

Supersymmetry and Phenomenology of Heterotic and Type I Superstring Models

David J Clements

June 18, 2018

Abstract

This work is the discussion of heterotic and type I string phenomenology. The heterotic string model is based on the free-fermionic formalism. In this scenario, one has the first case where non-Abelian VEV's, as opposed to singlet VEV's are required for the cancellation of the Fayet-Iliopoulos term. It is noted that non-Abelian fields are the only fields that can give rise to the satisfaction of the D -flat constraints in this model. In addition, there is an enhancement to the observable and hidden $SU(3)$ gauge groups to $SU(4)$.

The type I models discussed are based on $T^6/(\mathbb{Z}_2 \times \mathbb{Z}_2^s)$ and $T^6/(\mathbb{Z}_2 \times \mathbb{Z}_2 \times \mathbb{Z}_2^s)$ compactifications. The first example is a simpler case of the second model. It has $N = 2$ supersymmetry and includes a rank reduction of the $D5$ gauge groups as a result of using a freely acting Kaluza Klein shift \mathbb{Z}_2^s . The second case, is a freely acting Kaluza Klein shift of the $T^6/(\mathbb{Z}_2 \times \mathbb{Z}_2)$ orbifold $N = 1$ model. As such one has a choice of sign $\epsilon = \pm 1$ that arises in the model from terms not related to the principle orbits by S and T transformations. This allows the breaking of supersymmetry with the introduction of antibranes. In addition, one has four models for each choice of sign. However, I discuss the problems inherent in the $\epsilon = -1$ case with respect to particle interpretation.

I also discuss the $T^6/(\mathbb{Z}_2 \times \mathbb{Z}_2)$ model when background magnetic fields are introduced for the $\epsilon = -1$ case. In this scenario, one keeps the twisted terms in the transverse annulus which in turn does not allow for consistent cancellation of tadpoles. This is caused by a residual term that is proportional to the magnetic field. In this case I consider the magnetization of the first two tori. This leads to tadpole complications for the g and f twisted sectors, but allows the h twisted sector to behave normally. I discuss the issues of tachyonic excitations that arise from the low lying states in the direct channel.

Contents

1	Introduction	5
2	D-flatness in a 4D Heterotic Model Requiring Non-Abelian Fields	12
2.1	The Free Fermionic Construction	12
2.2	F - and D - Term Supersymmetry Breaking	15
2.3	The string model	16
2.4	Anomalous $U(1)$	21
2.5	Solutions of the D -Flat Constraint Equations	22
2.6	Discussion	25
3	Open Descendants of Type I $T^6/(\mathbb{Z}_2 \times \mathbb{Z}_2^s)$ and $T^6/(\mathbb{Z}_2 \times \mathbb{Z}_2 \times \mathbb{Z}_2^s)$ models	26
3.1	Type I Construction	26
3.1.1	Discrete and Continuous Wilson Lines	33
3.2	Open Descendants of a $T^6/(\mathbb{Z}_2 \times \mathbb{Z}_2^s)$ Model with $N = 2$ Supersymmetry .	36
3.3	$T^6/(\mathbb{Z}_2 \times \mathbb{Z}_2 \times \mathbb{Z}_2^s)$ model	45
3.3.1	Open Decedents	50
3.3.2	Models Without Discrete Torsion ($\epsilon = +1$)	51
3.3.3	Model Classes of $\epsilon = +1$	54
3.3.4	Models With Discrete Torsion ($\epsilon = -1$)	58
3.4	Discussion	63
4	Magnetic Deformation of the Type I $\mathbb{Z}_2 \times \mathbb{Z}_2$ Model with Discrete Torsion	65
4.1	Magnetic Background Construction for Bosons	65
4.1.1	Magnetically Deformed Fermions	67
4.2	$(T^6/\mathbb{Z}_2 \times \mathbb{Z}_2)(\mathbf{H})$ Structure	69
4.2.1	Tadpole Conditions	72
4.2.2	Mass Shifting and Tachyonic Instabilities	74
4.3	Discussion	75
5	Conclusions	77
A	General Mobius Origin for the A_1 Shift	83
B	$\mathbb{Z}_2 \times \mathbb{Z}_2$ Boundary Operators	85
C	Tadpole Diagrams	86
D	The Torus Amplitude from its Corresponding Action	87

E	Effect of Non-trivial Wilson Lines on Branes	90
F	Lattice Simplifications	91
G	Amplitudes of the $\mathbb{Z}_2 \times \mathbb{Z}_2$ Partition Function	92
H	Singular Valued Decomposition	94

List of Figures

3.1	Moving a brane off of the fixed point	34
3.2	Branes on the fixed points	42
B.1	Distinct boundary sets in the $\mathbb{Z}_2 \times \mathbb{Z}_2$	85
C.1	Distinct boundary sets in the $\mathbb{Z}_2 \times \mathbb{Z}_2$	86

List of Tables

3.1	Model classes with corresponding brane supersymmetry	35
3.2	Lattice S and P transforms	37
3.3	Unshifted fixed points	38
3.4	Remaining fixed points	39
3.5	Lattice restrictions	43
3.6	Lattice restrictions	53
3.7	Chiral multiplet representations for $\epsilon = (+, +, +)$	55
3.8	Chiral multiplet representations for $\epsilon = (+, -, -)$	56
3.9	Chiral multiplet representations for $\epsilon = (-, -, +)$	56
3.10	Chiral multiplet representations for $\epsilon = (-, +, -)$	57
3.11	$\epsilon = (1, 1, -1)$ Model Charges	61
4.1	Twisted sector mass shifts for $\mathbb{Z}_2 \times \mathbb{Z}_2$ model	75
G.1	Tadpole conditions	93

Chapter 1

Introduction

The standard model has provided a wealthy insight into low energy physics and interactions of fundamental particles and their respective force mediators. In particular, it has been shown to be consistent with virtually all physics down to scales approaching 10^{-16} cm. However, despite its success, the “Standard Model of Elementary Particles” could not support a theory in which the electromagnetic, weak, strong and gravity forces could be unified.

And so a new framework would be needed whereby the well known low energy behavior of particles is captured, and that the gauge symmetries could be unified at a higher scale. Along the path of understanding this framework, it would be hoped that other unsolved questions would also be answered. This motivation would provoke, and indeed require, an unprecedented level of insight into the mathematical and conceptual framework that represents the underlying principles of nature.

The standard model entails the symmetry of particles as the group $SU(3) \times SU(2)_L \times U(1)_Y$. The group structure describes the force mediators that set the multiplet families of matter. The matter multiplets organize as fifteen multiplets of spin- $\frac{1}{2}$ fermions in three generations of five. The Standard model force mediator particles are supplemented with gravity as a general relativistic theory.

There is a distinct conceptual underpinning of determinism versus uncertainty in the case of gravity and the force mediators of the standard model. In addition, there are a relatively large number of free parameters that determine the dynamics within the Lagrangian. From this, one must ask a question of the origin of the arrangements of multiplets and what mechanism might determine the particular values of the parameters used in the standard model structure.

Applying the highly successful method of field quantization (as used for the standard model forces) to gravitation has arguably proven to be the most complicated mathematical undertaking in theoretical physics. A conventional attempt to form a union between the quantum formalism and gravity yields a nonrenormalizable theory. This suggests that if gravity is to be unified consistently with the concept of uncertainty, there are physical mechanisms at work that exist at higher probing scales that are beyond the scope of standard model physics.

String theory is at present the best candidate for a unified framework for fundamental forces. Of the many attractive features it provides, it solves certain divergence problems that occur in equivalent point particle field theory diagrams because of the extended nature of a string. String theory includes gravitation defined within its own framework

as a spin-2 closed string. Indeed, it is capable of describing physics of gravity well beyond the point where details of processes no longer have a consistent interpretation (when, for example, approaching a singular point in general relativity, which is not possible at the resolution of standard model physics).

By contrast to the rather large number of parameters that reside in the Lagrangian of the standard model, String theory has one freedom which involves the string tension. This presents a striking first move toward a final theory, since such a theory (or theories at scales approaching it) would necessarily involve fewer or no freely fixable parameters. It has been argued that a final theory (that would necessarily include a unified description of fundamental forces) might show itself by means of self consistent and self explanatory mathematical structure.

While great strides are being made to develop the mathematical ideas and tools necessary to explore strings, future generations of accelerators will prompt the direction of such research with the production of related data. Although, there is still a gap in cooperation between theory development and corroborative data at scales beyond the standard model.

The large number of additional dimensions (by comparison to the four that exist in the standard model case) allows significant freedom to include string states with differing polarizations in the spacetime and internal directions. The requirement of additional dimensions leads to interesting compactification scenarios that provide new quantum numbers and moduli. For example, in addition to the conventional Kaluza Klein quantum number (which generically manifests itself in periodic or confined particle quantum systems) resulting from compactification on a circle, one also has towers of states that correspond to winding modes. Whereby the extended nature of the string allows it to wrap around a compact dimension.

With the introduction of left and right moving oscillators that involve left and right momentum components (that are symmetric and antisymmetric under interchange of winding and Kaluza Klein states) one has a simple duality relation for two theories defined at two different radii. The two radii are inversely related. The idea of this duality, combined with other operations that identify different string theories has become a pivotal point in contemporary research of string theory.

The picture that has emerged so far is that there are different perturbative string theories that are related and exist in ten dimensions, in addition to eleven dimensional supergravity. Collectively, these theories are linked by duality relations form perturbative limits of an underlying theory that doesn't have a clearly defined formulation. This more fundamental theory, is traditionally called M-theory.

In the context of M-theory, the true fundamental theory of nature, the theory should realize itself in a nonperturbative description. However, at the current level of understanding, what is known about this illusive theory are its perturbative limits, which are the $SO(32)$ and $E_8 \times E_8$ heterotic, type I, IIA and IIB along with eleven dimensional supergravity theories. Therefore, one should regard these limits as tools that allow the ability to probe the properties of the fundamental vacuum. But it may well be that none of these limits is capable of characterizing the vacuum completely. It is likely that all perturbative limits will need to be used to isolate the true M-theory vacuum. As such, it may well be that different perturbative string limits may provide more useful means to study different properties of the true nonperturbative vacuum.

There is yet no dynamical mechanism that provides instructions on how to select, and for what reason, a particular vacua. Indeed, while there are attempts in progress, such a mechanism may well lead to, or otherwise outline the form of the underlying M–theory.

The additional area of freedom that exists to explore appealing models resides in the concept of compactification. Since current accelerators are not able to probe the scales at which these hidden dimensions would allow their properties to be tested, there is at present a wide range of possibilities for their structure that are being considered. In this way, we can probe those properties that pertain to the observed experimental and cosmological data by using low energy effective field theory. The study of the perturbative limits in both their low and high energy behavior is the focus of intense study in the strings community. Much progress has been made in recent years in the basic understanding and intuitive meaning of the many new concepts and ideas related to compactification that have unfolded as a result.

The study of the $\mathbb{Z}_2 \times \mathbb{Z}_2$ modulated spectrum, which is an orbifold structure upon which all models in the work are considered, provides very appealing phenomenology. In the heterotic limit, the models that are based on this compactification have given rise to the most realistic superstring models to date. They contain the three generation structure with each of the standard model generations contained in one of the twisted sectors. One would conclude that this group structure provides some reason as to the manifest nature of the three generation family as being dependant on the underlying geometry.

In addition, models based on the $\mathbb{Z}_2 \times \mathbb{Z}_2$ orbifold have the $SO(10)$ embedding of the standard model spectrum. As such, in these models $U(1)_Y$ has the standard $SO(10)$ normalization with $k_Y = \frac{5}{3}$. In fact, the $E_8 \times E_8$ [12] heterotic construction is the only perturbative limit that contains the standard $SO(10)$ embedding of the standard model. The reason for this is that it contains the spinorial **16** representation in the perturbative massless spectrum. In this respect it may well be that other perturbative string limits may provide more useful means to study different properties of the true nonperturbative vacuum.

In terms of vacuum selection, while a dynamical mechanism for choosing one which is preferred is not known, it is appropriate to suggest that the realistic vacuum resides in the vicinity of the $\mathbb{Z}_2 \times \mathbb{Z}_2$ class of models. In addition, with the standard model compatibility that the $E_8 \times E_8$ model has, it is certainly suggested that a true vacuum would favor this limit. The full study of phenomenological aspects of the $\mathbb{Z}_2 \times \mathbb{Z}_2$ orbifold is therefore of significant benefit. It would then follow that the study of other limits based on the $\mathbb{Z}_2 \times \mathbb{Z}_2$ compactification scheme would also be of benefit.

Much of string physics, with the exception of recent work being done with time varying backgrounds, takes place on backgrounds that are fixed. This is largely because of the geometrical dependency that extended objects have when propagating on or interacting with a boundary that changes with time.

There is yet no known general approach to tackling the different limits with dynamical backgrounds. In order to make steps in this direction, it is very informative to understand such limits in the context of their behavior under different fixed backgrounds. Attempts to provide a greater picture in this way may well highlight some mechanism that is present which allows such string models to be defined consistently.

Such a mechanism might be extrapolated to show a more general framework of string scenarios with dynamical backgrounds.

It would be a very strong step forward if such a potential mechanism were to enlighten, or perhaps solve the problem of stabilizing the "unfrozen moduli" that exist in string theory (for example, in the case of the magnetized type I theory etc. . .). In looking at increasingly complicated backgrounds, such as allowing the presence of magnetic monopoles in the type I setting, or antisymmetric \mathbf{B} field have the effect of adding to the number of free moduli.

In the type I picture, the effect of magnetic monopoles admit an alternative interpretation in terms of rotated branes in the type IIA orientifold. The properties of the spectral content in this scenario, with respect to three-generation like properties, have been studied in [28]. However, the type I framework offers this description in terms of background magnetic fields [24, 32].

The six-dimensional case of the T^4/\mathbb{Z}_2 with two homogeneous magnetic fields in each T^2 (resulting from $T^4/\mathbb{Z}_2 \rightarrow (T^2(H_1) \times T^2(H_2))/\mathbb{Z}_2$ after introducing the two magnetic fields H_1 and H_2) was demonstrated in [25]. This was a particular case in which all tachyon's and possible terms that could give rise to divergences and inconsistencies are absent for the case that the two background field values are the same.

In extending this case to the study of the interesting class of $\mathbb{Z}_2 \times \mathbb{Z}_2$ models in four dimensions, such background fields present difficulties. Tachyonic instabilities present themselves without regard to the number of tori one wishes to magnetize (where $T^6/\mathbb{Z}_2 \times \mathbb{Z}_2$ has a torus structure $T^2 \times T^2 \times T^2$). This is due to the very nature of the $\mathbb{Z}_2 \times \mathbb{Z}_2$ orbifold generators which means that the compact directions have arrangements of orbifold operations that include $(+, -, -)$, $(-, +, -)$ and $(-, -, +)$. In addition, the magnetically shifted spectral states will have a dependence on the magnetic fields that can break supersymmetry.

This shift happens in a twofold way. The contributions from world sheet fermions give an addition to the mass squared term as a magnetic moment term that is sensitive to the helicity of the state in the directions of the tori that carry a magnetic field. Secondly, one has a tower of states that arise from the zero mode contributions for untwisted bosonic excitations as another contribution. The magnetic moment couplings will be sensitive to the sign of both the overall magnetic charge and the spin of the state. In this way, it is thus possible to introduce a mass splitting in supersymmetric multiplets.

So it is appreciated that if one is to assert that a magnetically deformed type I stable vacua exists, then there must exist an additional mechanism to prevent these excitations.

Moreover, the twisted structure of type I strings on such manifolds (and indeed in the simpler T^4/\mathbb{Z}_2 case for general choices of background fields) gives rise to divergences at massless level in the tube (or transverse) channel. These divergences take the form of residual terms that do not depend on the measure parameter τ_2 , which would normally cancel as a tadpole condition (in the absence of background magnetic fields). For the T^4/\mathbb{Z}_2 example, however, these are easily resolved with an appropriate field choice. This is not possible in the $\mathbb{Z}_2 \times \mathbb{Z}_2$ case, due to the structure of the generators (demonstrated in chapter 4 with two magnetic fields). These effects have not been studied with the choice of saturating the compact directions with magnetic fields.

These are then examples of how the study of increasingly complicated background scenarios cause further questions on realizing an underlying structure of string vacua that is capable of simulating the real world.

In the work presented here, phenomenological aspects of the heterotic $E_8 \times E_8$ NAHE based free fermionic and $SO(32)$ type I models are considered. In the light of the motivations for research already given, this work is intended to highlight particular points and phenomenology of these theories.

In the first chapter, the work is centered on the heterotic free fermionic models which discusses a particular extension of the NAHE set. The choice of extended vectors $\{\alpha, \beta, \gamma\}$ with appropriate GSO coefficients give rise to a low lying spectrum that will allow a satisfaction of the D -flat constraints only for the use of VEVs of non-Abelian fields. This is the first time that non-Abelian VEVs have been required for D -flat consistency as opposed to other possible phenomenological reasons.

In chapter 3, the effect of discrete Wilson lines is discussed in type I strings compactified on $T^6/(\mathbb{Z}_2 \times \mathbb{Z}_2^s)$ and $T^6/(\mathbb{Z}_2 \times \mathbb{Z}_2 \times \mathbb{Z}_2^s)$ manifolds. In the first case, I discuss a toy model which has one \mathbb{Z}_2 orbifold generator accompanied by a freely acting shift (\mathbb{Z}_2^s). The second case, which is essentially a generalization of this relies on the $\mathbb{Z}_2 \times \mathbb{Z}_2$ orbifold structure.

As described previously, the NAHE heterotic models are underlined by a geometric manifold which is an orbifold compactification of the type $\mathbb{Z}_2 \times \mathbb{Z}_2$. This structure is common to all the three generation free fermionic models.

The type I models show the effects on the open and closed spectrum from the projection of the torus with a freely acting momentum shift. It will be seen that while the first model is straightforwardly consistent, the second model presents some subtleties. Specifically, the symmetrization of states in the open and closed sectors.

Projections involving shifts that are defined as part of the $\mathbb{Z}_2 \times \mathbb{Z}_2$ structure have been studied in [1]. In this case, the shifts were not freely acting since they involve projectors of the form $(\delta, -\delta, -)$ for example. Here, a shift operation, denoted by δ , acts simultaneously with an orbifold operation. These models remove twisted terms in the torus that are independent orbits (terms that are not related to the principle orbits $\{(o, o), (o, g), (o, f), (o, h)\}$ by the generators of modular invariance, which is demonstrated in appendix B). The presence of such terms, as will be seen in the second model, allow a sign freedom ($\epsilon = \pm 1$). This freedom will allow for the introduction of eight possible subclasses of models. However, I show that the subclasses belonging to $\epsilon = -1$, has a problem with particle interpretation.

I will demonstrate the mechanisms of supersymmetry breaking that result in the four subclasses of models belonging to $\epsilon = +1$. The sign ϵ is defined in terms of three signs $\epsilon_i = \pm 1$ for $i = 1, 2, 3$ where $\epsilon = \epsilon_1 \epsilon_2 \epsilon_3$ and the models are classified by $(\epsilon_1, \epsilon_2, \epsilon_3)$. The only fully supersymmetric model in all eight that are possible from $\epsilon = \pm 1$ is the $(+, +, +)$ model.

In the third chapter, I demonstrate the appearance of residual terms in the $\mathbb{Z}_2 \times \mathbb{Z}_2$ open spectrum with two background magnetic fields in a model with discrete torsion. These terms give rise to tadpoles in the twisted sector that do not cancel. In the light of this model, it is appropriate to discuss the details of consistency conditions in type I strings. Additionally, the models in chapter 3 also show interesting deviations from the satisfaction of these consistency requirements.

In the ten dimensional case, the orientifold projection of the type IIB superstring torus amplitude, which is of course the ten dimensional type I superstring, gives rise to

$$\begin{aligned}\mathcal{J} &= \frac{1}{2} \int_{\mathcal{F}} \frac{d^2\tau}{\tau_2^2} \frac{1}{\tau_2^4} \frac{|V_8 - S_8|^2(\tau)}{\eta(\tau)} \\ \mathcal{K} &= \frac{1}{2} \int_0^\infty \frac{d\tau_2}{\tau_2^2} \frac{1}{\tau_2^4} \frac{(V_8 - S_8)(2i\tau_2)}{\eta(2i\tau_2)}\end{aligned}\tag{1.0.1}$$

where the second case is the Klein bottle amplitude, and in both cases their respective dependencies on the measures τ and $2i\tau_2$ are shown. The details of the construction are found in chapter 3. After an S transformation, the Klein can be written in terms of a closed string propagating between two non-dynamical objects known as $O9$ -planes. This is illustrated in the diagrams of appendix (C) for the Klein, annulus and Mobius couplings. However, this closed string coupling has the interpretation of two one-point functions at the $O9$ -planes with a propagator of

$$\frac{1}{p^2 + m^2}.\tag{1.0.2}$$

The factor of $\frac{1}{\tau_2^4}$ can be converted into a momentum integral according to equation (D.0.11). So at zero momentum (and after the appropriate rescaling of $2i\tau_2 = it = \frac{i}{l}$) the Klein amplitude has the form

$$\tilde{\mathcal{K}} = \frac{2^5}{2} \int_0^\infty dl \frac{(V_8 - S_8)(il)}{\eta(il)} \sim \frac{2^5}{2} \int_0^\infty dl e^{-lm^2} = \frac{1}{m^2}.\tag{1.0.3}$$

This of course carries a divergence, comparing with equation (1.0.2) at zero momentum.

So, part of the rationale for having an open sector is to allow cancellation of this tadpole divergence term. The transverse annulus and Mobius amplitudes are

$$\begin{aligned}\tilde{\mathcal{A}} &= \frac{2^{-5}N^2}{2} \int_0^\infty dl \frac{(V_8 - S_8)(il)}{\eta(il)} \\ \tilde{\mathcal{M}} &= \frac{2\epsilon N}{2} \int_0^\infty dl \frac{(\hat{V}_8 - \hat{S}_8)(il)}{\hat{\eta}(il)}.\end{aligned}\tag{1.0.4}$$

The Chan-Paton charges N count the stacks of dynamical objects known as $D9$ -branes to which the open string ends couple (in the direct channel). In the present discussion, one has closed strings propagating between branes. This then shows the contributions from $\tilde{\mathcal{K}} + \tilde{\mathcal{A}} + \tilde{\mathcal{M}}$ as proportional to

$$\frac{2^{-5}}{2} (2^5 + \epsilon N)^2 \int_0^\infty dl e^{-lm^2}.\tag{1.0.5}$$

The low energy effective action that describes these $O9$ - and $D9$ - brane Neveu-Schwarz couplings is

$$S_{NS} \sim (2^5 + \epsilon N)^2 \int d^{10}x e^{-\phi} \sqrt{-\det(G_{\mu\nu})}\tag{1.0.6}$$

for dilaton field ϕ and ten dimensional metric $G_{\mu\nu}$. So one has a cancellation of the divergence (1.0.5) for the the choice of $\epsilon = -1$. Moreover this confines $N = 32$, which

of course allows the ten dimensional type I gauge group of $SO(32)$. The other choice of $\epsilon = +1$ leads to a gauge group of $USp(32)$. These gauge groups can be seen from the direct channel expansion of the open sector as the number of vector bosons (coming from V_8) that act as the generators with

$$\mathcal{A} + \mathcal{M} \sim \frac{N(N + \epsilon)}{2}(V_8 - S_8). \quad (1.0.7)$$

Moving to describe the Ramond sector couplings, one has to take into account the potentials that arise from the bi-spinor expansion

$$\Phi_\alpha \bar{\Phi}_\beta = C_0 \Gamma_{\alpha\beta}^0 + C_{\mu\nu} \Gamma_{\alpha\beta}^{\mu\nu} + C_{\mu\nu\rho\kappa} \Gamma_{\alpha\beta}^{\mu\nu\rho\kappa}. \quad (1.0.8)$$

The low energy effective action is of the form

$$S_R \sim (2^5 + \epsilon N)^2 \mu_{(9)} \int C_{10}. \quad (1.0.9)$$

In this case one has both $O9$ -planes and the $D9$ branes carrying the Ramond charge $\mu_{(9)}$. There must therefore be an overall vanishing of the Ramond contributions. In the case of the action (1.0.6), one has an interpretation in terms of an increased vacuum energy if $\epsilon = +1$. However, for contributions arising from (1.0.9) there are charges with associated field lines. In a noncompact space, one can simply have the vanishing of the C_{p+1} forms at infinity. In a compact space, as will be the case in the models discussed in this work, the fields lines must begin and end somewhere, which can only be accomplished if there as many sources as sinks. In this case, there are exactly 32 sources as $D9$ -branes and an $O9$ -plane. The relative charges carried by a $D9$ -brane and an $O9$ -plane is of course 32.

In the magnetic chapter, it will be shown that the residual terms appearing in the transverse twisted sectors of the annulus cannot lead to consistent cancellation of both the Ramond and the Neveu-Schwarz sector tadpoles. This will therefore lead to an inconsistent model. While this is true for the case with discrete torsion, the model is completely consistent for the case without discrete torsion [30]

I now turn to the relevant discussions of the heterotic and type I string phenomenology.

Chapter 2

D-flatness in a 4D Heterotic Model Requiring Non-Abelian Fields

In this section I look at the necessity of non-Abelian *D*-flat constraints of a four dimensional toy model in the free fermionic construction for the one loop amplitude [15]. Unlike other models before it, it will be seen that the spectrum does not allow any solutions to the *D*-flat constraint equations for the use of VEVs of fields that are non-Abelian singlets.

The spectral content and phenomenology of these string models are determined by choices of boundary condition vectors and the one loop GSO phases. This model is underlined by the NAHE set which contains a set of boundary condition vectors that forms a base for a very large class of phenomenologically interesting models.

Although string consistency requirements impose conditions on the boundary conditions, there is freedom within the restrictions of consistency for models with greatly different phenomenology. In this toy model, the choice of boundary condition vectors plus an additional change to one of the GSO phases gives rise to:

- An enhancement in the observable and hidden sector gauge groups.
- Solution of the *D*-flat constraint equations exclusively through non-Abelian VEVs.

The string model discussed here belongs to a particular class of models known as Left-Right Symmetric models (LRS). These are free fermionic models with an observable sector gauge group that contains $SU(2)$ terms as $SU(2)_L \times SU(2)_R$.

I begin by reviewing the construction tools necessary for model building.

2.1 The Free Fermionic Construction

The free fermionic construction relies on an action that allows world sheet bosonic and fermionic fields to act freely of one another with no interaction. The heterotic action arises from taking left moving superstring degrees of freedom and right moving bosonic degrees of freedom and compactifying directly to four spacetime dimensions. In the fermionic formulation, one then applies fermionization to all internal bosonic fields. One finds that a complex fermionic field ψ and abosonic field H written as e^{iH} satisfy

the same operator product expansions. From each bosonic field H , two fermionic fields can be written as

$$\psi \sim e^{iH}, \quad \psi^* \sim e^{-iH} \quad (2.1.1)$$

The action for this construction is then defined by

$$\int d^2\sigma \left[\partial_\alpha X_L^\mu \partial^\alpha X_{\mu,L} + \partial_\alpha X_R^\mu \partial^\alpha X_{\mu,R} - i\bar{\psi}_L^\mu \gamma^\alpha \partial_\alpha \psi_{\mu,L} - i\bar{\psi}_L^I \gamma^\alpha \partial_\alpha \psi_{I,L} - i\bar{\psi}_R^\mu \gamma^\alpha \partial_\alpha \psi_{\mu,R} - i\bar{\psi}_R^I \gamma^\alpha \partial_\alpha \psi_{I,R} \right], \quad (2.1.2)$$

where $\mu = 1, 2$ are the spacetime indices and I are the internal ones. The labels L and R imply left and right moving fermions.

The spectrum is then composed of left moving coordinates X_L^μ , ψ_L^μ for transverse coordinates and eighteen internal real fermions, which in the notation used in this model, are denoted as six sets of three by the index $i = 1, \dots, 6$. The right moving sector has transverse bosonic coordinates X_R^μ and forty four ($j = 1, \dots, 44$) internal real fermionic coordinates as

$$\text{left moving } \begin{cases} X^\mu(z) \\ \Psi^\mu(z) \\ \chi_i(z), y_i(z), \omega_i(z) \end{cases} \quad \text{and right moving } \begin{cases} \bar{X}^\mu(\bar{z}) \\ \bar{\phi}_j(\bar{z}) \end{cases}. \quad (2.1.3)$$

The total of sixty four fermions are grouped as complex fermions

$$\psi = \frac{1}{\sqrt{2}}(\eta_j + i\eta_k), \quad \psi^* = \frac{1}{\sqrt{2}}(\eta_j - i\eta_k), \quad (2.1.4)$$

the particular grouping will of course rely on fermions having the same boundary condition where η_j and η_k are real.

A boundary condition vector defined as

$$\mathbf{a} = \{\mathbf{a}_L | \mathbf{a}_R\} = \{a_1, \dots, a_{10} | a_{11}, \dots, a_{22}\} \quad (2.1.5)$$

with components a_i will impose the condition on the i^{th} complex fermion as

$$\Psi^i(\tau, \sigma + 2\pi) = -e^{-\pi i a_i} \Psi^i(\tau, \sigma). \quad (2.1.6)$$

The labels L and R show the parts that act on the left and right moving fermions. One obtains NS (Neveu–Schwarz) and R (Ramond) boundary condition when the entries a_i are 0 or 1 respectively.

Model building begins with a prescription of vectors

$$\{\mathbf{b}_1, \dots, \mathbf{b}_n\} \quad (2.1.7)$$

that underly a general model. These vectors span a finite additive group

$$\Xi = \sum_{i=1}^n m_i \mathbf{b}_i \quad (2.1.8)$$

for $m_i = 0, \dots, N_i - 1$ such that $N_i \mathbf{b}_i = 0 \pmod{2}$.

In terms of boundary condition vectors $\alpha, \beta \in \Xi$ (with components α_l and β_l) the partition function will be written as

$$Z = \int \frac{d^2\tau}{[\text{Im}(\tau)]^2} Z_B(\tau, \bar{\tau}) \sum_{\alpha, \beta} C \begin{pmatrix} \alpha \\ \beta \end{pmatrix} \prod_{l=1}^{10} Z_l \begin{bmatrix} \alpha_l \\ \beta_l \end{bmatrix} \prod_{l=11}^{22} \bar{Z}_k \begin{bmatrix} \alpha_l \\ \beta_l \end{bmatrix}. \quad (2.1.9)$$

The phases $C \begin{pmatrix} \alpha \\ \beta \end{pmatrix}$ are chosen to allow the partition function to be modular invariant. Modular invariance is necessary to ensure that the partition function counts only distinct tori. A more formal discussion of modular invariance is left until the type I construction in the following chapter.

The phases that correspond to a given set of basis vectors, as will be clarified later, can introduce a freedom in the form of a choice of sign.

The invariance of Z will introduce rules or conditions on the basis vectors and phases introduced in (2.1.9). In addition, a GSO projection based on these vectors and phases will allow a projection of states of a given model to describe the spectral content. The calculation of these rules can be found in [34] and are summarized below.

Basis vectors that are consistent with modular invariance satisfy

$$N_{ij} \mathbf{b}_i \cdot \mathbf{b}_j = 0 \pmod{4}. \quad (2.1.10)$$

where N_{ij} is the least common multiple of the integers N_i and N_j . If one sets $i = j$, this condition holds for N_i odd. In the case that N_i is even, one has

$$N_i \mathbf{b}_i \cdot \mathbf{b}_i = 0 \pmod{8}. \quad (2.1.11)$$

The operation (\cdot) counts the left and right components of two parameters \mathbf{a} and \mathbf{b} as

$$\mathbf{a} \cdot \mathbf{b} = \left(\sum_{\text{Left}} - \sum_{\text{right}} \right) a_j b_j. \quad (2.1.12)$$

The GSO projection is defined as

$$e^{i\pi \mathbf{b}_j \cdot F \alpha} |s \rangle_{\alpha} = \delta_{\alpha} C \begin{pmatrix} \alpha \\ \mathbf{b}_j \end{pmatrix}^* |s \rangle_{\alpha} \quad (2.1.13)$$

with $\alpha \in \Xi$ and $|s \rangle_{\alpha}$ defines a state $|s \rangle$ in the sector α (* denotes complex conjugation), and

$$\delta_{\alpha} = e^{i\pi \alpha(\psi^{\mu})} = \begin{cases} -1 & \alpha(\psi^{\mu}) = 1 \\ +1 & \alpha(\psi^{\mu}) = 0 \end{cases}. \quad (2.1.14)$$

The phases that appear in the partition function, and thus the GSO projection, will have a sign freedom (in some sectors). Such choices can result in vastly different spectral content. In the case studied here, the choice of a different sign results, in particular, in an enhancement of the observable and hidden gauge groups.

The phases depend on the vectors according to

$$C \begin{pmatrix} \mathbf{b}_i \\ \mathbf{b}_j \end{pmatrix} = \delta_{\mathbf{b}_j} \exp \left(\frac{2i\pi m_i}{N_i} \right) \exp \left(\frac{i\pi \mathbf{b}_i \cdot \mathbf{b}_j}{2} \right) \quad (2.1.15)$$

where m_i and N_i are understood by equation (2.1.8).

The world sheet fermion number operator F acts on the complex modes ψ and ψ^* as a sign, so that $F\psi = +\psi$ and $F\psi^* = -\psi$.

The massless spectral content will generally have states that are pure vacuum which is degenerate. Such configurations have spinorial representations $|\pm\rangle$. As such, one has $F|+\rangle = 0|+\rangle$ and $F|-\rangle = -|-\rangle$ for these states.

The study of the phenomenology of these models involves the massless states from each sector. For each element $\alpha \in \Xi$, the oscillators allowed in the massless spectrum of the sector α are confined through the equations

$$\begin{aligned} M_L^2 = 0 &= -\frac{1}{2} + \frac{\alpha_L \cdot \alpha_L}{8} + N_L, \\ M_R^2 = 0 &= -1 + \frac{\alpha_R \cdot \alpha_R}{8} + N_R. \end{aligned} \quad (2.1.16)$$

Here, the terms $N_{L,R}$ are the left and right moving fermionic number operators and $\alpha_{L,R}$ are the components of α that act on the corresponding left and right fermions.

Thus, a model will be fully specified by the basis vectors and a choices for the phases, where such choices exists.

For an example of the choice that can arise, if one takes a vector S that has the boundary conditions on the fermions $\{\Psi^\mu, \chi_{1,2}, \chi_{3,4}, \chi_{5,6}\} = 1$ and all others 0, then $N_s = 2$. So $m_s \in \{0, 1\}$, and these two possibilities lead to different phases if one projects using the sector $\mathbf{b}_j = \mathbf{1}$, with reference to equation (2.1.15). As models become more complicated, so do the choices of the phases.

The following notation for the left and right sectors will be used for the total of sixty four fermions,

$$\psi_{1,2}^\mu (\chi_1 y_1 \omega_1) (\chi_2 y_2 \omega_2) (\chi_3 y_3 \omega_3) (\chi_4 y_4 \omega_4) (\chi_5 y_5 \omega_5) (\chi_6 y_6 \omega_6) \quad (2.1.17)$$

for the left sector, which carries the fermion spacetime field. In the right sector, one has

$$\bar{y}_1 \bar{\omega}_1 \bar{y}_2 \bar{\omega}_2 \bar{y}_3 \bar{\omega}_3 \bar{y}_4 \bar{\omega}_4 \bar{y}_5 \bar{\omega}_5 \bar{y}_6 \bar{\omega}_6 \bar{\Psi}_{1\dots 5} \bar{\eta}_1 \bar{\eta}_2 \bar{\eta}_3 \bar{\phi}_{1\dots 8}. \quad (2.1.18)$$

In all models, the fields $\bar{\Psi}_{1\dots 5}, \bar{\eta}_1, \bar{\eta}_2, \bar{\eta}_3$ and $\bar{\phi}_{1\dots 8}$ are complex. The pairings of the remaining internal fields will depend on the choice of boundary condition vectors.

2.2 $F-$ and $D-$ Term Supersymmetry Breaking

It will be helpful to review some of details of breaking supersymmetry through $F-$ and $D-$ terms. The Fayet–Iliopoulos (FI) term is an addition to the Lagrangian in the form ξD for the auxiliary field D [13, 14]. The variation with respect to this field then allows the inclusion of the factor ξ in the equation of motion. For the D terms, supersymmetry can be spontaneously broken via $\langle D_A \rangle \neq 0$ if there are no fields χ_k with charges Q_A^k such that $\sum_k Q_A^k |\langle \chi_k \rangle| = -\xi$. Similarly, supersymmetry is spontaneously broken via $\langle F \rangle \neq 0$.

The terms that result from variation with respect to the auxiliary fields D and F are

$$D_A = \sum_k Q_A^k |\chi_k|^2 + \xi, \quad (2.2.1)$$

$$D_\alpha = \sum_k Q_\alpha^k |\chi_k|^2 \quad (\alpha \neq A), \quad (2.2.2)$$

$$F_i = -\frac{\partial W}{\partial \eta_i}, \quad (2.2.3)$$

where

$$\langle D_A \rangle = \langle D_\alpha \rangle = \langle F_i \rangle = 0, \quad (2.2.4)$$

$$\xi = \frac{g^2 (\text{Tr} Q_A)}{192\pi^2} M_{\text{Pl}}^2. \quad (2.2.5)$$

The fields χ_k are those which acquire VEVs of order $\sqrt{\xi}$ and the η_i fields are scalars. W is the super potential, the terms Q_A^k and Q_α^k denote the anomalous and non-anomalous charges and $M_{\text{Pl}} \approx 2 \times 10^{18}$ GeV denotes the reduced Planck mass. The solution (*i.e.* the choice of fields with non-vanishing VEVs) to the set of equations (2.2.4)–(2.2.2), though nontrivial, is not unique. Therefore in a typical model there exist a moduli space of solutions to the F and D flatness constraints.

Very interesting aspects of the phenomenology of models involves the analysis and classification of flat directions. The methods for the analysis of D -flatness in string models, as the reader will appreciate from the discussion in section 2.5, have been made quite systematic [17, 10]. It has in general been assumed in the past that in a given string model there should exist a solution to the F and D flatness constraints. The simpler type of solutions to the flatness constraints utilize only fields that are singlets of all the non-Abelian groups in a given model (type I solutions).

In the following section, the string model discussed does not contain a type I solution. That is, the VEVs required to ensure that there are solutions to the flat directions must be from a set of fields that are not solely composed of singlet VEVs. Moreover, a solution using only singlet VEVs does not exist. This particular model was the first instance in which non-Abelian fields in the spectrum are required to have non vanishing VEVs if one insists on conforming to the constraints $\langle D_a \rangle = \langle D_\alpha \rangle = 0$.

2.3 The string model

The free fermionic string model discussed here is constructed by specifying a set of one loop GSO projection coefficients [5, 6] that correspond to the basis vectors $\{1, \mathbf{S}, \mathbf{b}_1, \mathbf{b}_2, \mathbf{b}_3\}$ and $\{\alpha, \beta, \gamma\}$. These vectors then form the set that was defined in (2.1.7).

The first set of vectors corresponds to the NAHE set [7, 8], which are common to all the semi-realistic free fermionic models. The second consists of three additional boundary condition basis vectors. The rules for extracting the superpotential terms were derived in ref. [19].

For the NAHE set, the boundary conditions on the left and right moving coordinates are defined in table 2.3.1.

	ψ^μ	χ^{12}	χ^{34}	χ^{56}	$\bar{\psi}^{1,\dots,5}$	$\bar{\eta}^1$	$\bar{\eta}^2$	$\bar{\eta}^3$	$\bar{\phi}^{1,\dots,8}$
1	1	1	1	1	1	1	1	1	1
S	1	1	1	1	0	0	0	0	0
b₁	1	1	0	0	1	1	0	0	0
b₂	1	0	1	0	1	0	1	0	0
b₃	1	0	0	1	1	0	0	1	0

	y^3y^6	$y^4\bar{y}^4$	$y^5\bar{y}^5$	$\bar{y}^3\bar{y}^6$	$y^1\omega^5$	$y^2\bar{y}^2$	$\omega^6\bar{\omega}^6$	$\bar{y}^1\bar{\omega}^5$	$\omega^2\omega^4$	$\omega^1\bar{\omega}^1$	$\omega^3\bar{\omega}^3$	$\bar{\omega}^2\bar{\omega}^4$
1	1	1	1	1	1	1	1	1	1	1	1	1
S	0	0	0	0	0	0	0	0	0	0	0	0
b₁	1	1	1	1	0	0	0	0	0	0	0	0
b₂	0	0	0	0	1	1	1	1	0	0	0	0
b₃	0	0	0	0	0	0	0	0	1	1	1	1

(2.3.1)

The boundary conditions of the three basis vectors which extend the NAHE set are shown in Table 2.3.2. This table as well as table 2.3.1 above show the pairings of left and right moving real fermions from the set $\{y_i, \omega_i | \bar{y}_i, \bar{\omega}_i\}$, for $i = 1, \dots, 6$. These fermions are paired to form complex left or right moving fermions. The particular pairings will of course vary with different models that assign alternate boundary conditions to these fermions.

The generalized GSO coefficients determining the physical massless states (through the GSO projection) of Model 1 appear in matrix 2.3.3.

	ψ^μ	χ^{12}	χ^{34}	χ^{56}	$\bar{\psi}^1$	$\bar{\psi}^2$	$\bar{\psi}^3$	$\bar{\psi}^4$	$\bar{\psi}^5$	$\bar{\eta}^{1,2,3}$	$\bar{\phi}^1$	$\bar{\phi}^{2,3,4}$	$\bar{\phi}^{5,6,7}$	$\bar{\phi}^8$
α	0	0	0	0	1	1	1	0	0	0	1	1	0	0
β	0	0	0	0	1	1	1	0	0	0	1	1	0	0
γ	0	0	0	0	$\frac{1}{2}$	$\frac{1}{2}$	$\frac{1}{2}$	0	0	$\frac{1}{2}$	0	$\frac{1}{2}$	$\frac{1}{2}$	0

	y^3y^6	$y^4\bar{y}^4$	$y^5\bar{y}^5$	$\bar{y}^3\bar{y}^6$	$y^1\omega^5$	$y^2\bar{y}^2$	$\omega^6\bar{\omega}^6$	$\bar{y}^1\bar{\omega}^5$	$\omega^2\omega^4$	$\omega^1\bar{\omega}^1$	$\omega^3\bar{\omega}^3$	$\bar{\omega}^2\bar{\omega}^4$
α	1	1	1	0	1	1	1	0	1	1	1	0
β	0	1	0	1	0	1	0	1	1	0	0	0
γ	0	0	1	1	1	0	0	0	0	1	0	1

(2.3.2)

LRS Model 1 Generalized GSO Coefficients:

$$\begin{array}{c}
 \mathbf{1} \quad \mathbf{S} \quad \mathbf{b}_1 \quad \mathbf{b}_2 \quad \mathbf{b}_3 \quad \alpha \quad \beta \quad \gamma \\
 \mathbf{1} \left(\begin{array}{ccccccccc}
 1 & 1 & -1 & -1 & -1 & 1 & 1 & i \\
 1 & 1 & 1 & 1 & 1 & -1 & -1 & -1 \\
 -1 & -1 & -1 & -1 & -1 & -1 & -1 & i \\
 -1 & -1 & -1 & -1 & -1 & -1 & -1 & i \\
 -1 & -1 & -1 & -1 & -1 & -1 & -1 & i \\
 1 & -1 & 1 & 1 & 1 & 1 & 1 & 1 \\
 1 & -1 & -1 & -1 & 1 & -1 & -1 & -1 \\
 1 & -1 & 1 & -1 & 1 & -1 & -1 & 1
 \end{array} \right) \\
 \mathbf{S} \\
 \mathbf{b}_1 \\
 \mathbf{b}_2 \\
 \mathbf{b}_3 \\
 \alpha \\
 \beta \\
 \gamma
 \end{array} \quad (2.3.3)$$

After the NAHE set, one has $N = 1$ supersymmetry with a gauge group of $SO(10) \times E_8 \times SO(6)^3$ and a total of 48 spinorial, with 16 of $SO(10)$, each 16 correspondingly arises from each sector b_1, b_2 and b_3 . The $SO(10)$ comes from the fermions $\bar{\Psi}^{1, \dots, 5}$.

In matrix (2.3.3) only the entries above the diagonal are independent and those below and on the diagonal are fixed by the modular invariance constraints. The relation between off diagonal components can be seen from

$$c \left(\begin{array}{c} \mathbf{b}_i \\ \mathbf{b}_j \end{array} \right) = \exp \left(\frac{i\pi \mathbf{b}_i \cdot \mathbf{b}_j}{2} \right) c \left(\begin{array}{c} \mathbf{b}_j \\ \mathbf{b}_i \end{array} \right)^* .$$

Blank lines are inserted to emphasize the division of the free phases between the different sectors of the realistic free fermionic models. Thus, the first two lines involve only the GSO phases of

$$c \left(\begin{array}{c} \{\mathbf{1}, \mathbf{S}\} \\ \mathbf{a}_i \end{array} \right) .$$

The set $\{\mathbf{1}, \mathbf{S}\}$ generates the $N = 4$ model with \mathbf{S} being the space–time supersymmetry generator.

Note that the boundary condition basis vectors that generate the string model are those of Model 3 [11]. The two models differ by a GSO phase with

$$c \left(\begin{array}{c} \mathbf{b}_3 \\ \beta \end{array} \right) = -1 \quad (2.3.4)$$

in this model, and

$$c \left(\begin{array}{c} \mathbf{b}_3 \\ \beta \end{array} \right) = +1 \quad (2.3.5)$$

in Model 3. As is elaborated on below, the consequence of this GSO phase change is that the gauge symmetry is enhanced, with one of the Abelian generators being absorbed into the enhanced non–Abelian gauge symmetry. Consequently, the number of Abelian group factors is reduced, which simplifies somewhat the analysis of the D –flat directions.

The final gauge group of the string model arises as follows: In the observable sector the NS boundary conditions produce gauge group generators for

$$SU(3)_C \times SU(2)_L \times SU(2)_R \times U(1)_C \times U(1)_{1,2,3} \times U(1)_{4,5,6}. \quad (2.3.6)$$

Thus, the $SO(10)$ symmetry, which arises from the fermion group $\bar{\Psi}^{1,\dots,5}$ is broken to $SU(3) \times SU(2)_L \times SU(2)_R \times U(1)_C$, where,

$$U(1)_C = \text{Tr } U(3)_C \Rightarrow Q_C = \sum_{i=1}^3 Q(\bar{\psi}^i). \quad (2.3.7)$$

The three symmetries denoted by $U(1)_j$ ($j = 1, 2, 3$) arise from the world-sheet currents $\bar{\eta}^j \bar{\eta}^{j*}$. These three $U(1)$ symmetries are present in all the three generation free fermionic models which use the NAHE set. Additional $U(1)$ symmetries, denoted by $U(1)_j$ ($j = 4, 5, 6$), arise by pairing two real fermions from the sets $\{\bar{y}^{3,\dots,6}\}$, $\{\bar{y}^{1,2}, \bar{\omega}^{5,6}\}$, and $\{\bar{\omega}^{1,\dots,4}\}$.

The final observable gauge group depends on the number of such pairings. From both tables 2.3.2 and 2.3.1, it can be seen that pairs can be formed out of $\bar{y}^{3,6}$, $\bar{y}^1 \bar{\omega}^5$ and $\bar{\omega}^{2,4}$, since they have identical boundary conditions for all basis vectors. In this model these are the pairings which generate the three additional $U(1)$ symmetries, denoted by $U(1)_{4,5,6}$.

In the hidden sector, which arises from the complex world-sheet fermions $\bar{\phi}^{1\dots 8}$, the NS boundary conditions produce the generators of

$$SU(3)_{H_1} \times U(1)_{H_1} \times U(1)_{7'} \times SU(3)_{H_2} \times U(1)_{H_2} \times U(1)_{8'}. \quad (2.3.8)$$

Here, the $U(1)$'s are rotated with the $U(1)_{7',8'}$ combinations of world-sheet charges given later, and $U(1)_{H_1}$ and $U(1)_{H_2}$ correspond to the combinations

$$Q_{H_1} = Q(\bar{\phi}^1) - Q(\bar{\phi}^2) - Q(\bar{\phi}^3) + Q(\bar{\phi}^4) - \sum_{i=5}^7 Q(\bar{\phi}^i) + Q(\bar{\phi}^8), \quad (2.3.9)$$

$$Q_{H_2} = \sum_{i=1}^4 Q(\bar{\phi}^i) - Q(\bar{\phi}^5) + \sum_{i=6}^8 Q(\bar{\phi}^i). \quad (2.3.10)$$

The sector $\zeta \equiv 1 + \mathbf{b}_1 + \mathbf{b}_2 + \mathbf{b}_3$ produces the representations $(3, 1)_{-2,0} \oplus (\bar{3}, 1)_{2,0}$ and $(1, 3)_{0,2} \oplus (1, \bar{3})_{0,-2}$ of $SU(3)_{H_1} \times U(1)_{H_1}$ and $SU(3)_{H_2} \times U(1)_{H_2}$. Thus, the E_8 symmetry reduces to $SU(4)_{H_1} \times SU(4)_{H_2} \times U(1)^2$. The additional $U(1)$'s in $SU(4)_{H_{1,2}}$ are given by the combinations in equations (2.3.9) and (2.3.10), respectively. The remaining $U(1)$ symmetries in the hidden sector, $U(1)_{7'}$ and $U(1)_{8'}$, correspond to the combinations of world-sheet charges

$$Q_{7'} = Q(\bar{\phi}^1) - Q(\bar{\phi}^8), \quad (2.3.11)$$

$$Q_{8'} = Q(\bar{\phi}^1) - \sum_{i=2}^4 Q(\bar{\phi}^i) + \sum_{i=5}^7 Q(\bar{\phi}^i) + Q(\bar{\phi}^8). \quad (2.3.12)$$

In addition to the NS and ζ sector the string model contains a combination of non-NAHE basis vectors with $\mathbf{X}_L \cdot \mathbf{X}_L = 0$, which therefore may give rise to additional

space–time vector bosons. The vector combination is given by $\mathbf{X} \equiv \zeta + 2\gamma$, where $\zeta \equiv 1 + \mathbf{b}_1 + \mathbf{b}_2 + \mathbf{b}_3$. This combination arises only from the NAHE set basis vectors plus 2γ , with γ inducing the left–right symmetry breaking pattern $SO(6) \times SO(4) \rightarrow SU(3) \times U(1) \times SU(2)_L \times SU(2)_R$. This vector combination is therefore generic for the pattern of symmetry breaking $SO(10) \rightarrow SU(3)_C \times U(1)_C \times SU(2)_L \times SU(2)_R$, in NAHE based models.

The sector \mathbf{X} gives rise to six additional space–time vector bosons which are charged with respect to the world–sheet $U(1)$ currents, and transform as $3 \oplus \bar{3}$ under $SU(3)_C$. These additional gauge bosons enhance the $SU(3)_C \times U(1)_{C'}$ symmetry to $SU(4)_C$, where $U(1)_{C'}$ is given by the combination of world–sheet charges,

$$Q_{C'} = Q(\bar{\psi}^1) - Q(\bar{\psi}^2) - Q(\bar{\psi}^3) - \sum_{i=1}^3 Q(\bar{\eta}^i) + Q(\bar{\phi}^1) - Q(\bar{\phi}^8). \quad (2.3.13)$$

The remaining orthogonal $U(1)$ combinations are

$$\begin{aligned} Q_{1'} &= Q(\bar{\eta}^1) - Q(\bar{\eta}^2), \\ Q_{2'} &= Q(\bar{\eta}^1) + Q(\bar{\eta}^2) - 2Q(\bar{\eta}^3), \\ Q_{3'} &= 3Q_C - (Q(\bar{\eta}^1) + Q(\bar{\eta}^2) + Q(\bar{\eta}^3)), \\ Q_{7''} &= Q_C + 3(Q(\bar{\eta}^1) + Q(\bar{\eta}^2) + Q(\bar{\eta}^3)) + 5Q_{7'}. \end{aligned} \quad (2.3.14)$$

and $Q_{4,5,6,8'}$ are unchanged. Thus, the full massless spectrum transforms under the final gauge group, $SU(4)_C \times SU(2)_L \times SU(2)_R \times U(1)_{1',2',3'} \times U(1)_{4,5,6} \times SU(4)_{H_1} \times SU(4)_{H_2} \times U(1)_{7'',8'}$.

In addition to the graviton, dilaton, antisymmetric sector and spin–1 gauge bosons, the NS sector gives three pairs of $SO(10)$ singlets with $U(1)_{1,2,3}$ charges; and three singlets of the entire gauge group.

The states from the sectors $\mathbf{b}_j \oplus \mathbf{b}_j + \mathbf{X}$ ($j = 1, 2, 3$) produce the three light generations. The states from these sectors and their decomposition under the entire gauge group are shown in Table 1 at the end of the Appendicies¹. The leptons (and quarks) are singlets of the color $SU(4)_{H_1, H_2}$ gauge groups and the $U(1)_{8'}$ symmetry of equation (2.3.12) becomes a gauged leptophobic symmetry.

The remaining massless states in the model and their quantum numbers are also given in Table 1.

I next turn to the definition of the weak–hypercharge in this LRS model. Due to the enhanced symmetry there are several possibilities to define a weak–hypercharge combination which is still family universal and reproduces the correct charge assignment for the Standard Model fermions. One option is to define the weak–hypercharge with the standard $SO(10)$ embedding, as in equation (2.3.15),

$$U(1)_Y = \frac{1}{3}U(1)_C + \frac{1}{2}U(1)_L. \quad (2.3.15)$$

This is identical to the weak–hypercharge definition in $SU(3) \times SU(2) \times U(1)_Y$ free fermionic models, which do not have enhanced symmetries, as for example in Model 3

¹The reader should note that all charges in this table have been scaled up by a factor of four.

of ref. [11]. Alternatively, one can define the weak–hypercharge to be the combination

$$U(1)_Y = \frac{1}{10} \left(U(1)_{3'} + \frac{1}{3} U_{7''} \right) + \frac{1}{2} U(1)_L \quad (2.3.16)$$

where $U(1)_{3'}$ and $U(1)_{7''}$ are given in (2.3.14). This combination still reproduces the correct charge assignment for the Standard Model states. The reason being that the states from the sectors \mathbf{b}_i $i = 1, 2, 3$ which are identified with the Standard Model states, are not charged with respect to the additional Cartan sub–generators that form the modified weak hypercharge definition. In some models it is found that such alternative definitions allow all massless exotic states to be integrally charged.

However, the study of this model is motivated by the possible existence of D –flat directions that use non–Abelian VEVs. It is not intended to be a semi–realistic candidate. It is therefore concluded that the model admits a sensible weak–hypercharge definition, which for the purpose of this work is sufficient.

2.4 Anomalous $U(1)$

The string model contains an anomalous $U(1)$ symmetry. The anomalous $U(1)$ is a combination of $U(1)_4$, $U(1)_5$ and $U(1)_6$, which are generated by the world–sheet complex fermions $\bar{y}^3 \bar{y}^6$, $\bar{y}^1 \bar{\omega}^5$ and $\bar{\omega}^2 \bar{\omega}^4$, respectively. So it is seen that $U_{4,5,6}$ arise from the internal “compactified” degrees of freedom.

It is convenient to rotate $U(1)_4$, $U(1)_5$ and $U(1)_6$ so that only one these symmetries is anomalous. The anomalous $U(1)_A$ combination in this model is given by

$$U_A \equiv U_4 + U_5 + U_6, \quad (2.4.1)$$

with $\text{Tr} Q_A = -72$. The two orthogonal linear combinations,

$$\begin{aligned} U_{4'} &= U_4 - U_5 \\ U_{5'} &= U_4 + U_5 - 2U_6 \end{aligned} \quad (2.4.2)$$

are then both traceless.

Since $\text{Tr} Q_A < 0$, the sign for the Fayet–Iliopoulos term (ξ) is negative, as can be seen from equation (2.2.5). Requiring D –flatness then implies that there must exist a field (or a combination of fields) with positive total $U(1)_A$ charge that receive a VEV (or VEVs) to cancel the $U(1)_A$ D –term. The equation that enforces this for D –flatness is shown in (2.2.1).

Looking at the massless spectrum of the model, given in Table 1 of the appendix (*Model 1 Fields*), it is immediately understood that the model does not contain any non–Abelian singlet fields with such a positive charge. Therefore, if D –flatness exists, some non–Abelian fields must acquire a VEV. The spectrum shows that the only states that carry positive $U(1)_A$ charge are the $SU(2)_L$ and $SU(2)_R$ (\mathcal{L}_{L_k, R_k}) doublets from the three sectors $\mathbf{b}_k + \zeta + 2\gamma \equiv \mathbf{1} + \mathbf{b}_i + \mathbf{b}_j + 2\gamma$, ($i, j, k = 1, 2, 3$) with i, j, k all distinct. These states are shown in Table 1 in the sectors $\mathbf{b}_k \oplus \mathbf{b}_k + \zeta + 2\gamma$. The same result holds also in Model 3 of ref. [11], in which there is no colour gauge enhancement from the sector $\zeta + 2\gamma$.

I next turn to discuss the possibility of D –flatness in this model.

2.5 Solutions of the D -Flat Constraint Equations

Table 1 in the appendices lists all of the massless states that appear in this LRS string model. There are a total of 68 fields, 38 of which may be used to form 19 sets of vector-like pairs of fields (which have opposite $U(1)$ charges). Of these 19 vector-like pairs, 13 pairs are singlets under all non-Abelian gauge groups, while three pairs are $\bar{\mathbf{4}}/\mathbf{4}$ (\bar{D}_i/D_i , $i = 1, 2, 3$) sets under $SU(4)_C$ and two pairs are $\mathbf{6}/\bar{\mathbf{6}}$'s ($\bar{\mathcal{H}}_i/\mathcal{H}_i$, $i = 1, 2$) sets under $SU(4)_{H_2}$. The 30 non-vector-like fields are all non-Abelian reps. That is, all singlets occur in vector-like pairs.

The anomalous charge trace of $U(1)_A$ is negative for this model. Thus, the anomaly can only be cancelled by fields with positive anomalous charge. In this model, as can be seen from Table 1, *none* of the non-Abelian singlets carry anomalous charge $Q^{(A)}$. The only fields with positive anomalous charge are three $SU(2)_L$ doublets, $\mathcal{L}_{L1,L2,L3}$ and three $SU(2)_R$ doublets, $\mathcal{L}_{R1,R2,R3}$.

To systematically study D -flatness for this model, first one must generate a complete basis of directions D -flat for all non-anomalous Abelian symmetries. These basis directions are provided in Table 2 at the end of the appendices.

The process begins from a set of simultaneous equations of the form

$$\mathbf{D}\cdot\mathbf{x} = \mathbf{b} \tag{2.5.1}$$

where the matrix \mathbf{D} has components $D_{ij} = Q_j^{(i)}$ which are the charges of the state ϕ_j with the norm squared of its VEV as the components of the vector \mathbf{x} , $x_j = |\langle\phi_j\rangle|^2$. The vector \mathbf{b} has zero entries except for the row $i = A$ which corresponds to the net anomalous charge, and has value $-\xi$. This is consistent with the equations (2.2.1) and (2.2.2).

From here, one uses the reduced matrix \mathbf{D}' which is simply the original matrix with the $i = A$ row removed. One then applies the SVD method² to systematically provide a set of basis directions. These are then rotated to give the basis directions in the form

$$\mathbf{x}_1 = \begin{pmatrix} |\langle\mathcal{L}_{R1}\rangle|^2 \\ 0 \\ 0 \\ \vdots \\ \text{common fields} \\ 0 \\ \vdots \end{pmatrix}, \quad \mathbf{x}_2 = \begin{pmatrix} 0 \\ |\langle\mathcal{L}_{L1}\rangle|^2 \\ 0 \\ \vdots \\ \text{common fields} \\ 0 \\ \vdots \end{pmatrix}, \dots \tag{2.5.2}$$

so that each contains at least one unique field VEV and a group of field VEVs that are common to all directions.

For a given row in Table 2, the first column entry denotes the name of the D -flat basis direction (\mathbf{x}_i). The next row specifies the anomalous charge of the basis direction. The following seven entries specify the ratios of the norms of the VEVs of the fields common to these directions. The first five of these fields have vector-like partners. For

²This method is based on the ‘‘Singular Value Decomposition’’ method, which was demonstrated for the systematic resolution of D -flat constraint equations by G. Cleaver. The method itself is reviewed in appendix H.

these, a negative norm indicates the vector–partner acquires the VEV, rather than the field specified at the top of the respective column. The last two of these seven fields are not vector–like. Thus, the norm must be non–negative for each of these for a flat direction formed from a linear combination of basis directions to be physical. The next to last entry specifies the norm of the VEV of the field unique to a given basis direction, while the identity of the unique field is given by the last entry.

These D –flat directions have been labelled as \mathbf{x}_1 through \mathbf{x}_{41} . The first eight D –flat directions (\mathbf{x}_1 to \mathbf{x}_8) carry a positive net anomalous charge. The next fourteen (\mathbf{x}_9 to \mathbf{x}_{22}) carry a negative net anomalous charge, while the remaining nineteen (\mathbf{x}_{23} to \mathbf{x}_{41}) lack a net anomalous charge. There are two classes of basis vectors lacking anomalous charge. The first class contains six directions for which the unique field is non–vector–like. These directions also contain VEVs for \mathcal{H}_1 ($\bar{\mathcal{H}}_1$) and/or \mathcal{H}_2 ($\bar{\mathcal{H}}_2$). The second class contains thirteen basis directions wherein the unique fields are vector–like and which do not contain $\bar{H}_{2'}$ and/or $\bar{H}_{4'}$. Thus, these thirteen directions are themselves vector–like and are denoted as such by a superscript “ v ”. For each vector–like basis direction, \mathbf{x}^v there is a corresponding $-\mathbf{x}^v$ direction, wherein the fields in \mathbf{x}^v are replaced by their respective vector–like partners.

None of the positive $Q^{(A)}$ directions are good in themselves because one or both of $|\langle \bar{H}_{2'} \rangle|^2$ and $|\langle \bar{H}_{4'} \rangle|^2$ are non–zero and negative while $|\langle \bar{H}_{2'} \rangle|^2$ and $|\langle \bar{H}_{4'} \rangle|^2$ are not vector–like representations. In particular, the $Q^{(A)} = 12$ directions have either $|\langle \bar{H}_{2'} \rangle|^2 = -2$ and $|\langle \bar{H}_{4'} \rangle|^2 = 0$ or $|\langle \bar{H}_{2'} \rangle|^2 = 0$ and $|\langle \bar{H}_{4'} \rangle|^2 = -2$, while the $Q^{(A)} = 24$ directions all have $|\langle \bar{H}_{2'} \rangle|^2 = |\langle \bar{H}_{4'} \rangle|^2 = -4$. In this basis one also finds that the $|\langle \bar{H}_{2'} \rangle|^2$ and $|\langle \bar{H}_{4'} \rangle|^2$ charges of all of the $Q^{(A)} = 0$ directions are zero or negative. So the $|\langle \bar{H}_{2'} \rangle|^2$ and $|\langle \bar{H}_{4'} \rangle|^2$ negative charges on the positive $Q^{(A)}$ directions cannot be made zero or positive by adding $Q^{(A)} = 0$ directions to $Q^{(A)} > 0$ directions. In contrast, all of the $Q^{(A)} = -12$ directions have either $|\langle \bar{H}_{2'} \rangle|^2 = 2$ and $|\langle \bar{H}_{4'} \rangle|^2 = 0$ or $|\langle \bar{H}_{2'} \rangle|^2 = 0$ and $|\langle \bar{H}_{4'} \rangle|^2 = 2$; the $Q^{(A)} = -24$ directions all have either $|\langle \bar{H}_{2'} \rangle|^2 = |\langle \bar{H}_{4'} \rangle|^2 = 4$ or $|\langle \bar{H}_{2'} \rangle|^2 = |\langle \bar{H}_{4'} \rangle|^2 = 2$; while the $Q^{(A)} = -48$ directions all have $|\langle \bar{H}_{2'} \rangle|^2 = |\langle \bar{H}_{4'} \rangle|^2 = 4$. Therefore, physical D –flat directions must necessarily be formed from linear combinations of $Q^{(A)} > 0$ and $Q^{(A)} < 0$ directions such that the net $Q^{(A)}$, $|\langle \bar{H}_{2'} \rangle|^2$, and $|\langle \bar{H}_{4'} \rangle|^2$ are all positive. Physical D –flat directions may also contain $Q^{(A)} = 0$ components that keep $|\langle \bar{H}_{2'} \rangle|^2, |\langle \bar{H}_{4'} \rangle|^2 \geq 0$.

The specific values of $Q^{(A)}$, $|\langle \bar{H}_{2'} \rangle|^2$, and $|\langle \bar{H}_{4'} \rangle|^2$ in the basis directions indicate that the roots of all physical flat directions must contain either \mathbf{x}_{19} or \mathbf{x}_{20} and combinations of basis vectors $\mathbf{x}_1, \mathbf{x}_2, \mathbf{x}_3$, and \mathbf{x}_4 of the form

$$n_1 \mathbf{x}_1 + n_2 \mathbf{x}_2 + n_3 \mathbf{x}_3 + n_4 \mathbf{x}_4 + n_{19} \mathbf{x}_{19} + n_{20} \mathbf{x}_{20}. \quad (2.5.3)$$

The non–negative integers $n_1, n_2, n_3, n_4, n_{19}, n_{20}$ satisfy the constraints

$$n_1 + n_2 + n_3 + n_4 - 2n_{19} - 2n_{20} > 0, \quad (2.5.4)$$

$$-n_1 - n_2 + 2n_{19} + 2n_{20} \geq 0, \quad (2.5.5)$$

$$-n_3 - n_4 + 2n_{19} + 2n_{20} \geq 0. \quad (2.5.6)$$

which provide the positivity requirements, in agreement with the Fayet–Iliopoulos term ξ , and the positive semi–definiteness of the norm squared of the field VEVs for $\bar{H}_{4'}$ and $\bar{H}_{2'}$ so that they represent fields with physical VEVs.

For example, one of the simplest D -flat solutions for all Abelian gauge groups is $n_1 = n_2 = n_3 = n_4 = 2$, $n_{19} = n_{20} = 1$. This direction is simply $|\langle \mathcal{L}_{L1} \rangle|^2 = |\langle \mathcal{L}_{L2} \rangle|^2 = |\langle \mathcal{L}_{L3} \rangle|^2 = |\langle \mathcal{L}_{R1} \rangle|^2 = |\langle \mathcal{L}_{R2} \rangle|^2 = |\langle \mathcal{L}_{R3} \rangle|^2$. The corresponding fields are three exotic $SU(2)_L$ doublets, \mathcal{L}_{L1} , \mathcal{L}_{L2} , and \mathcal{L}_{L3} , and three exotic $SU(2)_R$ doublets, \mathcal{L}_{R1} , \mathcal{L}_{R2} , and \mathcal{L}_{R3} . These six fields are singlets under all other non-Abelian groups.

For this model any D -flat direction must contain $SU(2)_L$ or $SU(2)_R$ fields. Thus, let us examine more closely $SU(2)$ D -flat constraints. The only $SU(2)$ fields in this model are doublet representations, which are generically denoted L_i . Thus, the related three $SU(2)$ D -terms,

$$D_{a=1,2,3}^{SU(2)} \equiv \sum_m L_i^\dagger T_{a=1,2,3}^{SU(2)} L_i, \quad (2.5.7)$$

contain matrix generators $T_a^{SU(2)}$ that take on the values of the three Pauli matrices,

$$\sigma_x = \begin{pmatrix} 0 & 1 \\ 1 & 0 \end{pmatrix}, \quad \sigma_y = \begin{pmatrix} 0 & -i \\ i & 0 \end{pmatrix}, \quad \sigma_z = \begin{pmatrix} 1 & 0 \\ 0 & -1 \end{pmatrix}, \quad (2.5.8)$$

respectively.

As discussed in [23], each component of the vector $\vec{D}^{SU(2)}$ is the total ‘‘spin expectation value’’ in the given direction of the internal space, summed over all $SU(2)$ doublet fields of the gauge group. Thus, for all of the $\langle D_a^{SU(2)} \rangle$ to vanish, the $SU(2)$ VEVs must be chosen such that the total \hat{x} , \hat{y} , and \hat{z} expectation values are zero.

I take the explicit representation of a generic $SU(2)$ doublet [23] $L(\theta, \phi)$ as

$$L(\theta, \phi) \equiv A \begin{pmatrix} \cos \frac{\theta}{2} e^{-i\frac{\phi}{2}} \\ \sin \frac{\theta}{2} e^{+i\frac{\phi}{2}} \end{pmatrix}, \quad (2.5.9)$$

where A is the overall amplitude of the VEV. The range of physical angles, $\theta = 0 \rightarrow \pi$ and $\phi = 0 \rightarrow 2\pi$ provide for the most general possible doublet

The contribution of $L(\theta, \phi)$ to each $SU(2)$ D -term is,

$$D_1^{SU(2)}(L) \equiv L^\dagger \begin{pmatrix} 0 & 1 \\ 1 & 0 \end{pmatrix} L = |A|^2 \sin \theta \cos \phi \quad (2.5.10)$$

$$D_2^{SU(2)}(L) \equiv L^\dagger \begin{pmatrix} 0 & -i \\ i & 0 \end{pmatrix} L = |A|^2 \sin \theta \sin \phi \quad (2.5.11)$$

$$D_3^{SU(2)}(L) \equiv L^\dagger \begin{pmatrix} 1 & 0 \\ 0 & -1 \end{pmatrix} L = |A|^2 \cos \theta. \quad (2.5.12)$$

From this one can see that the VEVs of three $SU(2)$ doublets $\mathcal{L}_{i=1,2,3}$ with equal norms $|A_1|^2 = |A_2|^2 = |A_3|^2 \equiv |A|^2$ can, indeed, produce an $SU(2)$ D -flat direction with the choice of angles, $\theta_1 = 0$, $\theta_2 = \theta_3 = 2\pi/3$, $\phi_2 = 0$, $\phi_3 = \pi$. For these angles, the total \hat{x} , \hat{y} , and \hat{z} expectation values are all zero.

This flat direction gives a specific example of what will occur for every flat direction of this model: non-Abelian VEVs (for at least $SU(2)_L$ or $SU(2)_R$ doublets) are a necessary if one requires D -flatness, or a solution to the equations of motion (2.2.1) and (2.2.2)).

I now consider the status of F -flatness at the FI scale. By $U(1)$ gauge invariance (by referring to table 1), the direction $|\langle \mathcal{L}_{L1} \rangle|^2 = |\langle \mathcal{L}_{L2} \rangle|^2 = |\langle \mathcal{L}_{L3} \rangle|^2 = |\langle \mathcal{L}_{R1} \rangle|^2 =$

$|\langle \mathcal{L}_{R2} \rangle|^2 = |\langle \mathcal{L}_{R3} \rangle|^2$ was found to comply with F -flatness. This is understood since one of the constraints to forming superpotential terms is that each should have vanishing total $U(1)$ charge. From this, F -flatness remains the case to all finite order in the superpotential. While this is true for the simplest flat direction as is used in this example, it is expected that dangerous F -terms will arise for all but a few of the more complicated directions.

2.6 Discussion

This is a toy model with specific choices of GSO phases and boundary condition vectors (consistent with modular invariance) that give rise to a spectrum which supports D - and F -flatness for the use of non-Abelian terms. Of course, this is certainly the case for the simple direction where the only fields that take on VEVs are the exotic $SU(2)_{L,R}$ doublets \mathcal{L}_{L_i,R_i} , for $i = 1, 2, 3$ where $|\langle \mathcal{L}_{L1} \rangle|^2 = |\langle \mathcal{L}_{L2} \rangle|^2 = |\langle \mathcal{L}_{L3} \rangle|^2 = |\langle \mathcal{L}_{R1} \rangle|^2 = |\langle \mathcal{L}_{R2} \rangle|^2 = |\langle \mathcal{L}_{R3} \rangle|^2$. As was mentioned before, this expected not to be the case for most of the other directions that are solutions of equations (2.5.4), (2.5.5) and (2.5.6).

As the reader will appreciate, the number of massless sectors that derive from the NAHE plus $\{\alpha, \beta, \gamma\}$ sectors is large. Generally there is no mechanism, other than computing and examining a model, for determining the appropriate vectors and GSO phases to obtain the precisely desired phenomenology. However, it is through the collective study of different models that one might begin to understand a mechanism behind the freedom to choose the vectors and GSO phases.

This work is not intended to elaborate on such a mechanism. Presented here is simply a four dimensional scenario whereby the choices (2.3.1), (2.3.2) and (2.3.3) lead to new and interesting spectral, and most importantly, D -flatness aspects.

It was pointed out before that this model could not be admitted as a possible realistic candidate. The non-Abelian fields \mathcal{L} , that were used here for D -flatness, carry fractional electric charge. In addition to this, all Higgs doublets from the Neveu-Schwarz sector are projected out by the choice of GSO phases. This makes it problematic to obtain realistic fermion mass spectrum.

This was the first instance in the study of the realistic free fermionic models in which non-Abelian VEVs are enforced by the requirement of D -flatness rather than by other possible phenomenological considerations.

Chapter 3

Open Descendants of Type I $T^6/(\mathbb{Z}_2 \times \mathbb{Z}_2^s)$ and $T^6/(\mathbb{Z}_2 \times \mathbb{Z}_2 \times \mathbb{Z}_2^s)$ models

In this and the next chapter, I will discuss phenomenological aspects of type I models in four spacetime dimensions whereby the internal coordinates are compactified on orbifolds [16]. Unlike toroidal compactification, orbifolds are the compactification of string coordinates on singular manifolds. The presence of orbifold identifications of these coordinates will lead to a much richer spectrum than compactification on an equivalent dimension torus.

The first chapter will involve a discussion of the open descendants and their spectral content with compactification on $T^6/(\mathbb{Z}_2 \times \mathbb{Z}_2^s)$ and $T^6/(\mathbb{Z}_2 \times \mathbb{Z}_2 \times \mathbb{Z}_2^s)$ orbifolds. The additional \mathbb{Z}_2^s group is a \mathbb{Z}_2 shift, which in both cases will be freely acting in that it will not generate any additional fixed points with respect to the orbifold fixed points.

In the $T^6/(\mathbb{Z}_2 \times \mathbb{Z}_2 \times \mathbb{Z}_2^s)$ case, the freely acting shift will allow for the inclusion of twisted sectors that appear in the $T^6/(\mathbb{Z}_2 \times \mathbb{Z}_2)$ case, this is illustrated in appendix B.

The construction of these models uses the Hamiltonian formulation, and details of the language used will now follow [25].

3.1 Type I Construction

The discussions that will follow on type I phenomenology involve amplitudes that have zero Euler character. The Euler character $\chi = 2 - 2h - b - c$ defines an invariant number of a surface with h handles, b boundaries and c cross caps. The parent amplitude is the torus ($h = 1, b = 0, c = 0$). The remaining surfaces are the Klein bottle ($h = 0, b = 0, c = 2$), annulus ($h = 0, b = 2, c = 0$) and Mobius strip ($h = 0, b = 1, c = 1$). The torus is formed by first taking the complex coordinates

$$z = \sigma_1 + \tau\sigma_2, \quad \bar{z} = \sigma_1 + \bar{\tau}\sigma_2 \tag{3.1.1}$$

for the complex parameter $\tau = \tau_1 + i\tau_2$, which defines the shape of the torus, and the two coordinates σ_1 and σ_2 . The relation

$$z \sim z + m + n\tau \tag{3.1.2}$$

periodically identifies the coordinates of each direction σ_1 and σ_2 so that the shape of the torus can be controlled by the parameter τ . However, counting over these surfaces involves summing over some equivalent tori. These equivalent surfaces are identified by the transformation

$$\tau \rightarrow \frac{a\tau + b}{c\tau + d} \quad (3.1.3)$$

which defines the modular group

$$\mathrm{SL}(2, \mathbb{Z})/\mathbb{Z}_2 = \mathrm{PSL}(2, \mathbb{Z}) \quad (3.1.4)$$

for integers a, b, c, d and $ad - bc = 1$. The modulating group \mathbb{Z}_2 ensures that tori which are equivalent under the transformation $\{a, b, c, d\} \rightarrow \{-a, -b, -c, -d\}$ are not doubly counted, since this would leave the transformation (3.1.3) unchanged.

The transformation (3.1.3) is generated by S and T operations which act on τ as

$$\begin{aligned} T : \tau &\rightarrow \tau + 1 \\ S : \tau &\rightarrow -\frac{1}{\tau}. \end{aligned} \quad (3.1.5)$$

The fundamental region of integration for the parameters τ_1 and τ_2 , which defines the shape of the torus sheet, is given by

$$\mathcal{F} = \left\{ -\frac{1}{2} < \tau_1 \leq \frac{1}{2}, |\tau| \geq 1 \right\}. \quad (3.1.6)$$

The amplitudes that are to be discussed are represented in terms of Jacobi theta functions and the Dedekind eta function. I will review their structure and transformation properties here.

The Dedekind eta function is defined as

$$\eta(\tau) = q^{\frac{1}{24}} \prod_{n=1}^{\infty} (1 - q^n) \quad (3.1.7)$$

for

$$q = e^{2\pi i\tau}. \quad (3.1.8)$$

It transforms under S and T as

$$\begin{aligned} \eta(\tau + 1) &= e^{i\frac{\pi}{12}} \eta(\tau), \\ \eta\left(-\frac{1}{\tau}\right) &= \sqrt{-i\tau} \eta(\tau) \end{aligned} \quad (3.1.9)$$

respectively, which shows the function

$$\frac{1}{\sqrt{\tau_2} |\eta(\tau)|^2} \quad (3.1.10)$$

has a modular invariant form.

The Jacobi theta functions are defined by the infinite product

$$\theta(z|\tau) \begin{bmatrix} \gamma \\ \vartheta \end{bmatrix} = e^{2i\pi\gamma(z+\vartheta)} q^{\frac{\gamma^2}{2}} \prod_{n=1}^{\infty} (1 - q^n)(1 + q^{n+\gamma-\frac{1}{2}} e^{2i\pi(z+\vartheta)})(1 + q^{n-\gamma-\frac{1}{2}} e^{-2i\pi(z+\vartheta)}). \quad (3.1.11)$$

which has an equivalent expression (which is more convenient to identify particular massive modes in the spectrum)

$$\theta \begin{bmatrix} \gamma \\ \vartheta \end{bmatrix} (z|\tau) = \sum_n q^{\frac{1}{2}(n+\gamma)^2} e^{2\pi i(n+\gamma)(z+\vartheta)} \quad (3.1.12)$$

The elements γ and φ describe the periodic boundary conditions $\gamma, \varphi = 0$ or anti periodic with $\gamma, \varphi = \frac{1}{2}$.

The periodicity values of 0 and $\frac{1}{2}$ define NS (Neveu–Schwarz) and R (Ramond) boundary conditions for the upper γ characteristic.

The four separate theta functions arising from all possible boundary conditions are defined as

$$\begin{aligned} \theta_1(z|\tau) &= \begin{bmatrix} \frac{1}{2} \\ \frac{1}{2} \end{bmatrix} (z|\tau), & \theta_2(z|\tau) &= \begin{bmatrix} \frac{1}{2} \\ 0 \end{bmatrix} (z|\tau), \\ \theta_3(z|\tau) &= \begin{bmatrix} 0 \\ 0 \end{bmatrix} (z|\tau), & \theta_4(z|\tau) &= \begin{bmatrix} 0 \\ \frac{1}{2} \end{bmatrix} (z|\tau). \end{aligned} \quad (3.1.13)$$

However, it can easily be seen by (3.1.11), that θ_1 vanishes identically for argument $z = 0$. The parameter $z \neq 0$ will play a crucial role in the type I models with magnetic deformations, in other cases that are studied it has a value $z = 0$.

The behavior of (3.1.11) under S and T transformations is shown by

$$\theta \begin{bmatrix} \gamma \\ \vartheta \end{bmatrix} \left(\frac{z}{\tau} \middle| -\frac{1}{\tau} \right) = (-i\tau)^{\frac{1}{2}} e^{2\pi i\gamma\varphi + i\pi \frac{z^2}{\tau}} \theta \begin{bmatrix} \vartheta \\ -\gamma \end{bmatrix} (z|\tau) \quad (3.1.14)$$

and

$$\theta \begin{bmatrix} \gamma \\ \vartheta \end{bmatrix} (z|\tau + 1) = e^{-\pi i\gamma(\gamma-1)} \theta \begin{bmatrix} \gamma \\ \vartheta + \gamma - \frac{1}{2} \end{bmatrix} (z|\tau) \quad (3.1.15)$$

respectively.

Now that the preliminary elements have been discussed, I turn to the construction techniques of type I model building.

The technology used to describe the open and closed sectors of the type I models [25] discussed in this chapter are based on the partition function in the Hamiltonian formulation. The form of the generator of translation, or Laurent zero mode, will depend on the 10-dimensional superstring action

$$S = -\frac{1}{4\pi\alpha'} \int d^2\zeta (\partial^\alpha X^\mu \partial_\alpha X^\nu \eta_{\mu\nu} + i\bar{\psi}^\mu \gamma^\alpha \partial_\alpha \psi_\mu). \quad (3.1.16)$$

The action contains two dimensional Majorana spinors and corresponding bosonic superpartners X^μ .

One obtains a description of closed string spectra in terms of four sectors, the first two of which are the left-right pairings of antiperiodic (NS) and periodic (R) fields NS - NS and R - R respectively. These account for fields that behave as spacetime bosons. The two remaining pairings are R - NS and NS - R , and these describe spacetime fermions.

In the case of the open spectrum, the fields are the left moving fields of the closed string. In this case, the R fields describe spacetime fermions and those of the bosons correspond to NS fields.

The zero Laurent mode has the form

$$L_o = \frac{1}{2} : \sum_l \alpha_{-l}^i \alpha_{l,i} : + \frac{1}{2} : \sum_w w \phi_{-w}^i \phi_{w,i} : + \Delta \quad (3.1.17)$$

Where the string spectrum is built by acting on the vacuum using the creation operators from X^μ as α_{-l}^μ and Ψ^μ as ϕ_{-w}^μ . The world sheet fermion modes (ϕ_w^μ) are summed over the index w which is integer for the R sector and half-odd integer for the NS .

The quantity Δ is a normal ordering constant, and acquires contributions of $-\frac{1}{48}$ from the NS sector and $\frac{1}{24}$ from the R of the fermionic coordinates. The bosonic coordinates provide $-\frac{1}{24}$. As such, the total in D spacetime dimensions is given by

$$\Delta = -\frac{1}{16}(D-2) \quad (3.1.18)$$

for the NS sector and 0 for the R sector.

The type I theory is the orientifold projection (or world sheet parity projection) of the type IIB open and closed theory under Ω . The action of Ω on the world sheet modes is defined as

$$\Omega : \alpha_n^\mu \leftrightarrow \tilde{\alpha}_n^\mu \quad (3.1.19)$$

for the left and right modes of the closed string and

$$\Omega : \alpha_n^\mu \rightarrow (-1)^n \alpha_n^\mu \quad (3.1.20)$$

for the open string.

With the insertion of the world sheet parity projection in the partition function as

$$\text{Tr} \frac{(1+\Omega)}{2} q^{L_o} \bar{q}^{\bar{L}_o}, \quad (3.1.21)$$

the closed sector comprises the torus amplitude and the Klein bottle. The torus being defined by the insertion of 1 and the Klein by Ω .

It will be seen that as a consequence of the orbifold operation, that the orientifold planes that exist in the Klein are $O9$ and $O5$ planes. Additionally, the action of Ω on the left and rights states is simply seen to reduce the counting of states according to

$$\sum_{L,R} \langle L, R | \Omega q^{L_o-1} \bar{q}^{\bar{L}_o-1} | L, R \rangle = \sum_R \langle R, R | (\bar{q}q)^{L_o-1} | R, R \rangle. \quad (3.1.22)$$

This identification will also have a non-trivial effect on the lattices that involve quantum numbers in the form of Kaluza Klein and winding states. Closed string momentum is

defined by

$$\begin{aligned} p_L &= \frac{m}{R} + \frac{nR}{\alpha'}, \\ p_R &= \frac{m}{R} - \frac{nR}{\alpha'}. \end{aligned} \tag{3.1.23}$$

So the left right identification of a state $|p_L, p_R\rangle$ necessarily confines the counting to either pure winding of Kaluza Klein towers.

The different topologies that result from the Ω projection define different forms for the Teichmüller parameter $\tau = \tau_1 + i\tau_2$.

The open sector has contributions from the annulus and Mobius amplitudes. The modulus for the Mobius amplitude is not purely imaginary, it transforms according to

$$P : \frac{1}{2} + \frac{i\tau_2}{2} \rightarrow \frac{1}{2} + \frac{i}{2\tau_2} \tag{3.1.24}$$

It is straight forward to see that this can be written in terms of the conventional S and T operators as

$$P = TST^2S. \tag{3.1.25}$$

The action of S and T are defined by their actions on the Teichmüller parameter in (3.1.5).

Under the P transform, the η function behaves as

$$P : \hat{\eta}\left(\frac{it}{2} + \frac{1}{2}\right) \rightarrow \hat{\eta}\left(\frac{i}{2t} + \frac{1}{2}\right) = \sqrt{t}\hat{\eta}\left(\frac{it}{2} + \frac{1}{2}\right). \tag{3.1.26}$$

The S transformation has an interesting effect on the Klein, annulus and Mobius amplitudes. In the direct channel of the annulus and Mobius amplitudes one has an interpretation of an open string coupling to endpoint boundaries. An S transformation allows a $\frac{\pi}{2}$ coordinate rotation that now defines world sheet time running from one boundary to the other (as can be seen by the tadpole diagrams illustrated in appendix C). This is understood as a closed string propagating in the bulk between the boundaries.

The consideration of diagrams under S transformation will be a convenient frame in which to extract tadpole cancellation conditions.

It is constructive to demonstrate the representations of (3.1.17) in terms of Jacobi theta functions, in the presence and absence of orbifold operations.

In addition to the untwisted bosonic contribution in the absence of an orbifold identification, which has the form

$$\text{Tr} q^{\sum n\alpha_n \cdot \alpha_{-n}} = \prod_{n=1}^{\infty} \frac{1}{1 - q^n} = \frac{q^{\frac{1}{24}}}{\eta} \tag{3.1.27}$$

the other possible states are combinations of twisted strings with or without orbifold insertions, and untwisted strings with the action of an orbifold.

The effect of twisting and the presence of orbifold operations in the trace of (3.1.27) will provide rich spectral content. Twisted states are associated with strings, in the

open sector, with ends terminating on different boundaries such as $D9$ and $D5$ branes. The modes of these strings appear with the mode shift $n \rightarrow n - \frac{1}{2}$.

The orbifold operation in the trace of the torus allows (by enforcing modular invariance) a much extended spectrum, this will be appreciated in models described later. An orbifold can be reached by subjecting smooth covering manifolds to discrete identifications. This action in general leaves points that are fixed on the original manifold. For example, an orbifold projection in a trace can be realized by the identification of a compact coordinate

$$X^\mu \sim -X^\mu \quad (3.1.28)$$

and so leaving only states that are even under this parity operation. This type of operation is a \mathbb{Z}_2 identification. This action results from the effect on the string modes as $\beta : \alpha_n^\mu \rightarrow -\alpha_n^\mu$, for $\beta \in \mathbb{Z}_2$.

So to exhaust the remaining bosonic states, one has

$$\begin{aligned} \text{Tr} \beta q^{\sum n \alpha_n \cdot \alpha_{-n}} &= \prod_{n=1}^{\infty} \frac{1}{1+q^n} = q^{\frac{1}{24}} \left(\frac{2\eta}{\theta_2} \right)^{\frac{1}{2}}, \\ \text{Tr} q^{\sum (n-\frac{1}{2}) \alpha_n \cdot \alpha_{-n}} &= \prod_{n=1}^{\infty} \frac{1}{1-q^{(n-\frac{1}{2})}} = q^{-\frac{1}{48}} \left(\frac{\eta}{\theta_4} \right)^{\frac{1}{2}}, \\ \text{Tr} \beta q^{\sum (n-\frac{1}{2}) \alpha_n \cdot \alpha_{-n}} &= \prod_{n=1}^{\infty} \frac{1}{1+q^{(n-\frac{1}{2})}} = q^{-\frac{1}{48}} \left(\frac{\eta}{\theta_3} \right)^{\frac{1}{2}}. \end{aligned} \quad (3.1.29)$$

The boundary conditions and their particular forms of the Jacobi theta function can be seen from equations (3.1.13) and (3.1.11) respectively.

The effect of the orbifold identification (3.1.28) on the torus coordinates (3.1.2), is to create the four fixed points

$$z_i = \{0, 1/2, \tau/2, (1+\tau)/2\} \quad (3.1.30)$$

which are the points left invariant under the \mathbb{Z}_2 action (in both directions of the torus)

$$z_i \sim -z_i. \quad (3.1.31)$$

In the case of the fermionic states, the Pauli exclusion principle requires only one fermion in each state, and so one has

$$\text{Tr} q^{\sum_w w \phi_w \cdot \phi_w} = \prod_w (1+q^w)^8 \quad (3.1.32)$$

which applies to both the NS and R sectors with the simple modification of $w \rightarrow w - \frac{1}{2}$ for the NS fields. Therefore, one has the full expression for R states as

$$\text{Tr} q^{L_0} = 16 \frac{\prod_{n=1}^{\infty} (1+q^n)^8}{\prod_{n=1}^{\infty} (1-q^n)^8} \quad (3.1.33)$$

where the factor of 16 takes into account the overall degeneracy of the R vacuum ($|\pm, \pm, \pm, \pm\rangle \sim 2^4$ states). In the NS case, the expression

$$\text{Tr} q^{L_0} = \frac{1}{q^{\frac{1}{2}}} \frac{\prod_{n=1}^{\infty} (1+q^{n-\frac{1}{2}})^8}{\prod_{n=1}^{\infty} (1-q^n)^8} \quad (3.1.34)$$

shows an additional factor of $q^{-\frac{1}{2}}$ which arises from equation (3.1.18).

The *GSO* projection

$$\text{Tr} \left(\frac{(1 - (-1)^F)}{2} q^{L_0} \right) = \frac{1}{2q^{\frac{1}{2}}} \frac{\prod_{n=1}^{\infty} (1 + q^{n-\frac{1}{2}})^8 - \prod_{n=1}^{\infty} (1 - q^{n-\frac{1}{2}})^8}{\prod_{n=1}^{\infty} (1 - q^n)^8} \quad (3.1.35)$$

is exactly the eight dimensional representation of the vector denoted by V_8 , as defined more generally below for $SO(2n)$ representations. This involves a restriction to odd numbers of modes by use of the fermion number operator F .

In the lightcone gauge, one has eight transverse directions which corresponds to an $SO(8)$ invariance. The $SO(2n)$ Lie group contains four conjugacy classes of representations which include the scalar, vector and two spinors. The representations of the *NS* fields that include the scalar and vector for $SO(2n)$ are given by the "constant" theta functions $z = 0$

$$O_{2n}(0|\tau) = \frac{\theta_3^n(0|\tau) + \theta_4^n(0|\tau)}{2\eta^n} \quad (3.1.36)$$

which is the scalar, and by reference to (3.1.35) shows it to correspond to a restriction to even numbers of modes. This expression thus contains the tachyon. Similarly

$$V_{2n}(0|\tau) = \frac{\theta_3^n(0|\tau) - \theta_4^n(0|\tau)}{2\eta^n} \quad (3.1.37)$$

begins with lowest contribution $q^{\frac{1}{2}}$ for all $n = 1, 2, \dots$

In the *R* case, one has two characters of opposite chirality. The characters

$$S_{2n}(0|\tau) = \frac{\theta_2^n(0|\tau) + i^{-n}\theta_1^n(0|\tau)}{2\eta^n} \quad (3.1.38)$$

and

$$C_{2n}(0|\tau) = \frac{\theta_3^n(0|\tau) - i^{-n}\theta_1^n(0|\tau)}{2\eta^n} \quad (3.1.39)$$

provide such a description. In both cases the low lying modes begin with the wights $q^{\frac{n}{8}}$. They are projections of the spectrum by

$$\frac{(1 + \Gamma_9(-1)^F)}{2}. \quad (3.1.40)$$

The characters used in the discussion of Mobius amplitudes involve real *hatted* characters. A given character χ_i is inherently complex, due to the additional $\frac{1}{2}$ piece in the measure ($il + \frac{1}{2}$ in the transverse channel). One can then define the real hatted character $\hat{\chi}_i$ which then differs from χ_i by a phase.

The string models which include the presence of antibranes, provide a subtle change to the spectrum for certain couplings. For strings coupling to $D5$ branes, the possible arrangements are $D5 - D5$, $\bar{D}5 - \bar{D}5$ and two copies of $\bar{D}5 - D5$. The former two have no effect on the projection, however, the latter will introduce a sign change in the GSO projection that will change the characters.

In the $T^6/(\mathbb{Z}_2 \times \mathbb{Z}_2 \times \mathbb{Z}_2^s)$ model, there will be a sign freedom in the parent amplitude, in the first case I consider, such a freedom will not exist. This sign freedom will realize the presence of antibranes.

All models in the following sections will be compactifications in four dimensions of the $SO(8)$ type I string to $SO(4)^2$ and $SO(2)^4$ which begins as the orientifold projection of the parent type IIB torus with fermion contributions

$$\mathcal{T} \sim |V_8 - S_8|^2, \quad (3.1.41)$$

This form gives rise to open descendants that allow an $SO(32)$ gauge group. The type IIA theory is described by the torus

$$\mathcal{T} \sim (V_8 - S_8)(\bar{V}_8 - \bar{C}_8) \quad (3.1.42)$$

which has the standard left–right handed relative chirality difference.

3.1.1 Discrete and Continuous Wilson Lines

Now that models compactified on both orbifold and toroidal topologies have been considered, it is lastly constructive to detail the effect of Wilson lines on the open spectrum and brane multiplets [1, 2, 3, 4]. The details that will enable the reader to understand the specifics of constructing amplitudes is left until I discuss particular examples in the following section. The purpose of the illustration below is simply to highlight some generic effects that result from the use of Wilson lines.

Introducing Wilson lines has a direct effect on branes that are transverse to a compact direction, in particular the lowest mass state of a string stretched between two branes is discussed in appendix E.

The distinct possibilities of the discrete operations that affect the compact coordinates are [9]:

$$\begin{aligned} A_1 : X_{L,R} &\rightarrow X_{L,R} + \frac{\pi R}{2}, \\ A_2 : X_{L,R} &\rightarrow X_{L,R} + \frac{1}{2} \left(\pi R \pm \frac{\pi \alpha'}{R} \right), \\ A_3 : X_{L,R} &\rightarrow X_{L,R} \pm \frac{\pi \alpha'}{2R}. \end{aligned} \quad (3.1.43)$$

for a circle of radius $2\pi R$. The shift which will be of interest in this work is the A_1 operator. This will affect the state $e^{ip \cdot X}$ as

$$A_1 : e^{ip_L X + ip_R \tilde{X}} \rightarrow (-1)^m e^{ip_L X + ip_R \tilde{X}} \quad (3.1.44)$$

As an example of the continuous case with the six dimensional orbifold compactification (T^4/\mathbb{Z}_2) [25], introducing Wilson lines in the last direction involves a transverse channel amplitude of the annulus as

$$\begin{aligned} \tilde{\mathcal{A}} = \frac{2^{-5}}{4} \left\{ (Q_o + Q_v) \left[N^2 v W_4 + \frac{1}{v} \sum_m (D + \frac{d}{2} e^{2i\pi\alpha m} + \frac{d}{2} e^{-2i\pi\alpha m})^2 P_3 P_m \right] \right. \\ \left. + 2N(D + d)(Q_o - Q_v) \left(\frac{2\eta}{\theta_2} \right)^2 + 4(Q_s + Q_c)(N_g^2 + D_g^2) \left(\frac{2\eta}{\theta_4} \right)^2 \right. \\ \left. - 2N_g D_g (Q_s - Q_c) \left(\frac{2\eta}{\theta_3} \right)^2 \right\}. \end{aligned} \quad (3.1.45)$$

The original T^4/\mathbb{Z}_2 amplitude is recovered by setting $\alpha = 0$.

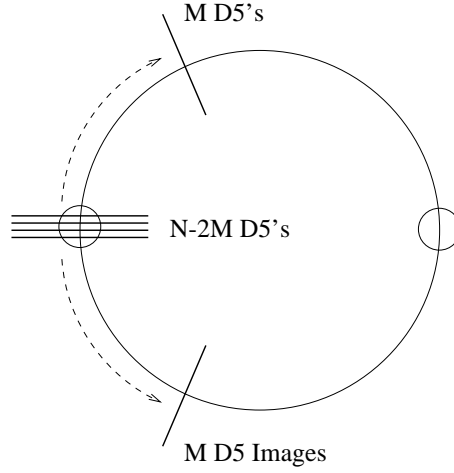


Figure 3.1: Moving a brane off of the fixed point

Here a stack of $D5$'s (denoted as d) and their images are moved a distance $2\pi\alpha R$ away from the fixed point they originally occupied to the second one. This is illustrated in figure 3.1.

In the direct channel, Poisson resummation

$$\sum_{n_i} e^{-\pi n^T A n + 2i\pi b n} = \frac{1}{\sqrt{\det(A)}} \sum_{m_i} e^{-\pi(m-b)^T A^{-1}(m-b)} \quad (3.1.46)$$

allows the lifting of states in mass, so that

$$\begin{aligned} \mathcal{A} = \frac{1}{4} \left\{ (Q_o + Q_v) \left[N^2 P_4 + (D^2 + \frac{d^2}{2}) W_4 + \frac{d^2}{4} W_3 (W_{n+2\alpha} + W_{n-2\alpha}) \right. \right. \\ \left. \left. + D d W_3 (W_{n+\alpha} + W_{n-\alpha}) \right] + (Q_o - Q_v) (N_g^2 + D_g^2) \left(\frac{2\eta}{\theta_2} \right)^2 \right. \\ \left. + 2N_g D_g (Q_s - Q_c) \left(\frac{\eta}{\theta_3} \right)^2 \right\}. \quad (3.1.47) \end{aligned}$$

Here it is seen that for $\alpha = \frac{1}{2}$, lattice states coupling to the Dd configuration have $n + \frac{1}{2}$ windings. In the general case that $\alpha \neq \frac{1}{2}$, one has a generic gauge group braking of $U(16)_9 \times U(16 - 2s) \times USp(2s)$, where $d = 2s$ which is required by consistency. For the interesting discrete case, (3.1.45) allows d $D5$ branes to move from one fixed point to the opposite one. This has the effect of projecting the spectrum by $\frac{1}{2}(1 + (-1)^m)$.

The use of shifts in the context of $\mathbb{Z}_2 \times \mathbb{Z}_2$ (shift) orbifolds have been exhaustively studied in [1]. These models are descriptions of a partition function that is projected by $\mathbb{Z}_2 \times \mathbb{Z}_2$ generators that incorporate the shift operators within the orbifold generators themselves. The shifts in these models act discretely. The projections in the trace are defined as

$$\sigma_1(\delta_1, \delta_2, \delta_3) = \begin{pmatrix} \delta_1 & -\delta_2 & -1 \\ -1 & \delta_2 & -\delta_3 \\ -\delta_1 & -1 & \delta_3 \end{pmatrix}, \quad \sigma_2(\delta_1, \delta_2, \delta_3) = \begin{pmatrix} \delta_1 & -1 & -1 \\ -1 & \delta_2 & -\delta_3 \\ -\delta_1 & -\delta_2 & \delta_3 \end{pmatrix}. \quad (3.1.48)$$

It is then clear that these models necessarily involve simultaneous actions of both shift

models	$D5_1$	$D5_2$	$D9$
p_3	$N = 2$	$N = 2$	$N = 1$
$w_2 p_3$	$N = 2$	$N = 4$	$N = 2$
$w_1 w_2 p_3$	$N = 4$	$N = 4$	$N = 4$
p_{23}	$N = 2$	—	$N = 1$
$w_1 p_2$	$N = 4$	—	$N = 2$
$w_1 p_2 p_3$	$N = 4$	—	$N = 2$
$w_1 p_2 w_3$	$N = 4$	—	$N = 4$
p_{123}	—	—	$N = 1$
$p_1 w_2 w_3$	—	—	$N = 2$
$w_1 w_2 w_3$	—	—	$N = 4$

Table 3.1: Model classes with corresponding brane supersymmetry

and orbifold operations. As such these are not freely acting orbifolds, but they can be interpreted as conventional $\mathbb{Z}_2 \times \mathbb{Z}_2$ orbifolds with unconventional Ω projections.

In these models, one can see that the modulating group generators given by equation (3.1.48) will involve terms of the form

$$\text{Tr}_{tw} \delta q^{L_0} \bar{q}^{\tilde{L}_0}. \quad (3.1.49)$$

This term is zero as the twisted trace involves a sum over fixed points of the states. As will be shown later by equation (3.2.7), δ has the effect of shifting the fixed point occupied by a state. As such, twisted states with shift insertions in the trace are zero.

In the freely acting shift case studied later, one can retain the twisted terms corresponding to independent orbits (appendix B) which give rise to two classes of sub models of the parent torus (each containing four sub models in the open sector). These terms are not present in the models generated by (3.1.48) for the reason given above.

The various supersymmetries present on the branes for these projections are displayed in table 3.1.1. From the table, the notations p_i and w_i are meant as a Kaluza Klein shift $(-1)^{m_i}$ and winding shift $(-1)^{n_i}$ in the direction of the i^{th} torus. Terms such as p_{ij} are shorthand for the product shift $(-1)^{m_i+m_j}$. In addition, — denotes the absence of the corresponding brane.

In these cases, the presence of $D5$ brane types is determined by the types of shift present. If a shift is present in a line in table 3.1.1, the corresponding $D5$ brane is absent for that direction. This is determined by the requirement of tadpole cancellation. The presence of shifts will lift those states in the Klein and Mobius that would normally contribute a condition that would allow the $D5$ to remain. Therefore, cancellation of the tadpole requires that the $D5$ (that would otherwise contribute massless modes) be absent.

In the cases I turn to now the presence of shifts, which in this case are freely acting, will not affect the numbers of $D5$'s in the model. However, the first model I consider has only one orbifold element and in this case, for the same reasons of tadpole cancellation, only one species of $D5$ exists. The second model has all possible types present.

3.2 Open Descendants of a $T^6(\mathbb{Z}_2 \times \mathbb{Z}_2^s)$ Model with $N = 2$ Supersymmetry

To illustrate the effects of the freely acting shifts of the type in equation (3.1.43) on the open descendants, I start with a simpler example of a \mathbb{Z}_2 orbifold, with orbifold operation denoted g and an additional freely acting shift h . The particular actions of g and h and their product on coordinates and lattices are given in equation (3.2.1)¹.

The $\mathbb{Z}_2 \times \mathbb{Z}_2^s$ generators comprise a freely acting orbifold and shift. In this case the effect of the $\mathbb{Z}_2 \times \mathbb{Z}_2^s$ is to break the $SO(8)$ group to $SO(4)^2$ by virtue of the \mathbb{Z}_2 orbifold operation. The shift of course has no effect in this breaking.

While the structure of the compact directions is $T^6 \rightarrow T_{45}^2 \times T_{67}^2 \times T_{89}^2$, with subscripts referring to the 2-tori directions, this model is (as far as the fermionic excitations are concerned) effectively a compactification on $(T^2 \times (T^4/\mathbb{Z}_2))/\mathbb{Z}_2^s$.

The original type IIB theory is projected using

$$\begin{aligned} g &= (\quad 1, \quad 1; \quad -1, \quad -1; \quad -1, \quad -1 \quad), \\ h &= (\quad A_1, \quad 1; \quad A_1, \quad 1; \quad 1, \quad 1 \quad), \\ f &= (\quad A_1, \quad 1; \quad -A_1, \quad -1; \quad -1, \quad -1 \quad). \end{aligned}$$

for A_1 defined in (3.1.43). The generators, (3.2.1) illustrates the shift action on only one of the coordinates of the relevant torus. The orbifolds act on all coordinates within a given torus to provide four fixed points in each that they act.

This is an interesting model that has a $\mathbb{Z}_2 \times \mathbb{Z}_2$ structure while preserving $N = 2$ supersymmetry in the open sector. The particular form of generators, that includes one as a pure shift operator, implies that the independent orbit diagrams (those not related by modular transformation, appendix B) do not contribute to the torus amplitude.

This takes away the consideration of a sub class of models associated with a sign freedom. These terms will appear in the generalized version of this model in section (3.3).

The way the modulating group generators are written with composite shift operators, has a twofold effect, firstly it will necessarily force the number of distinct $D5$ types to become only one (in this case, the $D5$ sitting in the first torus is the only one present).

The character set is derived from the breaking of the original $SO(8)$ characters O_8 , V_8 , C_8 and S_8 to supersymmetric representations involving O_4 , V_4 , C_4 and S_4 . Their representations in terms of theta functions can be found in section 3.1.

The supersymmetric world sheet fermion contributions are written as

$$\begin{aligned} Q_o &= V_4 O_4 - C_4 C_4 & Q_v &= O_4 V_4 - S_4 S_4 \\ Q_s &= O_4 C_4 - S_4 O_4 & Q_c &= V_4 S_4 - C_4 V_4. \end{aligned} \tag{3.2.1}$$

The function $\eta(\tau)$ is defined by equation (3.1.7), with the $SO(4)$ characters defined by equations (3.1.36), (3.1.37), (3.1.38) and (3.1.39).

¹This model was analyzed in collaboration with Carlo Angelantonj and Emilian Dudas.

In a given direction of a torus, one has a lattice of the form

$$\Lambda_{m+a,n+b} = \frac{q^{\frac{\alpha'}{4} \left(\frac{(m+a)}{R} + \frac{(n+b)R}{\alpha'} \right)^2} q^{\frac{\alpha'}{4} \left(\frac{(m+a)}{R} - \frac{(n+b)R}{\alpha'} \right)^2}}{\eta(q)\eta(\bar{q})}, \quad (3.2.2)$$

The form of which is demonstrated by equation (D.0.13). In the models presented in this study, this notation will include the lattice states of both directions. The labels a and b are in anticipation of the effects of momentum and winding shifts, which will of course only apply to the direction in which the relevant shift acts.

To obtain modular invariance under $PSL(2, \mathbb{Z})$, as required by the topology of the one loop string amplitude, one must perform S and T transforms on the torus states. The actions defined in (3.1.5) imply that the boundary operations of states transform as

$$\begin{aligned} S &: (a, b) \rightarrow (b, a^{-1}) \\ T &: (a, b) \rightarrow (a, ab). \end{aligned} \quad (3.2.3)$$

Here, a and b label the boundary operations that pertain to orbifold/twist's that are placed on world sheet fields. The full orbit configuration of these operators is described for the $\mathbb{Z}_2 \times \mathbb{Z}_2$ case in figure B.1.

Lattice (in $\tilde{\mathcal{A}}, \mathcal{K}$ and $\tilde{\mathcal{M}}$)	$S(\tilde{\mathcal{A}})$	$S(\mathcal{K})$ and $P(\tilde{\mathcal{M}})$
P_m	W_n	W_{2n}
P_{2m}	$W_n + W_{n+\frac{1}{2}}$	W_n
$(-1)^m P_m$	$W_{n+\frac{1}{2}}$	W_{2n+1}
$(-1)^m P_{2m}$	$W_{n+\frac{1}{2}} + W_n$	$W_{n+\frac{1}{2}}$
W_n	P_m	P_m
W_{2n}	$P_m + P_{m+\frac{1}{2}}$	P_{2m}
W_{2n+1}	$P_m - P_{m+\frac{1}{2}}$	$(-1)^m P_m$

Table 3.2: Lattice S and P transforms

Table 3.2 summarizes some useful S and P transforms for lattice states that will be encountered in determining the amplitude lattices in different channels. Here, \mathcal{A} , \mathcal{K} and \mathcal{M} are the annulus Klein and Mobius contributions. The tilde denotes the transverse amplitude. These results are obtained from equation (F.0.2) with the appropriate boundary condition ($m = 0$ or $n = 0$), modular parameter rescaling and equation (3.1.46) in combination with S transformation (3.1.5).

P and W are the restriction of $\Lambda_{m,n}$ to pure Kaluza-Klein (P) or winding (W) modes. The more compact notation of P_e and P_o will be used in the calculations (and similarly for the winding sums) which are the restriction of the counting to even or odd modes respectively.

T transforms on the lattices behave as

$$\begin{aligned} \Lambda_{m,n} &\rightarrow \Lambda_{m,n}, & \Lambda_{m,n+\frac{1}{2}} &\rightarrow (-1)^m \Lambda_{m,n+\frac{1}{2}}, \\ \Lambda_{m+\frac{1}{2},n} &\rightarrow (-1)^n \Lambda_{m+\frac{1}{2},n}, & \text{and } \Lambda_{m+\frac{1}{2},n+\frac{1}{2}} &\rightarrow i(-1)^{m+n} \Lambda_{m+\frac{1}{2},n+\frac{1}{2}}. \end{aligned} \quad (3.2.4)$$

These are easily seen by performing the T operation defined in (3.2.3) on the lattice of equation (3.2.2)

The torus resulting from the projections (3.2.1) is generated by enforcing modular invariance under (3.2.3) on

$$\mathcal{T} = \int \frac{d^2\tau}{\tau_2^2} \frac{1}{\tau_2^4} \text{Tr} \frac{(1+g)(1+h)}{2} \frac{(1+h)}{2} q^{L_o} \bar{q}^{\bar{L}_o}, \quad (3.2.5)$$

which of course will include the effect on lattice terms through equation (D.0.13). The modular invariant torus amplitude then simplifies to

$$\begin{aligned} \mathcal{T} = \frac{1}{4} & \left\{ [1 + (-1)^{m_1+m_2}] (\Lambda^1 \Lambda^2 + \Lambda_{m,n+\frac{1}{2}}^1 \Lambda_{m,n+\frac{1}{2}}^2) \Lambda^3 |Q_o + Q_v|^2 \right. \\ & + [1 + (-1)^{m_1}] \Lambda^1 |Q_o - Q_v|^2 \left| \frac{2\eta}{\theta_2} \right|^4 \\ & + 16 (\Lambda^1 + \Lambda_{m,n+\frac{1}{2}}^1) \left| \frac{\eta}{\theta_4} \right|^4 |Q_s + Q_c|^2 \\ & \left. + 16 (\Lambda^1 + (-1)^{m_1} \Lambda_{m,n+\frac{1}{2}}^1) \left| \frac{\eta}{\theta_3} \right|^4 |Q_s - Q_c|^2 \right\}. \end{aligned} \quad (3.2.6)$$

World-sheet supersymmetry requires the actions on bosons and fermions to be properly correlated, this is achieved by assigning positive eigenvalues to O_{2n} and C_{2n} and negative ones to V_{2n} and S_{2n} , under the action of an orbifold element.

With the A_1 shift operator, the number of fixed points can be seen to be halved. It acts on the fixed point coordinates, for example, as

$$(x_2, y_2; x_3, y_3) \rightarrow (x_2 + \frac{1}{2}, y_2; x_3 + \frac{1}{2}, y_3). \quad (3.2.7)$$

Where the labelling $(x_2, y_2; x_3, y_3)$ defines the collective fixed point coordinates for the space $T_{67}^2 \times T_{89}^2$, with the values $\{x_i, y_i | x_i \in \{0, \frac{1}{2}\}, y_i \in \{0, \frac{1}{2}\}\}$.

The total number of fixed points without the shift operation is $16 = 4 \times 4$, which are detailed in table (3.3).

$(0, 0; 0, 0)_1$	$(0, \frac{1}{2}; 0, 0)_2$	$(\frac{1}{2}, 0; 0, 0)_3$	$(\frac{1}{2}, \frac{1}{2}; 0, 0)_4$
$(0, 0; 0, \frac{1}{2})_5$	$(0, 0; \frac{1}{2}, 0)_6$	$(0, 0; \frac{1}{2}, \frac{1}{2})_7$	$(0, \frac{1}{2}; 0, \frac{1}{2})_8$
$(0, \frac{1}{2}; \frac{1}{2}, 0)_9$	$(0, \frac{1}{2}; \frac{1}{2}, \frac{1}{2})_{10}$	$(\frac{1}{2}, 0; 0, \frac{1}{2})_{11}$	$(\frac{1}{2}, 0; \frac{1}{2}, 0)_{12}$
$(\frac{1}{2}, 0; \frac{1}{2}, \frac{1}{2})_{13}$	$(\frac{1}{2}, \frac{1}{2}; 0, \frac{1}{2})_{14}$	$(\frac{1}{2}, \frac{1}{2}; \frac{1}{2}, 0)_{15}$	$(\frac{1}{2}, \frac{1}{2}; \frac{1}{2}, \frac{1}{2})_{16}$

Table 3.3: Unshifted fixed points

The origin of the lattice contributions of the torus amplitude is

$$\mathcal{T}_0 = |Q_o|^2 + |Q_v|^2 + 8|Q_s|^2 + 8|Q_c|^2 \quad (3.2.8)$$

and shows as expected 8 fixed points, reduced from 16. The independent coordinates of which are as in table 3.4.

$(0, 0; 0, 0)_1$	$(0, \frac{1}{2}; 0, 0)_2$	$(\frac{1}{2}, 0; 0, 0)_3$	$(\frac{1}{2}, \frac{1}{2}; 0, 0)_4$
$(0, 0; 0, \frac{1}{2})_5$	$(0, 0; \frac{1}{2}, \frac{1}{2})_7$	$(0, \frac{1}{2}; 0, \frac{1}{2})_8$	$(0, \frac{1}{2}; \frac{1}{2}, \frac{1}{2})_{10}$

Table 3.4: Remaining fixed points

Vertex operators of states flowing in \mathcal{K} and $\tilde{\mathcal{A}}$ will acquire from the torus, by virtue of the action of the shift in T_{45}^2 and T_{67}^2 , a state projector

$$V = [1 + (-1)^{m_1+m_2}]V_{T_2 \times (T^4/\mathbb{Z}_2)}. \quad (3.2.9)$$

For the Klein amplitude, Ω makes an effective identification of the left and right modes. As such, orbifold elements in the trace of (3.2.5) acting on the world sheet bosonic or fermionic oscillators are made ineffective by Ω . This is easily seen by a series expansion of such terms, since the left and right modes contribute $(-1)^{k+\tilde{k}}$, $k, \tilde{k} \in \mathbb{Z}$, the Ω identification then neglects the orbifold presence.

In a similar fashion, this projection also reduces the lattice modes to become either pure momentum or pure winding, this situation is inverted with the assistance of an inserted orbifold action α :

$$\begin{aligned} \Omega|p_L, p_R\rangle &= |p_R, p_L\rangle \Rightarrow n = 0, \\ \Omega\alpha|p_L, p_R\rangle &= | -p_R, -p_L\rangle \Rightarrow m = 0. \end{aligned} \quad (3.2.10)$$

Ω does not change the effect of twisting operations, since these are realized as a shift in the oscillator modes. The Klein amplitude thus takes the form,

$$\begin{aligned} \mathcal{K} = \frac{1}{8} \left\{ \right. & \left[(1 + (-1)^{m_1+m_2})P_1P_2P_3 \right. \\ & \left. + (1 + (-1)^{m_1})P_1W_2W_3 \right] (Q_o + Q_v) \\ & \left. + 32(Q_s + Q_c)P_1 \left(\frac{\eta}{\theta_4} \right)^2 \right\}. \end{aligned} \quad (3.2.11)$$

To derive the Klein amplitude in the transverse channel, one must perform an S transformation on the direct channel amplitude. The measure and lattice resummations give rise to the factors of 2^2 from the measure part and $\sqrt{2}$ from each internal direction. These results can be seen more clearly by equation (D.0.13). Moreover, table 3.2 shows the effect on lattice state counting after S transformation in the Klein, annulus and Mobius amplitudes.

The S transform of theta functions that are associated with modes that are acted on by orbifold or twist operations are shown by equation (3.1.14). For the $SO(2n)$ characters, the action of S is represented as a matrix of the form

$$S_{2n} = \frac{1}{2} \begin{pmatrix} 1 & 1 & 1 & 1 \\ 1 & 1 & -1 & -1 \\ 1 & -1 & i^{-n} & -i^{-n} \\ 1 & -1 & -i^{-n} & i^{-n} \end{pmatrix}, \quad (3.2.12)$$

and acts on the characters $(O_{2n}, V_{2n}, S_{2n}, C_{2n})^T$. This can be seen by deforming the individual theta functions of the $SO(2n)$ characters (3.1.36), (3.1.37), (3.1.38) and (3.1.39)

The direct Klein then has corresponding transverse amplitude

$$\begin{aligned} \tilde{\mathcal{K}} = \frac{2^5}{8} & \left\{ \left[(W_1^e W_2^e + W_1^o W_2^o) W_3^e v_1 v_2 v_3 + W_1 P_2^e P_3^e \frac{v_1}{v_2 v_3} \right] (Q_o + Q_v) \right. \\ & \left. + 2v_1 W_1^e (Q_o - Q_v) \left(\frac{2\eta}{\theta_2} \right)^2 \right\}. \end{aligned} \quad (3.2.13)$$

With the parity projection, the torus must be defined with an additional factor of $\frac{1}{2}$. It is seen that the torus has the massive $\Lambda_{n+\frac{1}{2}}^1 \Lambda_{n+\frac{1}{2}}^2 \Lambda^3$ lattice term in the untwisted sector that must symmetrize by itself. The presence of the operators Ω and g allow this to have the correct numerical factor to cancel the $\frac{1}{8}$ from the projections. For all unshifted winding and momentum quantum numbers set to zero, this state is simply

$$|n + \frac{1}{2}, n + \frac{1}{2}\rangle \quad (3.2.14)$$

for the remaining non-zero lattice states that are counted in the first two of the three tori. The spectrum must be invariant under the operators g , and Ω (δ acts trivially on these states), these have the actions

$$\begin{aligned} g : (m, n) & \rightarrow (-m, -n), \\ \Omega : (m, n) & \rightarrow (m, -n), \\ g\Omega : (m, n) & \rightarrow (-m, n). \end{aligned} \quad (3.2.15)$$

So their action on (3.2.14) is

$$\begin{aligned} 4|n + \frac{1}{2}, n + \frac{1}{2}\rangle = & |n + \frac{1}{2}, n + \frac{1}{2}\rangle_1 \oplus |n + \frac{1}{2}, -n - \frac{1}{2}\rangle_g \\ & \oplus | -n - \frac{1}{2}, -n - \frac{1}{2}\rangle_\Omega \oplus | -n - \frac{1}{2}, n + \frac{1}{2}\rangle_{g\Omega} \end{aligned} \quad (3.2.16)$$

which can be seen by reference to (3.2.2). The labels 1, g, \dots simply refer to the action that has been taken on a given state. The degeneracy factor then gives the correct counting.

Although the O -planes present are not indicated explicitly within amplitudes, their presence and dimension are understood from the toroidal volumes given by the v_i terms. $O9$ -plane's occupy the entire compact space and correspond to the term $v_1 v_2 v_3$. The $O5$ -plane only has a presence in the first of the three 2-tori, and has a volume term $\frac{v_1}{v_2 v_3}$.

In the transverse, or tube channel, the coefficients of the characters must arrange themselves as perfect squares at the origin of the lattices. These coefficients contain all the boundary terms that correspond to the $O9$ and $O5$ planes (in the case of the Klein bottle). Appendix C illustrates the diagrams associated with a closed string propagating between two boundaries, with world sheet time in the direction of propagation. The perfect square thus reflects the invariance of the amplitude under the interchange of the boundaries. The cross terms of the squares then give the mixing of different orientifold types. The same is true in the transverse annulus for brane couplings.

The transverse Klein amplitude shows the perfect square structure

$$\tilde{\mathcal{K}}_o = \frac{2^5}{8} v_1 \left\{ \left(\sqrt{v_2 v_3} + \frac{1}{\sqrt{v_2 v_3}} \right)^2 Q_o + \left(\sqrt{v_2 v_3} - \frac{1}{\sqrt{v_2 v_3}} \right)^2 Q_v \right\}. \quad (3.2.17)$$

The transverse annulus is directly derived from the states that flow in the torus. The annulus in this channel involves closed strings propagating between boundaries, or branes of the type $D9$, represented by the factor N , and $D5_1$ in this case, which is shown as D . As such, the structure of the states that flow in the annulus reflect the boundary conditions of the brane couplings. With the restriction to winding (Neumann boundary conditions) or Kaluza Klein (Dirichlet boundary conditions) for given boundaries, the transverse amplitude is

$$\begin{aligned} \tilde{\mathcal{A}} = & \frac{2^{-5}}{8} v_1 \left\{ \left[N^2 v_2 v_3 (W_1 W_2 + W_1^{n+\frac{1}{2}} W_2^{n+\frac{1}{2}}) W_3 \right. \right. \\ & + \left. \frac{4D^2}{v_2 v_3} W_1 P_2^e P_3 \right] (Q_o + Q_v) + 4NDW_1 (Q_o - Q_v) \left(\frac{2\eta}{\theta_2} \right)^2 \left. \right\} \\ & + \frac{2^{-3}}{8} v_1 \left\{ \left[R_N^2 (W_1 + W_1^{n+\frac{1}{2}}) + 2R_D^2 W_1 \right] (Q_s + Q_c) \left(\frac{2\eta}{\theta_4} \right)^2 \right. \\ & \left. - 4R_N R_D W_1 (Q_s - Q_c) \left(\frac{\eta}{\theta_3} \right)^2 \right\}. \end{aligned} \quad (3.2.18)$$

Some explanation of the numerical coefficients in the above amplitude is necessary. In the case of the untwisted terms, one must satisfy the perfect square structure for the $D5$ and $D9$ terms, as shown more clearly in (3.2.22).

The twisted terms are more subtle. Since such terms highlight the occupation of branes on the fixed points, their numerical coefficients must therefore reflect this. The breaking term R_N corresponds to the effect of the orbifold on the $D9$ -brane which fills all compact and non-compact dimensions. Since it is wrapped around all compact dimensions it therefore *sees* all the fixed points. The coefficient formula is

$$\sqrt{\frac{\text{total number of fixed points}}{\text{number of seen fixed points}}}. \quad (3.2.19)$$

R_N thus has the coefficient

$$\sqrt{\frac{16}{16}} \sqrt{v_1}. \quad (3.2.20)$$

With the volume v_1 being provided by the remaining compact directions that are not acted on by the orbifold element $(+, -, -)$. The $D5$ breaking term, R_D , involves a brane which wraps only the first tori, and is transverse to the remaining ones. Since the orbifold element $(+, -, -)$ provides sixteen fixed points in the second and third tori, this term therefore has a coefficient of 4, as it sits at the origin of the other tori, and hence sees only that fixed point.

Now, under the identification of the fixed points, one can categorize the types of brane that see certain fixed points. All brane types see the fixed point $(0, 0; 0, 0)$ (the fixed point at the origin of the tori T_{67}^2 and T_{89}^2). So one has the perfect square

$$(R_N \pm 4R_D)^2 v_1 \quad (3.2.21)$$

for the fixed point coordinates $(0, 0; 0, 0)$, where the sign depends on which character they couple to. For all other fixed points, R_D does not contribute to the counting since it only sees $(0, 0; 0, 0)$. So, the remaining seven fixed points are taken into account by R_N alone. There is an overall factor of 2 that reflects the degeneracy of the original sixteen fixed points (where half of the sixteen are identified), which is also required for proper particle interpretation in the direct channel.

These details provide the form for the lattice origin of the transverse annulus as

$$\begin{aligned} \tilde{A}_o = & \frac{2^{-5}}{8} v_1 \left\{ \left(N\sqrt{v_2 v_3} + \frac{2D}{\sqrt{v_2 v_3}} \right)^2 Q_o + \left(N\sqrt{v_2 v_3} - \frac{2D}{\sqrt{v_2 v_3}} \right)^2 Q_v \right. \\ & + 2 \left[(R_N - 4R_D)^2 + 7R_N^2 \right] Q_s \\ & \left. + 2 \left[(R_N + 4R_D)^2 + 7R_N^2 \right] Q_c \right\}. \end{aligned} \quad (3.2.22)$$

Since the transverse annulus describes closed strings coupling to boundaries, one can read off the boundary positions with reference to the dilaton wave function

$$\phi(y_1, y_2) = \sum_{m_1, m_2} \left(\cos\left(\frac{m_1 y_1}{R_1}\right) \cos\left(\frac{m_2 y_2}{R_2}\right) + \sin\left(\frac{m_1 y_1}{R_1}\right) \sin\left(\frac{m_2 y_2}{R_2}\right) \right) \phi^{(m_1, m_2)}.$$

The dilaton is encoded in Q_o , and thus equation (3.2.18) gives the positions of the branes. After the use of T -dualities (as indicated by the primes in a given direction) figure 3.2 shows the positions of the $D9$ (now a $D5$ brane) shown as the dashed line and the two stacks of rotated $D5$ branes sitting at the fixed points. By virtue of the shift, the f and h operations interchange the brane stacks while g leaves them unchanged.

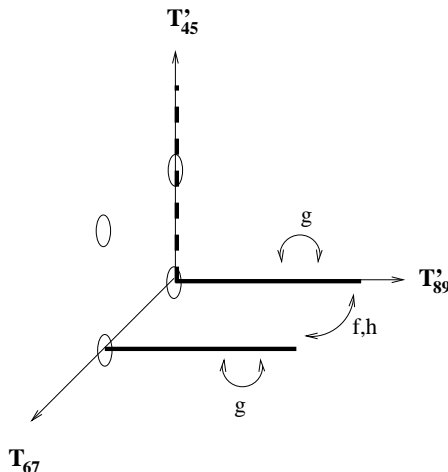


Figure 3.2: Branes on the fixed points

The lattice origin of the Mobius amplitude is the product of reflection coefficients from the transverse Klein and Annulus amplitudes, with appropriate factors as shown for the $O9-D9$ coupling in (3.2.24). This is done for all the common character sets in these two amplitudes, which includes only those that are untwisted, since the transverse

D -brane and O -plane couplings	Volumes
$D9 - D9, D9 - O9, O9 - O9$ $D5_1 - D5_1, D5_1 - O5_1, O5_1 - O5_1$ $D9 - O5_l, O9 - D5_l$	$v_1 v_2 v_3$ $\frac{v_1}{v_2 v_3}$ v_1
Couplings from \mathcal{A} and \mathcal{K}	Lattice States
$D9 - D9$ $O9 - O9$ $D5_1 - D5_1$ $O5_1 - O5_1$	$(W^1 W^2 + W_{n+\frac{1}{2}}^1 W_{n+\frac{1}{2}}^1) W^3$ $(W_e^1 W_e^2 + W_o^1 W_o^2) W_e^3$ $W_e^1 P_e^2 P_e^3$ $W_e^1 P_e^2 P_e^3$
$O - D$ Couplings in $\tilde{\mathcal{M}}$	Lattice States
$D9 - O9$ $D9 - O5_1$ $D5_1 - O9$ $D5_1 - O5_1$	$(W_e^1 W_e^2 + W_o^1 W_o^2) W_e^3$ W^1 W_e^1 $W_e^1 P_e^2 P_e^3 + (-1)^{m_2} W_o^1 P_e^2 P_e^3$

Table 3.5: Lattice restrictions

Klein amplitude has only untwisted states. The resulting Mobius origin expression is then dressed with the corresponding common lattice states of the transverse Klein and annulus terms, such that the direct annulus and Mobius symmetrize properly. These states are fully illustrated in table 3.5. From the expressions (3.2.17) and (3.2.22), the lattice origin expression for the transverse Mobius is

$$\begin{aligned} \tilde{\mathcal{M}}_o = & -\frac{1}{4} \left\{ \left(\sqrt{v_1 v_2 v_3} + \sqrt{\frac{v_1}{v_2 v_3}} \right) \left(N \sqrt{v_1 v_2 v_3} + 2D \sqrt{\frac{v_1}{v_2 v_3}} \right) \hat{Q}_o \right. \\ & \left. + \left(\sqrt{v_1 v_2 v_3} - \sqrt{\frac{v_1}{v_2 v_3}} \right) \left(N \sqrt{v_1 v_2 v_3} - 2D \sqrt{\frac{v_1}{v_2 v_3}} \right) \hat{Q}_v \right\}. \end{aligned} \quad (3.2.23)$$

There is an ambiguity in the form of a sign in the Mobius, it is chosen so as to allow a consistent tadpole cancellation. This ambiguity comes from the square root of various coupling terms, for example, the $D9-O9$ term is given by

$$\tilde{\mathcal{M}}_{D9-O9} = \pm 2 \times \sqrt{\frac{2^5}{8}} \times \sqrt{\frac{2^{-5} N^2}{8}}. \quad (3.2.24)$$

This reflects the closed string coupling to an O -plane and a D -brane, which includes a diagram factor of two for the orientation of the boundaries.

The coupling of the $D5$ -brane and the $O5$ -plane presents a subtlety. Since the shift h acts in one coordinate of the first two tori, the direct channel Klein $O5 - O5$ coupling has a projected momentum lattice as $(1 + (-1)^{m_1}) P^1$. This leads to the common lattice modes between the transverse annulus and Klein amplitudes to have all winding modes. This would naively lead to inconsistent symmetrization with the direct channel annulus, since the corresponding lattice in the annulus is P^k , and that of the direct Mobius would be $2P_e^k$. This can be rectified by splitting the winding mode lattice to $W_e + W_o$ and introducing a phase for the second momentum tower that exist with the odd winding modes, as shown for the $D5_1-O5_1$ coupling in table 3.5. This then allows the proper symmetrization between the direct annulus and Mobius for integer lattice modes.

With the remaining common states shown in table 3.5, the transverse Mobius results as

$$\begin{aligned} \tilde{\mathcal{M}} = & -\frac{v_1}{4} \left\{ \left[N v_2 v_3 (W_1^e W_2^e + W_1^o W_2^o) W_3^e \right. \right. \\ & \left. \left. + \frac{2D}{v_2 v_3} (W_1^e P_2^e + W_1^o (-1)^{m_2} P_2^e) P_3^e \right] (\hat{Q}_o + \hat{Q}_v) \right. \\ & \left. + (N W_1 + 2D W_1^e) (\hat{Q}_o - \hat{Q}_v) \left(\frac{2\hat{\eta}}{\hat{\theta}_2} \right)^2 \right\}. \end{aligned} \quad (3.2.25)$$

The direct channel amplitude for the annulus is

$$\begin{aligned} \mathcal{A} = & \frac{1}{8} \left\{ \left[N^2 (1 + (-1)^{m_1+m_2}) P_1 P_2 P_3 \right. \right. \\ & \left. \left. + 2D^2 P_1 (W_2 + W_2^{n+\frac{1}{2}}) W_3 \right] (Q_o + Q_v) \right. \\ & \left. + 4ND P_1 (Q_s + Q_c) \left(\frac{\eta}{\theta_4} \right)^2 + 2 \left[R_N^2 P_1^e + R_D^2 P_1 \right] (Q_o - Q_v) \left(\frac{2\eta}{\theta_2} \right)^2 \right. \\ & \left. + 4R_N R_D P_1 (Q_s - Q_c) \left(\frac{\eta}{\theta_3} \right)^2 \right\}. \end{aligned} \quad (3.2.26)$$

In deriving the direct channel Mobius it will be necessary to perform P transforms on the amplitude components. Formally, the P operator is a combination of the already understood S and T transforms as stated in equation (3.1.25). This acts on the measure parameter according to equation (3.1.24), where a change of variables $\tau_2 = \frac{1}{2l}$ allows the same dependency on il as the Klein and annulus transverse amplitudes (with the additional factor of $\frac{1}{2}$ in the Mobius).

The rescaling of the parameter τ_2 for the P transformation of the Mobius is identical to that used for the Klein for the S transformation. As such the P transformation on the Mobius lattice terms is the same as an S transformation on the Klein lattice states. The relevant lattice transformations are shown in table 3.2.

The P transformation acts on the $SO(2n)$ characters as

$$P_{2n} = \begin{pmatrix} c & s & 0 & 0 \\ s & -c & 0 & 0 \\ 0 & 0 & \chi c & i\chi s \\ 0 & 0 & i\chi s & \chi c \end{pmatrix} \quad (3.2.27)$$

for $s = \sin(n\pi/4)$, $c = \cos(n\pi/4)$ and $\chi = e^{-i\frac{n\pi}{4}}$.

The direct channel Mobius is then

$$\begin{aligned} \mathcal{M} = & -\frac{1}{8} \left\{ \left[N (1 + (-1)^{m_1+m_2}) P_1 P_2 P_3 \right. \right. \\ & \left. \left. + 2D (P_1 W_2 + (-1)^{m_1} P_1 W_2^{n+\frac{1}{2}}) W_3 \right] (\hat{Q}_o + \hat{Q}_v) \right. \\ & \left. - 2(N P_1^e + D P_1) (\hat{Q}_o - \hat{Q}_v) \left(\frac{2\hat{\eta}}{\hat{\theta}_2} \right)^2 \right\}. \end{aligned} \quad (3.2.28)$$

The massless modes in the amplitude $\tilde{\mathcal{K}} + \tilde{\mathcal{A}} + \tilde{\mathcal{M}}$, which correspond to $\mathcal{O}(q^0)$ terms, give rise to a divergence. Such terms correspond to tadpole diagrams, and consistency with the cancellation of these contributions forces a constraint on the gauge group. The construction so far then yields the following tadpole conditions

$$N = 32, \quad 2D = 32, \quad R_N = 0, \quad R_D = 0.$$

The Chan–Paton factors of the twisted sector (R_N and R_D) are identically zero as there are no complementary sectors in the Mobius or Klein to allow otherwise.

The required Chan-Paton parameterization is then

$$N = n + \bar{n}, \quad D = d + \bar{d}, \quad R_N = i(n - \bar{n}), \quad R_D = i(d - \bar{d}).$$

This Chan-Paton charge arrangement shows that the vector multiplet (contained in Q_o) is not present in the Mobius. However, the annulus does, and so the vector is oriented. As such the multiplicities have a unitary interpretation as shown above.

With these representations, one finds that the open sector has the gauge group (from the character Q_o)

$$U(16)_9 \times U(8)_5,$$

and shows the appropriate massless couplings in the open sector as

$$\begin{aligned} \mathcal{A}_o + M_o &= (n\bar{n} + d\bar{d})Q_o + \frac{1}{2}(n(n-1) + \bar{n}(\bar{n}-1) + d(d-1) + \bar{d}(\bar{d}-1))Q_v \\ &\quad + (n\bar{d} + \bar{n}d)Q_s + (nd + \bar{n}\bar{d})Q_c. \end{aligned} \quad (3.2.29)$$

This demonstrates the rank reduction of the group associated with the $D5$ brane. In the generic T^4/\mathbb{Z}_2 model, one has a gauge group of $U(16)_9 \times U(16)_5$.

It is now a simple matter to extract the interesting spectral content. The open descendants contain hypermultiplets in the representations $(120 \oplus \overline{120}, 1)$ and $(1, 28 \oplus \overline{28})$ from Q_v as

$$Q_v^h \sim O_2 O_2 (O_2 V_2 + V_2 O_2) - (S_2 S_2 + C_2 C_2) (S_2 S_2 + C_2 C_2)$$

and $(16, \overline{8})$ from Q_s as

$$Q_s^h \sim O_2 O_2 (C_2 S_2 + S_2 C_2) - (S_2 S_2 + C_2 C_2) O_2 O_2.$$

3.3 $T^6/(\mathbb{Z}_2 \times \mathbb{Z}_2 \times \mathbb{Z}_2^s)$ model

This model is in essence, a generalization of the previous one. The orbifold group is enhanced from \mathbb{Z}_2 to $\mathbb{Z}_2 \times \mathbb{Z}_2$. In addition, the momentum shift now extends to have an effect on modes in all three tori.

The projection that realizes the torus amplitude of this model has the form

$$\frac{1}{8}(1+g)(1+f)(1+\delta)$$

The $\mathbb{Z}_2 \times \mathbb{Z}_2 \times \mathbb{Z}_2^s$ elements are

$$\begin{aligned}
g &= (1, 1; -1, -1; -1, -1), \\
f &= (-1, -1; 1, 1; -1, -1), \\
h &= (-1, -1; -1, -1; 1, 1), \\
\delta &= (A_1, 1; A_1, 1; A_1, 1).
\end{aligned}$$

With an underlying $\mathbb{Z}_2 \times \mathbb{Z}_2$ group, there will be terms in the torus amplitude that are not connected by S and T transforms to the principle orbits $(o, o), (o, g), (o, f)$ and (o, h) , as better illustrated in appendix B. These terms will be realized in terms of modular orbits that are twisted sectors with different orbifold insertions, such as (f, g) . As such, an ambiguity will be present in the form of a sign freedom. This will give rise to models with $(\epsilon = -1)$ or without $(\epsilon = +1)$ discrete torsion, and necessitate the study of different classes of models within a choice of sign (as shown in [25] for the $\mathbb{Z}_2 \times \mathbb{Z}_2$ case without shifts).

The torus amplitude that results from the projection of the spectrum from (3.3.1) has $N = 2$ supersymmetry in both amplitudes (with or without discrete torsion). However, the supersymmetric multiplet structure in each is quite different.

The torus is

$$\begin{aligned}
\mathcal{T} &= \frac{1}{8} \left\{ |T_{oo}|^2 \left[\Lambda^1_{m,n} \Lambda^2_{m,n} \Lambda^3_{m,n} \right. \right. \\
&\quad \left. \left. + \Lambda^1_{m,n+\frac{1}{2}} \Lambda^2_{m,n+\frac{1}{2}} \Lambda^3_{m,n+\frac{1}{2}} \right] (1 + (-1)^{m_1+m_2+m_3}) \right. \\
&\quad \left. + |T_{ok}|^2 \Lambda^k_{m,n} (1 + (-1)^{m_k}) \left| \frac{2\eta^4}{\theta_2} \right|^4 \right. \\
&\quad \left. + 16 |T_{ko}|^2 (\Lambda^k_{m,n} + \Lambda^k_{m,n+\frac{1}{2}}) \left| \frac{\eta^4}{\theta_4} \right|^4 \right. \\
&\quad \left. + 16 |T_{kk}|^2 (\Lambda^k_{m,n} + (-1)^{m_k} \Lambda^k_{m,n+\frac{1}{2}}) \left| \frac{\eta^4}{\theta_3} \right|^4 \right. \\
&\quad \left. + \epsilon (|T_{gh}|^2 + |T_{gf}|^2 + |T_{fg}|^2 + |T_{fh}|^2 + |T_{hg}|^2 + |T_{hf}|^2) \left| \frac{8\eta^3}{\theta_2\theta_3\theta_4} \right|^2 \right\}. \quad (3.3.1)
\end{aligned}$$

The values k, m and l take the values $\{1, 2, 3\}$ for the bosonic lattice states, in correspondence with the generators $g \sim 1, f \sim 2$ and $h \sim 3$. The fermionic terms such as T_{kl} keep the labelling $l \in \{g, f, h\}$.

The origin of the lattice contributions has the form,

$$\begin{aligned}
\mathcal{T}_o &= (|\tau_{oo}|^2 + |\tau_{og}|^2 + |\tau_{of}|^2 + |\tau_{oh}|^2) \\
&\quad + 4(\epsilon + 1)(|\tau_{go}|^2 + |\tau_{gg}|^2 + |\tau_{gf}|^2 + |\tau_{gh}|^2) \\
&\quad + 4(1 - \epsilon)(\tau_{go}\bar{\tau}_{gg} + \tau_{gg}\bar{\tau}_{go} + \tau_{gf}\bar{\tau}_{gh} + \tau_{gh}\bar{\tau}_{gf}) \\
&\quad + 4(\epsilon + 1)(|\tau_{fo}|^2 + |\tau_{fg}|^2 + |\tau_{ff}|^2 + |\tau_{fh}|^2) \\
&\quad + 4(1 - \epsilon)(\tau_{fo}\bar{\tau}_{ff} + \tau_{fg}\bar{\tau}_{fh} + \tau_{ff}\bar{\tau}_{fo} + \tau_{fh}\bar{\tau}_{fg}) \\
&\quad + 4(\epsilon + 1)(|\tau_{ho}|^2 + |\tau_{hg}|^2 + |\tau_{hf}|^2 + |\tau_{hh}|^2) \\
&\quad + 4(1 - \epsilon)(\tau_{ho}\bar{\tau}_{hh} + \tau_{hg}\bar{\tau}_{hf} + \tau_{hf}\bar{\tau}_{hg} + \tau_{hh}\bar{\tau}_{ho}). \quad (3.3.2)
\end{aligned}$$

For either $\epsilon = \pm 1$, as in the last example, the presence of the shift reduces the independent fixed points from sixteen to eight. The original $\mathbb{Z}_2 \times \mathbb{Z}_2$ model has 52 hypermultiplets with 3 vector multiplets for $\epsilon = -1$ and 51 vector multiplets with 4 hypermultiplets for $\epsilon = +1$. The untwisted sector contains the supergravity multiplet, four hypermultiplets and 3 vector multiplets. Each of the three twisted sectors contains the remaining 48 hypermultiplets for $\epsilon = +1$ and 48 vector multiplets for $\epsilon = -1$. The Hodge numbers for these models are (51, 3) and (3, 51).

In this model, one has eight fixed points with the action of the freely acting shift. As such, equation (3.3.2) shows a model with the same multiplet structure in the untwisted sector but a reduction to 24 hypermultiplets for $\epsilon = +1$, and 24 vector multiplets for $\epsilon = -1$. As such, the models provide the Hodge numbers (27, 3) and (3, 27).

Again, a massive term $\Lambda_{n+\frac{1}{2}}^1 \Lambda_{n+\frac{1}{2}}^2 \Lambda_{n+\frac{1}{2}}^3$ appears that must symmetrize by itself. In precisely the same manor as the argument given for (3.2.16), one has states that correspond to the action of the operators 1, g , f , fg , Ω , $g\Omega$, $f\Omega$ and $fg\Omega$. These eight operators in addition to the factor of 2 from the shift projection cancels precisely the $\frac{1}{16}$ (which includes the factor of $\frac{1}{2}$ from the orientifold projection).

The torus amplitude (3.3.1) clearly shows the two separately connected parts, with the sign freedom ϵ associated with those orbits not related to the principle ones. Discrete torsion is obtained by taking $\epsilon = -1$. As shown, the resulting spectral content for cases with and without torsion are quite different.

This will also be the case for the open sector. In addition, there will be the possibility of SUSY breaking by the possible presence of anti-branes, which will be discussed in section (3.3.1).

With an underlying $\mathbb{Z}_2 \times \mathbb{Z}_2$ orbifold group, the $SO(8)$ characters break to $SO(2)^4$ characters that are defined by the following supersymmetric contributions:

$$\begin{aligned}
\tau_{oo} &= V_2 O_2 O_2 O_2 + O_2 V_2 V_2 V_2 - S_2 S_2 S_2 S_2 - C_2 C_2 C_2 C_2 \\
\tau_{og} &= O_2 V_2 O_2 O_2 + V_2 O_2 V_2 V_2 - C_2 C_2 S_2 S_2 - S_2 S_2 C_2 C_2 \\
\tau_{oh} &= O_2 O_2 O_2 V_2 + V_2 V_2 V_2 O_2 - C_2 S_2 S_2 C_2 - S_2 C_2 C_2 S_2 \\
\tau_{of} &= O_2 O_2 V_2 O_2 + V_2 V_2 O_2 V_2 - C_2 S_2 C_2 S_2 - S_2 C_2 S_2 C_2 \\
\\
\tau_{go} &= V_2 O_2 S_2 C_2 + O_2 V_2 C_2 S_2 - S_2 S_2 V_2 O_2 - C_2 C_2 O_2 V_2 \\
\tau_{gg} &= O_2 V_2 S_2 C_2 + V_2 O_2 C_2 S_2 - S_2 S_2 O_2 V_2 - C_2 C_2 V_2 O_2 \\
\tau_{gh} &= O_2 O_2 S_2 S_2 + V_2 V_2 C_2 C_2 - C_2 S_2 V_2 V_2 - S_2 C_2 O_2 O_2 \\
\tau_{gf} &= O_2 O_2 C_2 C_2 + V_2 V_2 S_2 S_2 - S_2 C_2 V_2 V_2 - C_2 S_2 O_2 O_2 \\
\\
\tau_{ho} &= V_2 S_2 C_2 O_2 + O_2 C_2 S_2 V_2 - C_2 O_2 V_2 C_2 - S_2 V_2 O_2 S_2 \\
\tau_{hg} &= O_2 C_2 C_2 O_2 + V_2 S_2 S_2 V_2 - C_2 O_2 O_2 S_2 - S_2 V_2 V_2 C_2 \\
\tau_{hh} &= O_2 S_2 C_2 V_2 + V_2 C_2 S_2 O_2 - S_2 O_2 V_2 S_2 - C_2 V_2 O_2 C_2 \\
\tau_{hf} &= O_2 S_2 S_2 O_2 + V_2 C_2 C_2 V_2 - C_2 V_2 V_2 S_2 - S_2 O_2 O_2 C_2
\end{aligned}$$

$$\begin{aligned}
\tau_{fo} &= V_2 S_2 O_2 C_2 + O_2 C_2 V_2 S_2 - S_2 V_2 S_2 O_2 - C_2 O_2 C_2 V_2 \\
\tau_{fg} &= O_2 C_2 O_2 C_2 + V_2 S_2 V_2 S_2 - C_2 O_2 S_2 O_2 - S_2 V_2 C_2 V_2 \\
\tau_{fh} &= O_2 S_2 O_2 S_2 + V_2 C_2 V_2 C_2 - C_2 V_2 S_2 V_2 - S_2 O_2 C_2 O_2 \\
\tau_{ff} &= O_2 S_2 V_2 C_2 + V_2 C_2 O_2 S_2 - C_2 V_2 C_2 O_2 - S_2 O_2 S_2 V_2.
\end{aligned} \tag{3.3.3}$$

Where one combines these into the character sums as

$$\begin{aligned}
T_{\gamma o} &= \tau_{\gamma o} + \tau_{\gamma g} + \tau_{\gamma h} + \tau_{\gamma f} & T_{\gamma g} &= \tau_{\gamma o} + \tau_{\gamma g} - \tau_{\gamma h} - \tau_{\gamma f} \\
T_{\gamma h} &= \tau_{\gamma o} - \tau_{\gamma g} + \tau_{\gamma h} - \tau_{\gamma f} & T_{\gamma f} &= \tau_{\gamma o} - \tau_{\gamma g} - \tau_{\gamma h} + \tau_{\gamma f}.
\end{aligned} \tag{3.3.4}$$

Which for the sake of clarification, $\gamma \in \{0, 1, 2, 3\}$ where $o \sim 0$ (the $\mathbb{Z}_2 \times \mathbb{Z}_2$ identity), with the normal relations for g , f and h in terms of the $\mathbb{Z}_2 \times \mathbb{Z}_2$ generators.

In the discussions that follow, where ever a sum occurs in character set such as T_{kl} , it is taken that the condition $k \neq l$ applies. For T_{kl} , the index k is the action of the corresponding k orbifold element, while l is a twist.

The case considered in the previous section was the projection of the partition function by $\mathbb{Z}_2 \times \mathbb{Z}_2^s$. Consequently, the counting of fixed points (multiplicity factor) for the twisted sector in the torus, in particular the $\Lambda_{m, n+\frac{1}{2}}$ massive states, is preserved as eight after the orientifold projection. This was realized by the factor of $\frac{1}{8}$ from the projection which includes $\frac{1}{2}$ from the orientifold projection. In the $\mathbb{Z}_2 \times \mathbb{Z}_2 \times \mathbb{Z}_2^s$ model, the freely acting shift acts as an additional modulating group outside the $\mathbb{Z}_2 \times \mathbb{Z}_2$ projection. This requires an extra factor of one half in the trace. As such, the $n + \frac{1}{2}$ massive states in the twisted sector of the torus have half the degeneracy they require for consistent interpretation as states that exist at the eight fixed points. Therefore, the Klein must also add an equal number of $n + \frac{1}{2}$ states to compensate the half from the orientifold projection

$$\frac{1}{2} (8_{\mathcal{T}} \Lambda_{m, n+\frac{1}{2}} + 8_{\mathcal{K}} W_{n+\frac{1}{2}}), \tag{3.3.5}$$

with eight from the torus $8_{\mathcal{T}}$, and eight from the Klein $8_{\mathcal{K}}$. However, the naive insertion of such a $W_{n+\frac{1}{2}}$ term leads to inconsistent factorization in the transverse Klein amplitude. This inconsistency arises due to the S transformation mapping $W_{n+\frac{1}{2}}$ states to $(-1)^m P$. In this case, the $O5_l - O5_k$ couplings would have a factor of two. A similar phenomenon arises in a six dimensional example in [25]. Here the authors consider T^4/\mathbb{Z}_2 with an unconventional orientifold projection $\xi\Omega$, for the phase $\xi^2 = 1$. This model defines a direct Klein amplitude

$$\begin{aligned}
\mathcal{K} &= \frac{1}{4} \left[(Q_o + Q_v) \left(\sum_m (-1)^m \frac{q^{(\frac{\alpha'}{2})m^T g^{-1}m}}{\eta^4} + \sum_n (-1)^n \frac{q^{(\frac{1}{2\alpha'})n^T g n}}{\eta^4} \right) \right. \\
&\quad \left. + 2 \times (n_+ + n_-) (Q_s + Q_c) \left(\frac{\eta}{\theta_4} \right)^4 \right].
\end{aligned} \tag{3.3.6}$$

As such, in the transverse channel amplitude, the twisted sector cannot be derived by factorization from the untwisted states that are now entirely massive, by virtue of a redefinition of the orientifold projection. This then requires equal but opposite

eigenvalue assignments to the twisted states that effectively render the counting zero with $n_+ = 8$ and $n_- = -8$.

The Klein amplitude for the $T^6/\mathbb{Z}_2 \times \mathbb{Z}_2 \times \mathbb{Z}_2^s$ model is then given by

$$\begin{aligned} \mathcal{K} = & \frac{1}{16} \left\{ \left(P^1 P^2 P^3 (1 + (-1)^{m_1+m_2+m_3}) + (1 + (-1)^{m_1}) P^1 W^2 W^3 \right. \right. \\ & \left. \left. + (1 + (-1)^{m_2}) W^1 P^2 W^3 + (1 + (-1)^{m_3}) W^1 W^2 P^3 \right) T_{oo} \right. \\ & \left. + 2 \times 16 \epsilon_k (P^k + \epsilon W^k) \left(\frac{\eta}{\theta_4} \right)^2 T_{ko} + 2 \times (8 - 8) W_{n+\frac{1}{2}}^k \left(\frac{\eta}{\theta_4} \right)^2 T_{ko} \right\} \end{aligned} \quad (3.3.7)$$

where the parameter ϵ satisfies

$$\epsilon = \epsilon_1 \epsilon_2 \epsilon_3. \quad (3.3.8)$$

The arrangements of ϵ_j in equation (3.3.7) are such that at the origin of the lattices, the left-right symmetric states in the torus (3.3.2) can be seen to vanish for $\epsilon = -1$ (which is provided for by the term $P^k + \epsilon W^k$). Moreover, the signs ϵ_j should arrange into the perfect square structure (3.3.11).

The transverse Klein amplitude is then

$$\begin{aligned} \tilde{\mathcal{K}} = & \frac{2^5}{16} \left\{ \left(v_1 v_2 v_3 (W_e^1 W_e^2 W_e^3 + W_o^1 W_o^2 W_o^3) + \frac{v_k}{2v_l v_m} W^k P_e^l P_e^m \right) T_{oo} \right. \\ & \left. + 2 \epsilon_k \left[v_k W_e^k + \epsilon \frac{P_e^k}{v_k} \right] \left(\frac{2\eta}{\theta_2} \right)^2 T_{ok} \right\}. \end{aligned} \quad (3.3.9)$$

The usual symmetrized summation convention is used for k, l and m .

The transverse Klein amplitude at the origin is

$$\tilde{\mathcal{K}}_o = \frac{2^5}{16} \left\{ \left(v_1 v_2 v_3 + \frac{v_k}{2v_l v_m} \right) T_{oo} + 2 \epsilon_k \left(v_k + \epsilon \frac{1}{v_k} \right) T_{ok} \right\} \quad (3.3.10)$$

which has an expanded form

$$\begin{aligned} \tilde{\mathcal{K}}_o = & \frac{2^5}{16} \left\{ \left(\sqrt{v_1 v_2 v_3} + \epsilon_1 \sqrt{\frac{v_1}{v_2 v_3}} + \epsilon_2 \sqrt{\frac{v_2}{v_1 v_3}} + \epsilon_3 \sqrt{\frac{v_3}{v_1 v_2}} \right)^2 \tau_{oo} \right. \\ & + \left(\sqrt{v_1 v_2 v_3} + \epsilon_1 \sqrt{\frac{v_1}{v_2 v_3}} - \epsilon_2 \sqrt{\frac{v_2}{v_1 v_3}} - \epsilon_3 \sqrt{\frac{v_3}{v_1 v_2}} \right)^2 \tau_{og} \\ & + \left(\sqrt{v_1 v_2 v_3} - \epsilon_1 \sqrt{\frac{v_1}{v_2 v_3}} + \epsilon_2 \sqrt{\frac{v_2}{v_1 v_3}} - \epsilon_3 \sqrt{\frac{v_3}{v_1 v_2}} \right)^2 \tau_{of} \\ & \left. + \left(\sqrt{v_1 v_2 v_3} - \epsilon_1 \sqrt{\frac{v_1}{v_2 v_3}} - \epsilon_2 \sqrt{\frac{v_2}{v_1 v_3}} + \epsilon_3 \sqrt{\frac{v_3}{v_1 v_2}} \right)^2 \tau_{oh} \right\}. \end{aligned} \quad (3.3.11)$$

In the above expression, it is seen that the charges for the orientifold planes can be changed in accordance to particular model classes of the parameter (3.3.8).

3.3.1 Open Decedents

By incorporating the signs ϵ_j into the annulus, one can introduce brane supersymmetry breaking. As such, it is convenient to use the compact notation

$$\tilde{T}_{nm}^{(\epsilon_i)} = T_{nm}^{NS} - \epsilon_i T_{nm}^R. \quad (3.3.12)$$

Strings that couple to brane–antibrane pairs provide character sets that now differ from the usual supersymmetric ones (3.3.3). Under S transformation, characters of the form $\tilde{T}_{nm}^{(-1)}$ go to $T_{nm}^{(-1)}$ which are the same as in (3.3.3) except for the changes of $O_2 \leftrightarrow V_2$ and $S_2 \leftrightarrow C_2$ in the last three factors. These sets are shown in equation (3.3.13). The characters that correspond to $\tilde{T}_{nm}^{(+1)}$ are simply denoted T_{nm} .

$$\begin{aligned}
\tau_{oo}^{(-1)} &= O_2 O_2 O_2 O_2 + V_2 V_2 V_2 V_2 - C_2 S_2 S_2 S_2 - S_2 C_2 C_2 C_2 \\
\tau_{og}^{(-1)} &= V_2 V_2 O_2 O_2 + O_2 O_2 V_2 V_2 - S_2 C_2 S_2 S_2 - C_2 S_2 C_2 C_2 \\
\tau_{oh}^{(-1)} &= V_2 O_2 O_2 V_2 + O_2 V_2 V_2 O_2 - S_2 S_2 S_2 C_2 - C_2 C_2 C_2 S_2 \\
\tau_{of}^{(-1)} &= V_2 O_2 V_2 O_2 + O_2 V_2 O_2 V_2 - S_2 S_2 C_2 S_2 - C_2 C_2 S_2 C_2 \\
\\
\tau_{go}^{(-1)} &= O_2 O_2 S_2 C_2 + V_2 V_2 C_2 S_2 - C_2 S_2 V_2 O_2 - S_2 C_2 O_2 V_2 \\
\tau_{gg}^{(-1)} &= V_2 V_2 S_2 C_2 + O_2 O_2 C_2 S_2 - C_2 S_2 O_2 V_2 - S_2 C_2 V_2 O_2 \\
\tau_{gh}^{(-1)} &= V_2 O_2 S_2 S_2 + O_2 V_2 C_2 C_2 - S_2 S_2 V_2 V_2 - C_2 C_2 O_2 O_2 \\
\tau_{gf}^{(-1)} &= V_2 O_2 C_2 C_2 + O_2 V_2 S_2 S_2 - C_2 C_2 V_2 V_2 - S_2 S_2 O_2 O_2 \\
\\
\tau_{ho}^{(-1)} &= O_2 S_2 C_2 O_2 + V_2 C_2 S_2 V_2 - S_2 O_2 V_2 C_2 - C_2 V_2 O_2 S_2 \\
\tau_{hg}^{(-1)} &= V_2 C_2 C_2 O_2 + O_2 S_2 S_2 V_2 - S_2 O_2 O_2 S_2 - C_2 V_2 V_2 C_2 \\
\tau_{hh}^{(-1)} &= V_2 S_2 C_2 V_2 + O_2 C_2 S_2 O_2 - C_2 O_2 V_2 S_2 - S_2 V_2 O_2 C_2 \\
\tau_{hf}^{(-1)} &= V_2 S_2 S_2 O_2 + O_2 C_2 C_2 V_2 - S_2 V_2 V_2 S_2 - C_2 O_2 O_2 C_2 \\
\\
\tau_{fo}^{(-1)} &= O_2 S_2 O_2 C_2 + V_2 C_2 V_2 S_2 - C_2 V_2 S_2 O_2 - S_2 O_2 C_2 V_2 \\
\tau_{fg}^{(-1)} &= V_2 C_2 O_2 C_2 + O_2 S_2 V_2 S_2 - S_2 O_2 S_2 O_2 - C_2 V_2 C_2 V_2 \\
\tau_{fh}^{(-1)} &= V_2 S_2 O_2 S_2 + O_2 C_2 V_2 C_2 - S_2 V_2 S_2 V_2 - C_2 O_2 C_2 O_2 \\
\tau_{ff}^{(-1)} &= V_2 S_2 V_2 C_2 + O_2 C_2 O_2 S_2 - S_2 V_2 C_2 O_2 - C_2 O_2 S_2 V_2.
\end{aligned} \quad (3.3.13)$$

Moreover, as will be seen, this arrangement defines a perfect square structure for the annulus R – R sector that agrees with that of the Klein amplitude, and will thus facilitate consistent R – R tadpole cancellation, as is required.

The differences in the closed amplitudes associated with the sign freedom $\epsilon = \pm 1$ have been demonstrated. The different choices lead to quite distinct open amplitudes with very different phenomenological characteristics.

In the transverse channel, the annulus is interpreted as closed string states propagating between D –branes, that in this case are either $D9$ or $D5_k$ branes. As was

done in the construction of the annulus of the previous case ($\mathbb{Z}_2 \times \mathbb{Z}_2^s$), one obtains the transverse annulus from the torus partition function. The previous case consisted of characters of $SO(8) \rightarrow SO(4)^2$ which from equations (3.1.38) and (3.1.39) can be seen to be real. With the breaking $SO(8) \rightarrow SO(2)^4$ the corresponding characters S_2 and C_2 are complex. The transverse annulus states are of the form

$$\langle \mathcal{T}(S) | q^{L_0} | S \rangle \quad (3.3.14)$$

(where \mathcal{T} is a time reversal operator). The operator \mathcal{T} maps complex values to their conjugates, thus interchanging S_2 and C_2 .

It is obvious from (3.3.2) and (3.3.3) that for $\epsilon = -1$, such terms which are of the form (3.3.14) exist for both the untwisted and twisted sectors of the torus. For the choice $\epsilon = +1$, it is seen that one can only retain such characters in the untwisted sector. Consequently, the open descendants of the two models $\epsilon = \pm 1$ have very different structures.

3.3.2 Models Without Discrete Torsion ($\epsilon = +1$)

The subclass of models is generated by $\epsilon = (+, +, +)$, where $\epsilon_k = +1$, and $(+, -, -)$ with two additional permutations $(-, +, -)$ and $(-, -, +)$. As has been shown in (3.3.12), the presence of any $\epsilon_k = -1$ breaks supersymmetry.

The transverse annulus amplitude is defined by

$$\begin{aligned} \tilde{\mathcal{A}} = & \frac{2^{-5}}{16} \left\{ \left(N^2 v_1 v_2 v_3 (W^1 W^2 W^3 + W_{n+\frac{1}{2}}^1 W_{n+\frac{1}{2}}^2 W_{n+\frac{1}{2}}^3) \right. \right. \\ & \left. \left. + D_{ko}^2 \frac{v_k}{2v_l v_s} W^k P^l P^s \frac{(1 + (-1)^{m_l + m_s})}{2} \right) T_{oo} \right. \\ & \left. + 2D_{ko} N v_k W^k \left(\frac{2\eta}{\theta_2} \right)^2 \tilde{T}_{ok}^{(\epsilon_k)} \right. \\ & \left. + D_{ko} D_{lo} \frac{1}{v_s} \frac{P^s (1 + (-1)^s)}{2} \left(\frac{2\eta}{\theta_2} \right)^2 \tilde{T}_{os}^{(\epsilon_k \epsilon_l)} \right\} \quad (3.3.15) \end{aligned}$$

where the construction follows from that done in the $\mathbb{Z}_2 \times \mathbb{Z}_2^s$ orientifold case, with the addition of strings stretched between the sets of $D5_k - D5_l$ branes. The brane configuration is of course similar to that of figure 3.2 (after relevant T -dualities) where one now has instead three species of $D5$ branes.

The numerical coefficients are constrained by the requiring that (3.3.16) is obeyed. The origin of the lattice towers shows the perfect square structure as

$$\begin{aligned} \tilde{\mathcal{A}}_o = & \frac{2^{-5}}{16} \left\{ \left(N \sqrt{v_1 v_2 v_3} + D_{go} \sqrt{\frac{v_1}{v_2 v_3}} + D_{fo} \sqrt{\frac{v_2}{v_1 v_3}} + D_{ho} \sqrt{\frac{v_3}{v_1 v_2}} \right)^2 \tau_{oo}^{NS} \right. \\ & - \left(N \sqrt{v_1 v_2 v_3} + \epsilon_1 D_{go} \sqrt{\frac{v_1}{v_2 v_3}} + \epsilon_2 D_{fo} \sqrt{\frac{v_2}{v_1 v_3}} + \epsilon_3 D_{ho} \sqrt{\frac{v_3}{v_1 v_2}} \right)^2 \tau_{oo}^R \\ & \left. + \left(N \sqrt{v_1 v_2 v_3} + D_{go} \sqrt{\frac{v_1}{v_2 v_3}} - D_{fo} \sqrt{\frac{v_2}{v_1 v_3}} - D_{ho} \sqrt{\frac{v_3}{v_1 v_2}} \right)^2 \tau_{og}^{NS} \right\} \end{aligned}$$

$$\begin{aligned}
& - \left(N\sqrt{v_1 v_2 v_3} + \epsilon_1 D_{go} \sqrt{\frac{v_1}{v_2 v_3}} - \epsilon_2 D_{fo} \sqrt{\frac{v_2}{v_1 v_3}} - \epsilon_3 D_{ho} \sqrt{\frac{v_3}{v_1 v_2}} \right)^2 \tau_{og}^R \\
& + \left(N\sqrt{v_1 v_2 v_3} - D_{go} \sqrt{\frac{v_1}{v_2 v_3}} + D_{fo} \sqrt{\frac{v_2}{v_1 v_3}} - D_{ho} \sqrt{\frac{v_3}{v_1 v_2}} \right)^2 \tau_{of}^{NS} \\
& - \left(N\sqrt{v_1 v_2 v_3} - \epsilon_1 D_{go} \sqrt{\frac{v_1}{v_2 v_3}} + \epsilon_2 D_{fo} \sqrt{\frac{v_2}{v_1 v_3}} - \epsilon_3 D_{ho} \sqrt{\frac{v_3}{v_1 v_2}} \right)^2 \tau_{of}^R \\
& + \left(N\sqrt{v_1 v_2 v_3} - D_{go} \sqrt{\frac{v_1}{v_2 v_3}} - D_{fo} \sqrt{\frac{v_2}{v_1 v_3}} + D_{ho} \sqrt{\frac{v_3}{v_1 v_2}} \right)^2 \tau_{oh}^{NS} \\
& - \left. \left(N\sqrt{v_1 v_2 v_3} - \epsilon_1 D_{go} \sqrt{\frac{v_1}{v_2 v_3}} - \epsilon_2 D_{fo} \sqrt{\frac{v_2}{v_1 v_3}} + \epsilon_3 D_{ho} \sqrt{\frac{v_3}{v_1 v_2}} \right)^2 \tau_{oh}^R \right\}. \tag{3.3.16}
\end{aligned}$$

An S transform shows the direct channel amplitude to be

$$\begin{aligned}
\mathcal{A} &= \frac{1}{16} \left\{ \left(N^2 P_1 P_2 P_3 (1 + (-1)^{m_1+m_2+m_3}) \right. \right. \\
& \quad \left. \left. + \frac{1}{4} D_{ko}^2 P^k (W^l W^s + W_{n+\frac{1}{2}}^l W_{n+\frac{1}{2}}^s) \right) T_{oo} \right. \\
& \quad \left. + 2 D_{ko} N P^k \left(\frac{\eta}{\theta_4} \right)^2 T_{ko}^{(\epsilon_k)} \right. \\
& \quad \left. \frac{1}{2} D_{ko} D_{lo} (W^s + W_{n+\frac{1}{2}}^s) \left(\frac{\eta}{\theta_4} \right)^2 T_{so}^{(\epsilon_k \epsilon_l)} \right\}. \tag{3.3.17}
\end{aligned}$$

Having fixed the relevant factors in the annulus, the Mobius can now be constructed. The Mobius is dressed with lattice states in the same manner as that of the previous model. However, with the shift acting in all tori, the phase that was introduced to give correct direct channel annulus-Mobius symmetrization is extended accordingly. The appropriate Mobius term is shown in table 3.6.

With the introduction of the signs ϵ_j into the annulus and Klein amplitudes, the Mobius shows these at its lattice origin accordingly:

$$\begin{aligned}
\tilde{\mathcal{M}}_o &= \pm \frac{1}{8} \left\{ N v_1 v_2 v_3 \hat{T}_{oo} + \epsilon_k D_{ko} \frac{v_k}{2 v_l v_m} \hat{T}_{oo}^{(\epsilon_k)} \right. \\
& \quad \left. + \epsilon_k N v_k \hat{T}_{ok} + D_{ko} v_k \hat{T}_{ok}^{(\epsilon_k)} + \epsilon_m D_{lo} \frac{1}{v_k} \hat{T}_{ok}^{(\epsilon_l)} \right\}. \tag{3.3.18}
\end{aligned}$$

With the correct lattice terms, one finds the full transverse Mobius amplitude to be

$$\begin{aligned}
\tilde{\mathcal{M}} &= -\frac{1}{8} \left\{ N v_1 v_2 v_3 (W_e^1 W_e^2 W_e^3 + W_o^1 W_o^2 W_o^3) \hat{T}_{oo} \right. \\
& \quad \left. + \epsilon_k D_{ko} \frac{v_k}{2 v_l v_s} (W_e^k P_e^l P_e^s + (-1)^{m_l+m_s} W_o^k P_e^l P_e^s) \hat{T}_{oo}^{(\epsilon_k)} \right\}
\end{aligned}$$

Plane diagrams	Volumes
$D9 - D9, D9 - O9, O9 - O9$	$v_1 v_2 v_3$
$D5_k - D5_k, D5_k - O5_k, O5_k - O5_k$	$\frac{v_k}{v_l v_m}$
$D5_k - D5_l, D5_k - O5_l, O5_k - O5_l$	$\frac{1}{v_m}$
$D9 - D5_k, D9 - O5_k, D5_k - O9$	v_k
$\tilde{\mathcal{A}}$ and $\tilde{\mathcal{K}}$ Plane Diagrams	Lattice Couplings
$D9 - D9$	$W^1 W^2 W^3 + W_{n+\frac{1}{2}}^1 W_{n+\frac{1}{2}}^2 W_{n+\frac{1}{2}}^3$
$D5_k - D5_k$	$W^k P^l P^m (1 + (-1)^{m_l + m_m})$
$O9 - O9$	$W_e^1 W_e^2 W_e^3 + W_o^1 W_o^2 W_o^3$
$O5_k - O5_k$	$W^k P_e^l P_e^m$
$\tilde{\mathcal{M}}$ plane diagrams	Lattice Couplings
$D9 - O9$	$W_e^1 W_e^2 W_e^3 + W_o^1 W_o^2 W_o^3$
$D9 - O5_k$	W^k
$D5_k - O9$	W_e^k
$D5_k - O5_k$	$W_e^k P_e^l P_e^m + (-1)^{m_l + m_m} W_o^k P_e^l P_e^m$
$D5_k - O5_l$	P_e^m

Table 3.6: Lattice restrictions

$$\begin{aligned}
& + (\epsilon_k N v_k W^k \hat{T}_{ok} + D_{ko} v_k W_e^k \hat{T}_{ok}^{(\epsilon_k)}) \left(\frac{2\hat{\eta}}{\hat{\theta}_2} \right)^2 \\
& + \epsilon_m D_{lo} \frac{P_e^k}{v_k} \hat{T}_{ok}^{(\epsilon_l)} \left(\frac{2\hat{\eta}}{\hat{\theta}_2} \right)^2 \} \quad (3.3.19)
\end{aligned}$$

where the sign ambiguity is -1 for consistent tadpole cancellation.

The corresponding direct channel is obtained by P transformation. It is noted that while P has non trivial effect of the lattice modes, it leaves the characters unchanged with the exception of a sign change for the orbifold sector. This can be seen by the representation defined in (3.2.27). As such

$$\begin{aligned}
\mathcal{M} = & -\frac{1}{16} \left\{ NP^1 P^2 P^3 (1 + (-1)^{m_1 + m_2 + m_3}) \hat{T}_{oo} \right. \\
& + \epsilon_k \frac{1}{2} D_{ko} (P^k W^l W^s + (-1)^{m_k} P^k W_{n+\frac{1}{2}}^l W_{n+\frac{1}{2}}^s) \hat{T}_{oo}^{(\epsilon_k)} \\
& - (2\epsilon_k N P_e^k \hat{T}_{ok} + D_{ko} P^k \hat{T}_{ok}^{(\epsilon_k)}) \left(\frac{2\hat{\eta}}{\hat{\theta}_2} \right)^2 \\
& \left. - \epsilon_m D_{lo} W^k \hat{T}_{ok}^{(\epsilon_l)} \left(\frac{2\hat{\eta}}{\hat{\theta}_2} \right)^2 \right\}. \quad (3.3.20)
\end{aligned}$$

The tadpole conditions for the $D9$ branes are

$$\frac{2^5}{16} + \frac{2^{-5}}{16} N^2 - \frac{N}{8} = 0 \Rightarrow N = 32. \quad (3.3.21)$$

It is seen that the tadpole conditions for the $D5$ branes in the NS and R sector cannot lead to mutual cancellation for cases other than $(+, +, +)$. The tadpole for N , as seen

by equation (3.3.21), is unaffected by this. However, allowing the cancellation of the R - R sector forces a tree level dilaton tadpole correlated with the creation of a potential for the NS - NS sector. This has an interpretation of increased vacuum energy. The tadpoles arising from the R - R sector must be satisfied in order to allow the total R - R charge to be cancelled.

From the amplitudes, one finds

$$D_{ko}^{(NS)} = \epsilon_k 32, D_{ko}^{(R)} = 32. \quad (3.3.22)$$

3.3.3 Model Classes of $\epsilon = +1$

The direct channel amplitudes defined by equations (3.3.17) and (3.3.20) require a rescaling of $N \rightarrow 2n$ and $D_{ko} \rightarrow 4d_k$ to give proper symmetrization. As such, one now has

$$\begin{aligned} \mathcal{A} = & \frac{1}{4} \left\{ \left(n^2 P_1 P_2 P_3 (1 + (-1)^{m_1+m_2+m_3}) \right. \right. \\ & + d_k^2 P^k (W^l W^s + W_{n+\frac{1}{2}}^l W_{n+\frac{1}{2}}^s) \left. \right) T_{oo} \\ & + 4d_k n P^k \left(\frac{\eta}{\theta_4} \right)^2 T_{ko}^{(\epsilon_k)} \\ & \left. + 4d_k d_l \frac{(W^s + W_{n+\frac{1}{2}}^s)}{2} \left(\frac{\eta}{\theta_4} \right)^2 T_{mo}^{(\epsilon_k \epsilon_l)} \right\} \end{aligned} \quad (3.3.23)$$

and

$$\begin{aligned} \mathcal{M} = & -\frac{1}{8} \left\{ n P^1 P^2 P^3 (1 + (-1)^{m_1+m_2+m_3}) \hat{T}_{oo} \right. \\ & + \epsilon_k d_k (P^k W^l W^s + (-1)^{m_k} P^k W_{n+\frac{1}{2}}^l W_{n+\frac{1}{2}}^s) \hat{T}_{oo}^{(\epsilon_k)} \\ & - (2\epsilon_k n P_e^k \hat{T}_{ok} + 2d_k P^k \hat{T}_{ok}^{(\epsilon_k)}) \left(\frac{2\hat{\eta}}{\hat{\theta}_2} \right)^2 \\ & \left. - 2\epsilon_m d_l W^k \hat{T}_{ok}^{(\epsilon_l)} \left(\frac{2\hat{\eta}}{\hat{\theta}_2} \right)^2 \right\}. \end{aligned} \quad (3.3.24)$$

Here, it appears that some massive modes, in particular the $(-1)^{m_k} P^k W_{n+\frac{1}{2}}^l W_{n+\frac{1}{2}}^s$ towers do not symmetrize with proper numerical factors. The annulus and Mobius are required to symmetrize modulo two. In this case, one has a multiplicity of the common states in the Mobius and annulus as

$$2^3 \times \left(\frac{d_k^2}{4} - \frac{d_k}{8} \right) = 3 \frac{d_k(d_k - 1)}{2} + \frac{d_k(d_k + 1)}{2} \quad (3.3.25)$$

where the multiplicity of 2^3 comes from the interchange of the indices l and s and the degeneracy of massive states under an orbifold element or Ω as $\alpha : n + \frac{1}{2} \rightarrow -n - \frac{1}{2}$. So one finds that the group interpretation is preserved as the decomposition into three orthogonal copies and one symplectic.

Firstly, I discuss the simplest and fully supersymmetric case of $(+, +, +)$. The expanded lattice origin form of the Mobius amplitude is shown in appendix A. The massless open spectra is given by

$$\begin{aligned}
\mathcal{A}_o + \mathcal{M}_o = & \left[\frac{n(n+1)}{2} + \frac{d_g(d_g+1)}{2} \right. \\
& \left. + \frac{d_f(d_f+1)}{2} + \frac{d_h(d_h+1)}{2} \right] \tau_{oo} \\
& + \left[\frac{n(n-1)}{2} + \frac{d_g(d_g-1)}{2} \right. \\
& \left. + \frac{d_f(d_f-1)}{2} + \frac{d_h(d_h-1)}{2} \right] (\tau_{og} + \tau_{of} + \tau_{oh}) \\
& + (nd_g + d_f d_h) (\tau_{go} + \tau_{gg} + \tau_{gf} + \tau_{gh}) \\
& + (nd_f + d_g d_h) (\tau_{fo} + \tau_{fg} + \tau_{ff} + \tau_{fh}) \\
& + (nd_h + d_g d_f) (\tau_{ho} + \tau_{hg} + \tau_{hf} + \tau_{hh}). \tag{3.3.26}
\end{aligned}$$

The vector multiplet, contained in τ_{oo} , combined with the tadpole conditions (3.3.21) and (3.3.22), and with the rescaling $N = 2n$ and $D_{ko} = 4d_k$, shows the gauge group to be $USp(16)_9 \times USp(8)_{5_{\{1,2,3\}}}$. The suffixes refer to the groups of the $D9$ and three copies of $D5$. From (3.3.3), one can see that $N = 1$ with chiral multiplets that arise in the untwisted sector from τ_{ok} and from the twisted sector in τ_{gf} , τ_{hg} and τ_{fg} . This model therefore has chiral multiplets in the representations described in table 3.7.

Sector	Characters	Reps. in $(D9; D5_1, D5_2, D5_3)$
Twisted	$\tau_{gf} + \tau_{gh}$	$(16; 8, 1, 1) + (1; 1, 8, 8)$
	$\tau_{fg} + \tau_{fh}$	$(16; 1, 8, 1) + (1; 8, 1, 8)$
	$\tau_{hg} + \tau_{hf}$	$(16; 1, 1, 8) + (1; 8, 8, 1)$
Untwisted	τ_{ok}	$(120; 1, 1, 1) + (1; 28, 1, 1)$ $+ (1; 1, 28, 1) + (1; 1, 1, 28)$

Table 3.7: Chiral multiplet representations for $\epsilon = (+, +, +)$

The remaining cases break supersymmetry for states coupling to $\bar{D}5_k$ branes, or antibranes that are aligned with the directions that satisfy $\epsilon_k = -1$. These are permutations of $(+, -, -)$.

For $(+, -, -)$, one has low lying spectrum

$$\begin{aligned}
\mathcal{A}_o + \mathcal{M}_o = & \left[\frac{n(n-1)}{2} + \frac{d_g(d_g-1)}{2} \right] (\tau_{oo} + \tau_{of} + \tau_{oh}) \\
& + \left[\frac{n(n+1)}{2} + \frac{d_g(d_g+1)}{2} \right] \tau_{og} \\
& + \left[\frac{d_f(d_f-1)}{2} + \frac{d_h(d_h-1)}{2} \right] \tau_{og}^{\text{NS}} \\
& + \left[\frac{d_f(d_f+1)}{2} + \frac{d_h(d_h+1)}{2} \right] \tau_{og}^{\text{R}}
\end{aligned}$$

$$\begin{aligned}
& + \left[\frac{d_f(d_f + 1)}{2} + \frac{d_h(d_h + 1)}{2} \right] (\tau_{oo}^{\text{NS}} + \tau_{of}^{\text{NS}} + \tau_{oh}^{\text{NS}}) \\
& + \left[\frac{d_f(d_f - 1)}{2} + \frac{d_h(d_h - 1)}{2} \right] (\tau_{oo}^{\text{R}} + \tau_{of}^{\text{R}} + \tau_{oh}^{\text{R}}) \\
& + (nd_g + d_f d_h)(\tau_{go} + \tau_{gg} + \tau_{gf} + \tau_{gh}) \\
& + (nd_f + d_g d_h)(\tau_{fo}^{(-)} + \tau_{fg}^{(-)} + \tau_{ff}^{(-)} + \tau_{fh}^{(-)}) \\
& + (nd_h + d_g d_f)(\tau_{ho}^{(-)} + \tau_{hg}^{(-)} + \tau_{hf}^{(-)} + \tau_{hh}^{(-)}). \tag{3.3.27}
\end{aligned}$$

Supersymmetry is seen to be broken in this expansion in a twofold way. Firstly, the

Sector	Characters	Reps. in $(D9; D5_1, D5_2, D5_3)$
Twisted	$\tau_{gf} + \tau_{gh}$	$(16; 8, 1, 1) + (1; 1, 8, 8)$
Untwisted	τ_{og}	$(136; 1, 1, 1) + (1; 36, 1, 1)$
	τ_{of}	$(120; 1, 1, 1) + (1; 28, 1, 1)$
	τ_{oh}	$(120; 1, 1, 1) + (1; 28, 1, 1)$

Table 3.8: Chiral multiplet representations for $\epsilon = (+, -, -)$

representations for the Neveu-Schwarz and Ramond terms are different in the untwisted sectors. Secondly, the presence of signs ϵ_k forces character sets to transform differently under S , as can be seen by reference to (3.3.13). So the f and h twisted characters are no longer supersymmetric.

In this case, the gauge group is $SO(16)_9 \times SO(8)_{5_1} \times USp(8)_{\bar{5}_{\{2,3\}}}$. The representations of the chiral multiplets in this model are displayed in table 3.8. For $(-, +, -)$, the low

Sector	Characters	Reps. in $(D9; D5_1, D5_2, D5_3)$
Twisted	$\tau_{hg} + \tau_{hf}$	$(16; 1, 1, 8) + (1; 8, 8, 1)$
Untwisted	τ_{og}	$(120; 1, 1, 1) + (1; 1, 1, 28)$
	τ_{of}	$(120; 1, 1, 1) + (1; 1, 1, 28)$
	τ_{oh}	$(136; 1, 1, 1) + (1; 1, 1, 36)$

Table 3.9: Chiral multiplet representations for $\epsilon = (-, -, +)$

lying modes correspond to

$$\begin{aligned}
\mathcal{A}_o + \mathcal{M}_o = & \left[\frac{n(n-1)}{2} + \frac{d_f(d_f-1)}{2} \right] (\tau_{oo} + \tau_{og} + \tau_{oh}) \\
& + \left[\frac{n(n+1)}{2} + \frac{d_f(d_f+1)}{2} \right] \tau_{of} \\
& + \left[\frac{d_g(d_g-1)}{2} + \frac{d_h(d_h-1)}{2} \right] \tau_{of}^{\text{NS}} \\
& + \left[\frac{d_g(d_g+1)}{2} + \frac{d_h(d_h+1)}{2} \right] \tau_{of}^{\text{R}}
\end{aligned}$$

$$\begin{aligned}
& + \left[\frac{d_g(d_g + 1)}{2} + \frac{d_h(d_h + 1)}{2} \right] (\tau_{oo}^{\text{NS}} + \tau_{og}^{\text{NS}} + \tau_{oh}^{\text{NS}}) \\
& + \left[\frac{d_g(d_g - 1)}{2} + \frac{d_h(d_h - 1)}{2} \right] (\tau_{oo}^{\text{R}} + \tau_{og}^{\text{R}} + \tau_{oh}^{\text{R}}) \\
& + (nd_g + d_f d_h) (\tau_{go}^{(-)} + \tau_{gg}^{(-)} + \tau_{gf}^{(-)} + \tau_{gh}^{(-)}) \\
& + (nd_f + d_g d_h) (\tau_{fo} + \tau_{fg} + \tau_{ff} + \tau_{fh}) \\
& + (nd_h + d_g d_f) (\tau_{ho}^{(-)} + \tau_{hg}^{(-)} + \tau_{hf}^{(-)} + \tau_{hh}^{(-)})
\end{aligned} \tag{3.3.28}$$

with gauge group $SO(16)_9 \times USp(8)_{\bar{5}_1} \times SO(8)_{\bar{5}_2} \times USp(8)_{\bar{5}_3}$ and representations for

Sector	Characters	Reps. in $(D9; D\bar{5}_1, D\bar{5}_2, D\bar{5}_3)$
Twisted	$\tau_{fg} + \tau_{fh}$	$(16; 1, 8, 1) + (1; 8, 1, 8)$
Untwisted	τ_{og}	$(120; 1, 1, 1) + (1; 1, 28, 1)$
	τ_{of}	$(136; 1, 1, 1) + (1; 1, 36, 1)$
	τ_{oh}	$(120; 1, 1, 1) + (1; 1, 28, 1)$

Table 3.10: Chiral multiplet representations for $\epsilon = (-, +, -)$

the chiral multiplets are displayed in table 3.10.

Finally, the $(-, -, +)$ model gives rise to

$$\begin{aligned}
\mathcal{A}_o + \mathcal{M}_o = & \left[\frac{n(n-1)}{2} + \frac{d_h(d_h-1)}{2} \right] (\tau_{oo} + \tau_{og} + \tau_{of}) \\
& + \left[\frac{n(n+1)}{2} + \frac{d_h(d_h+1)}{2} \right] \tau_{oh} \\
& + \left[\frac{d_g(d_g-1)}{2} + \frac{d_f(d_f-1)}{2} \right] \tau_{oh}^{\text{NS}} \\
& + \left[\frac{d_g(d_g+1)}{2} + \frac{d_f(d_f+1)}{2} \right] \tau_{oh}^{\text{R}} \\
& + \left[\frac{d_g(d_g+1)}{2} + \frac{d_f(d_f+1)}{2} \right] (\tau_{oo}^{\text{NS}} + \tau_{og}^{\text{NS}} + \tau_{of}^{\text{NS}}) \\
& + \left[\frac{d_g(d_g-1)}{2} + \frac{d_f(d_f-1)}{2} \right] (\tau_{oo}^{\text{R}} + \tau_{og}^{\text{R}} + \tau_{of}^{\text{R}}) \\
& + (nd_g + d_f d_h) (\tau_{go}^{(-)} + \tau_{gg}^{(-)} + \tau_{gf}^{(-)} + \tau_{gh}^{(-)}) \\
& + (nd_f + d_g d_h) (\tau_{fo}^{(-)} + \tau_{fg}^{(-)} + \tau_{ff}^{(-)} + \tau_{fh}^{(-)}) \\
& + (nd_h + d_g d_f) (\tau_{ho} + \tau_{hg} + \tau_{hf} + \tau_{hh})
\end{aligned} \tag{3.3.29}$$

with $SO(16)_9 \times USp(8)_{\bar{5}_{\{1,2\}}} \times SO(8)_{\bar{5}_3}$ gauge group. Representations for the chiral multiplets are displayed in table 3.9.

This then exhausts all possible configurations of the $\epsilon = +1$ models. I now turn to those with discrete torsion.

3.3.4 Models With Discrete Torsion ($\epsilon = -1$)

The oriented open sector for this class of models is far richer than those without discrete torsion. By reference to (3.3.2), one has the existence of left moving states coupled to their corresponding conjugates. In this case, in addition to the states in (3.3.15) there are twisted sectors.

In addition to the transverse untwisted states defined by (3.3.15), one now has

$$\begin{aligned}
\tilde{\mathcal{A}} = & \frac{2^{-5}}{16} \left\{ \left(N_o^2 v_1 v_2 v_3 (W^1 W^2 W^3 + W_{n+\frac{1}{2}}^1 W_{n+\frac{1}{2}}^2 W_{n+\frac{1}{2}}^3) \right. \right. \\
& + \frac{v_k}{2v_l v_s} D_{ko}^2 W^k P^l P^m \frac{(1 + (-1)^{m_l + m_s})}{2} \left. \right) T_{oo} \\
& + \left[M_1 N_k^2 v_k (W^k + W_{n+\frac{1}{2}}^k) \right. \\
& + M_2 D_{kk}^2 v_k W^k + M_3 D_{lk}^2 \frac{P^k}{v_k} \left. \right] T_{ko} \left(\frac{\eta}{\theta_4} \right)^2 \\
& + 2N_o D_{ko} v_k W^k \tilde{T}_{ok}^{(\epsilon_k)} \left(\frac{2\eta}{\theta_2} \right)^2 \\
& + M_4 N_k D_{kk} v_k W^k \tilde{T}_{kk}^{(\epsilon_k)} \left(\frac{\eta}{\theta_3} \right)^2 \\
& + M_5 N_l D_{kl} \tilde{T}_{lk}^{(\epsilon_k)} \frac{8\eta^3}{\theta_2 \theta_3 \theta_4} \\
& + D_{ko} D_{lo} \frac{P^s}{v_s} \frac{(1 + (-1)^{m_s})}{2} \tilde{T}_{os}^{(\epsilon_k \epsilon_l)} \left(\frac{2\eta}{\theta_2} \right)^2 \\
& + M_6 D_{km} D_{lm} \frac{P^m}{v_m} \tilde{T}_{mm}^{(\epsilon_k \epsilon_l)} \left(\frac{\eta}{\theta_3} \right)^2 \\
& \left. + M_7 D_{kk} D_{lk} \tilde{T}_{km}^{(\epsilon_k \epsilon_l)} \frac{8\eta^3}{\theta_2 \theta_3 \theta_4} \right\}. \tag{3.3.30}
\end{aligned}$$

The coefficients M_i are determined from the origin of the twisted sector with the same arguments as used for the $\mathbb{Z}_2 \times \mathbb{Z}_2^s$ model.

The N_g term fills all compact and non-compact dimensions and thus has the coefficient v_k . With the volume v_k being provided by the remaining compact directions that are not acted on by an orbifold. When considering the factors involved with terms like D_{kl} , l represents the fixed point configuration of $T_{45}^2 \times T_{67}^2 \times T_{89}^2$ and k represents whether the brane is wrapped or transverse. For example, D_{gf} has fixed points in the first and third torus corresponding to f . The index g implies that the D_{gf} brane is wrapped around the first tori and is transverse to the second and third, consistent with the representation $g = (+, -, -)$. Hence, it *sees* four fixed points.

Looking at the g -twisted sector of the $\epsilon = (+, +, -)$ model, this has a total of sixteen fixed points, four located in each of the second and third tori. Under the operation of the shift, half are identified. The independent fixed points are as in table 3.4.

For the g -twisted sector, one has terms in the annulus as

$$\begin{aligned}
\tilde{\mathcal{A}}^g = & \frac{2^{-5}}{16} \left\{ \left[(M_1 N_g^2 + M_2 D_{gg}^2) v_1 + M_3 D_{lg}^2 \frac{1}{v_1} \right] T_{go} \right. \\
& + M_4 N_g D_{gg} v_1 \tilde{T}_{gg}^{(\epsilon_1)} \\
& + 4M_5 N_g D_{kg} \tilde{T}_{gk}^{(\epsilon_k)} \\
& + M_6 D_{kg} D_{lg} \frac{1}{v_1} \tilde{T}_{gg}^{(\epsilon_k \epsilon_l)} \\
& \left. + 4M_7 D_{gg} D_{lg} \tilde{T}_{gm}^{(\epsilon_k \epsilon_l)} \right\}. \tag{3.331}
\end{aligned}$$

All brane types N_g , D_{gg} , D_{fg} and D_{hg} see the fixed point $(0, 0; 0, 0)$, and therefore arrange into a perfect square with multiplicity 1. The arguments set out in the simpler $\mathbb{Z}_2 \times \mathbb{Z}_2^s$ model with regard to the wrapping of $D5$ branes is generalized here with the inclusion of three distinct types. The counting of their fixed point occupation is then a little more complicated. N_g and D_{hg} see the fixed points $(0, 0; \frac{1}{2}, 0)$, $(0, 0; 0, \frac{1}{2})$ and $(0, 0; \frac{1}{2}, \frac{1}{2})$, which correspond to their own perfect square with multiplicity 3. The coefficients of the N_g and D_{hg} terms are 1 and 2 respectively, which can easily be seen by reference to (3.2.19). Similar holds for the square of N_g and D_{fg} . The remaining fixed points are taken into account by N_g alone.

The resulting perfect square structures for the NS - NS and R - R portions of τ_{gl} are

$$\begin{aligned}
& 2 \times \frac{2^{-5}}{16} \left\{ \left(\sqrt{v_1} N_g - 4\sqrt{v_1} D_{gg} - 2\frac{1}{\sqrt{v_1}} D_{fg} + 2\frac{1}{\sqrt{v_1}} D_{hg} \right)^2 \right. \\
& \left. + 3\left(\sqrt{v_1} N_g - 2\frac{1}{\sqrt{v_1}} D_{fg} \right)^2 + 3\left(\sqrt{v_1} N_g + 2\frac{1}{\sqrt{v_1}} D_{hg} \right)^2 + v_1 N_g^2 \right\}, \tag{3.332}
\end{aligned}$$

and

$$\begin{aligned}
& 2 \times \frac{2^{-5}}{16} \left\{ \left(\sqrt{v_1} N_g - 4\sqrt{v_1} D_{gg} - 2\frac{1}{\sqrt{v_1}} D_{fg} - 2\frac{1}{\sqrt{v_1}} D_{hg} \right)^2 \right. \\
& \left. + 3\left(\sqrt{v_1} N_g - 2\frac{1}{\sqrt{v_1}} D_{fg} \right)^2 + 3\left(\sqrt{v_1} N_g - 2\frac{1}{\sqrt{v_1}} D_{hg} \right)^2 + v_1 N_g^2 \right\} \tag{3.333}
\end{aligned}$$

respectively. Similar results follow for the same procedure in the f and h twisted sectors. The overall factor of 2 is to account for the multiplicity of the shifted fixed points in the same fashion as for the $\mathbb{Z}_2 \times \mathbb{Z}_2^s$ case.

With the aid of the identity

$$\theta_2 \theta_3 \theta_4 = 2\eta^3,$$

the transverse annulus is now seen to be

$$\begin{aligned}
\tilde{\mathcal{A}} = \frac{2^{-5}}{16} & \left\{ \left(N_o^2 v_1 v_2 v_3 (W^1 W^2 W^3 + W_{n+\frac{1}{2}}^1 W_{n+\frac{1}{2}}^2 W_{n+\frac{1}{2}}^3) \right. \right. \\
& + \frac{v_k}{2v_l v_s} D_{ko}^2 W^k P^l P^s \frac{(1 + (-1)^{m_l + m_s})}{2} \left. \right) T_{oo} \\
& + 2 \times 2 \left[N_k^2 v_k (W^k + W_{n+\frac{1}{2}}^k) \right. \\
& + 2D_{kk}^2 v_k W^k + 2D_{lk}^2 \frac{P^k}{v_k} \left. \right] T_{ko} \left(\frac{2\eta}{\theta_4} \right)^2 \\
& + 2N_o D_{ko} v_k W^k \tilde{T}_{ok}^{(\epsilon_k)} \left(\frac{2\eta}{\theta_2} \right)^2 \\
& + 2 \times 2N_k D_{kk} v_k W_k \tilde{T}_{kk}^{(\epsilon_k)} \left(\frac{2\eta}{\theta_3} \right)^2 \\
& + 2 \times 4N_l D_{kl} \tilde{T}_{lk}^{(\epsilon_k)} \frac{8\eta^3}{\theta_2 \theta_3 \theta_4} \\
& + D_{ko} D_{lo} \frac{P^s}{v_s} \frac{(1 + (-1)^{m_s})}{2} \tilde{T}_{os}^{(\epsilon_k \epsilon_l)} \left(\frac{2\eta}{\theta_2} \right)^2 \\
& + 2D_{km} D_{lm} \frac{P^m}{v_m} \tilde{T}_{mm}^{(\epsilon_k \epsilon_l)} \left(\frac{2\eta}{\theta_3} \right)^2 \\
& \left. + 2 \times 4D_{kk} D_{lk} \tilde{T}_{km}^{(\epsilon_k \epsilon_l)} \frac{8\eta^3}{\theta_2 \theta_3 \theta_4} \right\}. \tag{3.3.34}
\end{aligned}$$

With corresponding direct channel

$$\begin{aligned}
\mathcal{A} = \frac{1}{16} & \left\{ \left(N_o^2 P^1 P^2 P^3 (1 + (-1)^{m_1 + m_2 + m_3}) \right. \right. \\
& + \frac{1}{2} \frac{D_{ko}^2}{2} P^k (W^l W^m + W_{n+\frac{1}{2}}^l W_{n+\frac{1}{2}}^m) \left. \right) T_{oo} \\
& + \left[N_k^2 P^k (1 + (-1)^{m_k}) \right. \\
& + 2D_{kk}^2 P^k + 2D_{lk}^2 W^k \left. \right] T_{ok} \left(\frac{2\eta}{\theta_2} \right)^2 \\
& + 2N_o D_{ko} P^k T_{ko}^{(\epsilon_k)} \left(\frac{\eta}{\theta_4} \right)^2 \\
& - 2 \times 2N_k D_{kk} P^k T_{kk}^{(\epsilon_k)} \left(\frac{\eta}{\theta_3} \right)^2 \\
& + 2 \times 2i(-1)^{k+l} N_l D_{kl} T_{kl}^{(\epsilon_k)} \frac{2\eta^3}{\theta_2 \theta_3 \theta_4} \\
& \left. + \frac{1}{2} D_{ko} D_{lo} (W^m + W_{n+\frac{1}{2}}^m) T_{mo}^{(\epsilon_k \epsilon_l)} \left(\frac{\eta}{\theta_4} \right)^2 \right\}
\end{aligned}$$

N_o	$= (n + m + \bar{n} + \bar{m}),$	N_g	$= i(n + m - \bar{n} - \bar{m})$
N_f	$= i(n - m - \bar{n} + \bar{m}),$	N_h	$= (n - m + \bar{n} - \bar{m})$
D_{go}	$= 2(o_1 + g_1 + \bar{o}_1 + \bar{g}_1),$	D_{fo}	$= 2(o_2 + g_2 + \bar{o}_2 + \bar{g}_2)$
D_{ho}	$= 2(a + b + c + d),$	D_{gg}	$= i(o_1 + g_1 - \bar{o}_1 - \bar{g}_1)$
D_{ff}	$= i(o_2 + g_2 - \bar{o}_2 - \bar{g}_2),$	D_{hh}	$= a - b - c + d$
D_{gf}	$= o_1 - g_1 + \bar{o}_1 - \bar{g}_1,$	D_{gh}	$= -i(o_1 - g_1 - \bar{o}_1 + \bar{g}_1)$
D_{fg}	$= o_2 - g_2 + \bar{o}_2 - \bar{g}_2,$	D_{fh}	$= i(o_2 - g_2 - \bar{o}_2 + \bar{g}_2)$
D_{hg}	$= a + b - c - d,$	D_{hf}	$= a - b + c - d$

Table 3.11: $\epsilon = (1, 1, -1)$ Model Charges

$$\begin{aligned}
& -2 \times D_{km} D_{lm} W^m T_{mm}^{(\epsilon_k \epsilon_l)} \left(\frac{\eta}{\theta_3} \right)^2 \\
& + 2 \times 2i (-1)^{m+k} D_{kk} D_{lk} T_{mk}^{(\epsilon_k \epsilon_l)} \frac{2\eta^3}{\theta_2 \theta_3 \theta_4} \}. \tag{3.3.35}
\end{aligned}$$

It is here that consistent particle interpretation does not occur. The inconsistency is generated in the $D5_i - D5_j$ (for $i \neq j$) sector. All other sectors give rise to the proper massless and massive counting. Moreover, the problem exists in the twisted sector that has to symmetrize by itself, as the Mobius has only untwisted sectors present. The Mobius has the same form as for the case without discrete torsion, up to signs ϵ_k that in this case are required to give $\epsilon = -1$ (with reference to equation (3.3.8)), and a different definition of the Chan–Paton charges.

To begin with one must define the Chan-Paton charge parameterization which is given in table 3.11 for the case in consideration of $\epsilon = (+, +, -)$. As with the $\mathbb{Z}_2 \times \mathbb{Z}_2^s$ case, the parameterization involves factors of the form n, \bar{n} , etc. . . . These apply for branes that are aligned with $\epsilon_k = +1$ (i.e. D_{kl} and N_k for $l = 1, 2, 3$) for the cases which are permutations of $(+, +, -)$.

As with the previous models, the factors of two for the terms in each D_{ko} are necessary and induced by the shift to give proper integer particle interpretation. All sectors that involve a coupling to a $D9$ brane are consistent.

With this parameterization, the untwisted sector provides consistent massless spectrum as

$$\begin{aligned}
\mathcal{A}_o + \mathcal{M}_o &= (n\bar{n} + m\bar{m} + g_1\bar{g}_1 + o_1\bar{o}_1 + o_2\bar{o}_2 + g_2\bar{g}_2)\tau_{oo} \\
&+ (n\bar{m} + m\bar{n} + o_1\bar{g}_1 + g_1\bar{o}_1 + ab + cd)\tau_{og} \\
&+ (nm + \bar{n}\bar{m} + o_2\bar{g}_2 + g_2\bar{o}_2 + ac + bd)\tau_{of} \\
&+ (\bar{o}_1\bar{g}_1 + o_1g_1 + o_2g_2 + \bar{o}_2\bar{g}_1 + ad + bc)\tau_{oh} \\
&+ \frac{(a(a+1) + b(b+1) + c(c+1) + d(d+1))}{2} \tau_{oo}^{NS} \\
&+ \frac{(a(a-1) + b(b-1) + c(c-1) + d(d-1))}{2} \tau_{oo}^R \\
&+ \frac{(o_2(o_2-1) + g_2(g_2-1) + \bar{o}_2(\bar{o}_2-1) + \bar{g}_2(\bar{g}_2-1))}{2} \tau_{og}
\end{aligned}$$

$$\begin{aligned}
& + \frac{(o_1(o_1 - 1) + g_1(g_1 - 1) + \bar{o}_1(\bar{o}_1 - 1) + \bar{g}_1(\bar{g}_1 - 1))}{2} \tau_{of} \\
& + \frac{(n(n - 1) + m(m - 1) + \bar{n}(\bar{n} - 1) + \bar{m}(\bar{m} - 1))}{2} \tau_{oh}. \tag{3.3.36}
\end{aligned}$$

Indeed, the twisted massless spectrum also gives rise to a consistent particle interpretation in all sectors g , f and h . The spectrum obtained from the twisted $D9$ – $D5$ couplings also allows consistent state counting for all mass levels.

Turning lastly to the $D5_i - D5_j$ sector, one has consistency for massless and all integer massive levels. However, for the $n + \frac{1}{2}$ massive states one has the term

$$\frac{1}{2} D_{fo} D_{lo} W_{n+\frac{1}{2}}^m T_{mo}^{(\epsilon_k \epsilon_l)} \left(\frac{\eta}{\theta_4} \right)^2. \tag{3.3.37}$$

Any combination of the operators g , f , h and Ω will map $W_{n+\frac{1}{2}}$ to $W_{\pm(n+\frac{1}{2})}$, this winding tower will then have a degeneracy of two. Taking into account the interchange counting $k \leftrightarrow l$ and the rescaling defined in table 3.11, the end result is a state with numerical coefficient of $\frac{1}{2}$.

The same term occurred in the model without discrete torsion in equation (3.3.23). In that case, it did not cause any inconsistency because of the generic rescaling $N \rightarrow 2n$ and $D \rightarrow 2d$ in addition to the rescaling induced by the freely acting shift. In the models with discrete torsion, such a rescaling is taken into account (for the integer massive and massless levels) by the presence of the breaking terms N_k, D_{kk}, \dots

In the transverse annulus, one has the freedom to introduce Wilson lines via phases of the form $e^{2\pi i \alpha}$, for $\alpha \in (0, 1)$. If such phases are introduced, the resulting amplitude must respect symmetrization in the direct channel and the corresponding terms in the transverse annulus must exist in the torus. Introducing phases in the group of $D5_i - D5_j$ terms that must symmetrize together as

$$\begin{aligned}
& \frac{1}{2} D_{ko} D_{lo} (W^m + W_{n+\frac{1}{2}}^m) T_{mo}^{(\epsilon_k \epsilon_l)} \left(\frac{\eta}{\theta_4} \right)^2 \\
& - 2 \times D_{km} D_{lm} W^m T_{mm}^{(\epsilon_k \epsilon_l)} \left(\frac{\eta}{\theta_3} \right)^2 \\
& + 2 \times 2i (-1)^{m+k} D_{kk} D_{lk} T_{mk}^{(\epsilon_k \epsilon_l)} \frac{2\eta^3}{\theta_2 \theta_3 \theta_4} \tag{3.3.38}
\end{aligned}$$

only leads to amplitudes that violate this requirement, or indeed cause the same problem of incorrect counting at other mass levels.

To illustrate this point, I begin with a phase in the first term as

$$D_{ko} D_{lo} P^s \frac{(1 + (-1)^{m_s^1 + \beta m_s^2})}{2} \xrightarrow{\vec{S}} \frac{1}{2} D_{ko} D_{lo} (W^s + W_{n_1+\frac{1}{2}, n_2+\frac{\beta}{2}}^s). \tag{3.3.39}$$

Where m_s^1 and m_s^2 are the momentum quantum numbers on the first and second directions of the torus T^s . For $\beta = 1$, the momentum lattice in the transverse channel has expanded form

$$P_{2m_1, 2m_2}^s + P_{2m_1+1, 2m_2+1}^s \tag{3.3.40}$$

which includes odd states that do not exist in the torus. For $\beta \neq 1$, the projection which leads to the counting of even momentum states, as required by the torus, no longer exists unless $\beta = 0 \pmod{2}$. Therefore, the introduction of a phase for this term has to be one which multiplies the whole lattice expression. Doing this will however lift the massless spectrum in the direct channel amplitude of terms associated with $D_{k_o}D_{l_o}$ couplings.

Allowing a phase for the second term in (3.3.38), while solving the $n + \frac{1}{2}$ state counting problem, would then cause a similar effect of non-integer particle counting for the massless states.

The third term does not carry any momenta or winding states, and so any phase possibilities are only applicable to the first two.

I reiterate here that the spectrum is consistent at massive and massless levels for all other couplings in this model, consistency only breaks down for the $D5_i D5_j$ couplings.

3.4 Discussion

The spectra of freely acting orbifolds with non-freely acting winding and or Kaluza Klein shifts have been exhaustively studied in [1] as (shift) orbifolds. The inclusion of shift operators within the $\mathbb{Z}_2 \times \mathbb{Z}_2$ orbifold generators leads to (in the cases with two $D5$ branes, and some models with only one $D5$ brane) richer geometries. In particular, such cases involve shifted fixed points, which give rise to unique massive lattices of the form $W_{n+\frac{1}{2}}$ in the direct channel annulus. In addition, the arrangement of shifts within the $\mathbb{Z}_2 \times \mathbb{Z}_2$ generators imposes restrictions on the number of distinct $D5$ branes that can exist. The models defined by $\mathbb{Z}_2 \times \mathbb{Z}_2$ (shift) projections that essentially exhaust all interesting configurations are defined [1] by

$$\sigma_1(\delta_1, \delta_2, \delta_3) = \begin{pmatrix} \delta_1 & -\delta_2 & -1 \\ -1 & \delta_2 & -\delta_3 \\ -\delta_1 & -1 & \delta_3 \end{pmatrix}, \quad \sigma_2(\delta_1, \delta_2, \delta_3) = \begin{pmatrix} \delta_1 & -1 & -1 \\ -1 & \delta_2 & -\delta_3 \\ -\delta_1 & -\delta_2 & \delta_3 \end{pmatrix}. \quad (3.4.1)$$

The parameters δ_i are winding or momentum shifts. Wherever a δ operation exists in a column, the corresponding brane is eliminated.

In the freely acting shift models, all $D5$ branes are allowed to exist but have a more conventional geometry with regard to their relative placements.

The closed string states in the $\mathbb{Z}_2 \times \mathbb{Z}_2$ (shift) models are not as rich as those in the $\mathbb{Z}_2 \times \mathbb{Z}_2 \times \mathbb{Z}_2^s$ models. This is especially evident in that such (shift) orbifolds do not allow contributions from $\mathbb{Z}_2 \times \mathbb{Z}_2$ orbits that lie outside S and T transformations on the principle orbits (o, o) , (o, g) , (o, f) and (o, h) (as illustrated in appendix B).

With the inclusion of independent orbits, one has a class of models which exhibit possible scenarios of supersymmetry breaking (according to the sign freedom associated with the independent modular orbits). The cases without discrete torsion which include $(+, +, +)$, $(+, -, -)$, $(-, +, -)$ and $(-, -, +)$ lead to fully consistent amplitudes with $N = 1$ supersymmetry in the open sector with brane supersymmetry breaking associated with strings attached to a $\bar{D}5_k$ antibrane (which are aligned with the directions corresponding to $\epsilon_k = -1$).

There is however an unresolved problem of consistent particle interpretation for cases with discrete torsion for $n + \frac{1}{2}$ massive modes stretched between distinct $D5$ branes.

The spectral content is entirely consistent for the counting of string states which do not include $D5_i$ - $D5_j$ couplings. However, at the time of writing, a solution to this problem has not been found.

The sign ϵ associated with the inclusion of the additional independent orbits is a freedom. There is no mechanism outlined yet that guides the choice of which model is preferred, other than perhaps phenomenological requirements. In contrast to the (shift) orbifold models, although the closed spectrum is not as rich in such cases, they do eliminate this freedom.

Unitary groups are obtained only from the models in the $\epsilon = -1$ in using the underlying geometry $T^6(\mathbb{Z}_2 \times \mathbb{Z}_2)$. In many of the possible arrangements of (shift) orbifold models, the corresponding torus amplitude allows the propagation of twisted states that give three different models with unitary gauge groups (for models with both $D9$'s and $D5$'s present). However, none of these has all three twisted sectors contributing to the massless spectrum. Use of the freely acting shift allows one to keep the three twisted sectors at massless level.

Chapter 4

Magnetic Deformation of the Type I $\mathbb{Z}_2 \times \mathbb{Z}_2$ Model with Discrete Torsion

In this last discussion of type I phenomenology, I look at the interesting scenario of including background magnetic fields in the generic $\mathbb{Z}_2 \times \mathbb{Z}_2$ model (see appendix G). In particular, it is the model with discrete torsion ($\epsilon = -1$). It will be shown that magnetizing this model, which has twisted terms in the transverse annulus, causes complications that force the model to be inconsistent.

In addition, I will review the instabilities inherent with magnetizing the $\mathbb{Z}_2 \times \mathbb{Z}_2$ structure.

4.1 Magnetic Background Construction for Bosons

The effects of introducing background magnetic fields are discussed in [29], [25] and in the bosonic case [24]. I review the basic concepts in the context of the bosonic string here, so that the construction of the $\mathbb{Z}_2 \times \mathbb{Z}_2$ model is more transparent.

The terms in the standard bosonic action are supplemented with additional terms that allow a gauge field to interact with the string end points. The full bosonic action is

$$S_{\text{bosonic}} = -\frac{1}{4\pi\alpha'} \int d^2\sigma \partial_\alpha X_\mu \partial^\alpha X^\mu - q_L \int d\tau A_\mu \partial_\tau X^\mu \Big|_{\sigma=0} - q_R \int d\tau A_\mu \partial_\tau X^\mu \Big|_{\sigma=\pi} \quad (4.1.1)$$

with $A_\mu = -\frac{1}{2}F_{\mu\nu}X^\nu$ for a constant field tensor $F_{\mu\nu}$. In addition to the well know wave equation for the fields X^μ , one also has boundary conditions that now mix Dirichlet and Neumann conditions

$$\begin{aligned} \partial_\sigma X^\mu - 2\pi\alpha' q_L F_\nu^\mu \partial_\tau X^\nu &= 0, & \sigma = 0, \\ \partial_\sigma X^\mu + 2\pi\alpha' q_R F_\nu^\mu \partial_\tau X^\nu &= 0, & \sigma = \pi. \end{aligned} \quad (4.1.2)$$

The action (4.1.1) describes the effect of open strings coupling to boundaries that carry the source charge for such magnetic fields. As such, these boundaries are considered as magnetic monopoles, where the left and right boundaries carry the charges q_L and q_R respectively.

After the complex redefinitions $Z = \frac{1}{\sqrt{2}}(X^1 + iX^2)$ and $\bar{Z} = \frac{1}{\sqrt{2}}(X^1 - iX^2)$ in the j^{th} torus, in the case that the total charge

$$Q = q_L + q_R \quad (4.1.3)$$

is nonzero, the corresponding wave function has shifted mode numbers. This can be seen from the wave function

$$\psi_n(\tau, \sigma) = \frac{1}{\sqrt{|n - \xi_j|}} \cos[(n - \xi_j)\sigma + \gamma_j] e^{-i(n - \xi_j)\tau}, \quad (4.1.4)$$

with $\gamma_j = \tan^{-1}(2\pi\alpha'q_L H_j)$, of the string coordinate

$$Z = z + i\sqrt{2\alpha'} \left[\sum_{n=1}^{\infty} a_n \psi_n(\tau, \sigma) - \sum_{m=0}^{\infty} b_m^\dagger \psi_{-m}(\tau, \sigma) \right]. \quad (4.1.5)$$

Where ξ is defined as

$$\xi_j = \frac{1}{\pi} (\tan^{-1}(2\pi\alpha'q_L H_j) + \tan^{-1}(2\pi\alpha'q_R H_j)). \quad (4.1.6)$$

This will result in a modification to the components of the energy momentum tensor aligned with the magnetized torus, which defines the relevant parts of the zero Laurent mode as [24]

$$L_0 = \sum_{m=1}^{\infty} (m - \xi_j) a_m^\dagger \cdot a_m + \sum_{m=0}^{\infty} (m + \xi_j) b_m^\dagger \cdot b_m. \quad (4.1.7)$$

The general modes will have a modified Virasoro algebra

$$[L_n, L_m] = (n - m)L_{n+m} + \delta_{n+m,0} \left[\frac{c}{12}(n^3 - n) + n\xi_j(1 - \xi_j) \right], \quad (4.1.8)$$

with an additional c number piece. The original algebra [24] is recovered with the redefinition of the zero mode $L'_0 = L_0 + \frac{1}{2}\xi_j(1 - \xi_j)$. Hence, the contribution to states in the partition function is now

$$\text{Tr} q^{L'_0} = -i \left(q^{\frac{1}{24}} \right)^2 q^{-\frac{1}{2}\xi_j^2} \left(\frac{k_j \eta}{\theta_1(\xi_j \tau | \tau)} \right), \quad (4.1.9)$$

Including the presence of an orbifold operation and twisted modes, the results of (3.1.29) also deform in a similar way to (4.1.9).

The theta function θ_1 is defined by equations (3.1.13) and (3.1.11) with argument $z = \xi\tau$ in the direct channel.

The numbers k_j arise from the non-commutativity of the zero modes and the quantization condition (4.2.9) that allows a degeneracy of exactly k_j for states in of the j^{th} torus. Such numbers will only be present for the bosonic modes that are untwisted and not accompanied by an orbifold operation. Twisted strings will not have Landau levels as they do not have zero modes.

In what follows, I will use the shorthand notation

$$\alpha_j = 2\pi\alpha'qH_j. \quad (4.1.10)$$

for the j^{th} torus

In the case that the total charge is zero $q_L = -q_R$, which represent a dipole string, the situation is a little more subtle. The oscillator frequencies are no longer shifted as $\xi = 0$, although there is still a phase shift according to (4.1.4). As such, the spectrum for this solution is that of a string in the absence of magnetic fields, up to momenta that are now boosted as

$$\tilde{p} = \frac{m}{R\sqrt{1+\alpha^2}}. \quad (4.1.11)$$

This rescaling ensures the consistency of the massless transverse channel amplitude where contributions should form perfect squares.

As such, there will be momenta and winding lattices \tilde{P}^j and \tilde{W}^j that simply denote the conventional lattices with correspondingly altered radii. Under S transformation, one has

$$S : \tilde{P}^j \rightarrow \frac{v_j}{2}(1 + \alpha_j^2)\tilde{W}^j \quad (4.1.12)$$

For untwisted modes, the change in mass caused by the magnetic deformation in the direct channel relates to the field H_j in the following way

$$\Delta M^2 \sim \sum_{j=1,2,3} \{(2n_j + 1)|2\pi\alpha'(q_L + q_R)H_j| + 4\pi\alpha'(q_L + q_R)\Sigma_j H_j\}. \quad (4.1.13)$$

The first term originates from the Landau levels as can be seen from taking into account the contributions from the deformed world sheet bosons. The second arises from the magnetic moments due to spin Σ_j which arise from the world sheet fermions. In the case of contributions from the twisted sector, the Landau terms are absent. As will be discussed, with the absence of the term $(2n_j + 1)|2\pi\alpha'(q_L + q_R)H_j|$, problems with respect to stability in $\mathbb{Z}_2 \times \mathbb{Z}_2$ models will arise. For such cases, tachyonic modes will appear when the second term in ΔM^2 is negative.

4.1.1 Magnetically Deformed Fermions

I review the details of the action on fermionic states by magnetic fields [33].

In addition to the bosonic action defined in (4.1.1), fermions behave, with the introduction of magnetic fields, according to

$$S_{\text{fermionic}} = \frac{i}{4\pi\alpha'} \int d^2\sigma \bar{\psi}^\mu \gamma^\beta \partial_\beta \psi_\mu + \frac{iq_L}{2} \int d\tau F_{\nu\mu} \bar{\psi}^\nu \gamma^0 \psi^\mu \Big|_{\sigma=0} + \frac{iq_R}{2} \int d\tau F_{\nu\mu} \bar{\psi}^\nu \gamma^0 \psi^\mu \Big|_{\sigma=\pi}. \quad (4.1.14)$$

Where the matrices γ^β ($\beta = 0, 1$) satisfy the relation $\{\gamma_\alpha, \gamma_\beta\} = 2h_{\alpha\beta}$. In particular, one has

$$\gamma^0 = \begin{pmatrix} 1 & 0 \\ 0 & 1 \end{pmatrix}, \quad \gamma^1 = \begin{pmatrix} 1 & 0 \\ 0 & -1 \end{pmatrix}. \quad (4.1.15)$$

The variation of $S_{\text{fermionic}}$ with respect to the fields gives the following relations between the left and right moving parts as

$$\begin{aligned}\psi_L^\mu + (-1)^a \psi_R^\mu &= -\pi \alpha' q_R F_\nu^\mu (\psi_R^\nu - (-1)^a \psi_L^\nu) \quad (\sigma = \pi), \\ \psi_L^\mu - \psi_R^\mu &= \pi \alpha' q_L F_\nu^\mu (\psi_R^\nu + \psi_L^\nu) \quad (\sigma = 0).\end{aligned}\quad (4.1.16)$$

For a fermion written as $\psi = (\psi_R, \psi_L)^T$ with NS or R boundary condition $a = 0, 1$ respectively. The coordinates, when made complex using the two coordinates of a torus $\psi_{L,R}^\pm = \frac{1}{\sqrt{2}}(\psi_{L,R} \pm i\psi_{L,R})$, reduce (4.1.16) to

$$\begin{aligned}-(-1)^a \psi_R^\pm &= \frac{(1 \mp i\alpha_R)}{(1 \pm i\alpha_R)} \psi_L^\pm \quad (\sigma = \pi), \\ \psi_R^\pm &= \frac{(1 \pm i\alpha_L)}{(1 \mp i\alpha_L)} \psi_L^\pm \quad (\sigma = 0),\end{aligned}\quad (4.1.17)$$

using the notation (4.1.10) with charges q_L and q_R . The wave functions that satisfy these conditions are

$$\begin{aligned}\chi_{R,n}^\pm &= \frac{1}{\sqrt{2}} \exp[-i(n \pm \xi)(\tau - \sigma_2) \pm itan^{-1}\alpha_L], \\ \chi_{L,n}^\pm &= \frac{1}{\sqrt{2}} \exp[-i(n \pm \xi)(\tau + \sigma_2) \mp itan^{-1}\alpha_L],\end{aligned}\quad (4.1.18)$$

for the fermionic coordinates

$$\psi_{L,R}^\pm(\sigma, \tau) = \sum_n d_n^\pm \chi_{(n)L,R}^\pm(\sigma, \tau). \quad (4.1.19)$$

The resulting L_0 mode is [33]

$$L_0 = - \sum_{n \in \mathbb{Z} + \nu} (n + \xi) : d_{-n}^+ d_n^- : + \Delta \quad (4.1.20)$$

with normal ordering constants $\Delta = \frac{\xi^2}{2}$ (NS) and $\Delta = \frac{1}{8} - \frac{\xi}{2}(1 - \xi)$ (R).

The characters O_2 , V_2 , S_2 and C_2 are then deformed in the direct channel [25] according to

$$\begin{aligned}O_2(\xi) &= \frac{q^{\frac{1}{2}\xi^2}}{2\eta(\tau)} [\theta_3(\xi\tau|\tau) + \theta_4(\xi\tau|\tau)], \\ V_2(\xi) &= \frac{q^{\frac{1}{2}\xi^2}}{2\eta(\tau)} [\theta_3(\xi\tau|\tau) - \theta_4(\xi\tau|\tau)], \\ S_2(\xi) &= \frac{q^{\frac{1}{2}\xi^2}}{2\eta(\tau)} [\theta_2(\xi\tau|\tau) - i\theta_1(\xi\tau|\tau)], \\ C_2(\xi) &= \frac{q^{\frac{1}{2}\xi^2}}{2\eta(\tau)} [\theta_2(\xi\tau|\tau) + i\theta_1(\xi\tau|\tau)].\end{aligned}\quad (4.1.21)$$

The factor ξ contains the charge term which is associated to the magnetic charge of the $D9$ brane, to which the deformed open string is attached. In the case where

an open string is attached to two branes of like charge, this term appears in the theta functions as $\pm 2\xi$. Similarly, for strings stretched between a neutral and charged brane, the contributions are $\pm \xi$.

In studying the tadpole terms, it is only necessary to look at the low lying contributions associated with the deformed theta functions. Such modes, which here are written in the transverse channel, are given as

$$\begin{aligned}
\theta_1(\pm n\xi_j|\tau) &= \mp 2\sin(n\pi\xi_j)q^{\frac{1}{8}}(1 - 2q\cos(2n\pi\xi_j) + \dots) \\
\theta_2(\pm n\xi_j|\tau) &= 2\cos(n\pi\xi_j)q^{\frac{1}{8}}(1 + 2q\cos(2n\pi\xi_j) + \dots) \\
\theta_3(\pm n\xi_j|\tau) &= 1 + 2q^{\frac{1}{2}}\cos(2n\pi\xi_j) + \dots \\
\theta_4(\pm n\xi_j|\tau) &= 1 - 2q^{\frac{1}{2}}\cos(2n\pi\xi_j) + \dots
\end{aligned} \tag{4.1.22}$$

where n takes the value of 1 or 2, in accordance with the charged ends of the string. Here $\xi_j = 2\pi\alpha'qH_j$ (for small H_j) and the charge q is the absolute value of the charge associated with a brane m or \bar{m} .

The low lying character modes (4.1.21) in the transverse channel reduce to

$$\begin{aligned}
O_2(\pm\xi_j) &\sim O_2(\pm 2\xi_j) \sim \frac{1}{\eta}, \\
V_2(\pm\xi_j) &\sim \frac{q^{\frac{1}{2}}}{\eta} \left(\frac{1 - \alpha_j^2}{1 + \alpha_j^2} \right), \\
V_2(\pm 2\xi_j) &\sim \frac{q^{\frac{1}{2}}}{\eta} \left(\frac{1 - 6\alpha_j^2 + \alpha_j^4}{(1 + \alpha_j^2)^2} \right), \\
S_2(\pm n\xi_j) &\sim \frac{q^{\frac{1}{8}}}{\eta} \left(\frac{1 + (1 - n)\alpha_j^2 \pm in\alpha_j}{(1 + \alpha_j^2)^{\frac{n}{2}}} \right), \\
C_2(\pm n\xi_j) &\sim \frac{q^{\frac{1}{8}}}{\eta} \left(\frac{1 + (1 - n)\alpha_j^2 \mp in\alpha_j}{(1 + \alpha_j^2)^{\frac{n}{2}}} \right).
\end{aligned} \tag{4.1.23}$$

These relations illustrate how the tadpoles will be influenced by particular couplings to magnetically charged branes.

Now that the details for the building of magnetically deformed models have been discussed, I now turn to the case of the $\mathbb{Z}_2 \times \mathbb{Z}_2$ model.

4.2 $(T^6/\mathbb{Z}_2 \times \mathbb{Z}_2)(\mathbf{H})$ Structure

The structure of the generators of the $\mathbb{Z}_2 \times \mathbb{Z}_2$ allows a rather rich spectral content in the presence of background magnetic fields. However, the breaking terms that follow from the choice of models with discrete torsion ($\epsilon = -1$) provides inconsistencies. The second class of models belonging to $\epsilon = +1$ has been reported in [30], which does not experience such problems, as will be explained in more detail later.

To illustrate this, I only consider the case with two magnetized tori. As such, the

field tensor $F_{\mu\nu}$ has the block form ($\mu = 4, 5, 6, 7$)

$$\begin{pmatrix} 0 & H_1 & 0 & 0 \\ -H_1 & 0 & 0 & 0 \\ 0 & 0 & 0 & H_2 \\ 0 & 0 & -H_2 & 0 \end{pmatrix}. \quad (4.2.1)$$

The model that is considered here is one with $\epsilon = (+, +, -)$. As such, the Chan-Paton charges corresponding to $D9$ branes, which have been defined for the model with freely acting shifts in table 3.11, break according to

$$\begin{aligned} N'_o &= n' + s + \bar{n}' + \bar{s} \rightarrow N_o + m + \bar{m} \\ N'_g &= i(n' + s - \bar{n}' - \bar{s}) \rightarrow N_g + i(m - \bar{m}) \\ N'_f &= i(n' - s - \bar{n}' + \bar{s}) \rightarrow N_f + i(m - \bar{m}) \\ N'_h &= n' - s + \bar{n}' - \bar{s} \rightarrow N_h + m + \bar{m}. \end{aligned} \quad (4.2.2)$$

Where $n' = n + m$, $\bar{n}' = \bar{n} + \bar{m}$, the prime therefore refers the original non-deformed stack of branes.

One begins with a stack of l parent $D9$ branes, $2p$ of them are then charged magnetically, p with charge q and the same number of charge $-q$. This allows the compact tori to support fields from monopoles to have vanishing total charge. Any factors assigned to the parent Chan-Paton charges are inherited by the magnetically charged stacks, as shown in (4.2.2).

The direct channel annulus that results from such breaking's of the $D9$'s separates into three pieces. Firstly, the uncharged sectors, or $Q = 0$, are given by

$$\begin{aligned} \mathcal{A}_{(Q=0)} &= \frac{1}{8} \left\{ \left(N_o^2 P^1 P^2 P^3 + 2m\bar{m}\tilde{P}_1\tilde{P}_2P_3 \right) T_{oo}(0,0) + \frac{D_{ko}^2}{2} P^k W^l W^s T_{oo} \right. \\ &\quad + \left(N_g^2 P^1 + 2m\bar{m}\tilde{P}^1 \right) T_{og}(0,0) \left(\frac{2\eta}{\theta_2(0)} \right)^2 \\ &\quad + \left(N_f^2 P^2 + 2m\bar{m}\tilde{P}^2 \right) T_{of}(0,0) \left(\frac{2\eta}{\theta_2(0)} \right)^2 \\ &\quad + \left(N_h^2 P^3 + 2m\bar{m}\tilde{P}^3 \right) T_{oh}(0,0) \left(\frac{2\eta}{\theta_2(0)} \right)^2 \\ &\quad + \left(D_{kk}^2 P^k + D_{lk}^2 W^k \right) T_{ok} \left(\frac{2\eta}{\theta_2} \right)^2 \\ &\quad + 2N_o D_{ko} P^k T_{ko}^{(\epsilon_k)}(0,0) \left(\frac{\eta}{\theta_4} \right)^2 \\ &\quad - 2N_k D_{kk} P_k T_{kk}^{(\epsilon_k)}(0,0) \left(\frac{\eta}{\theta_3} \right)^2 \\ &\quad \left. + 2i(-1)^{k+l} N_l D_{kl} T_{kl}^{(\epsilon_k)}(0,0) \frac{2\eta^3}{\theta_2\theta_3\theta_4} \right\} \end{aligned}$$

$$\begin{aligned}
& +D_{ko}D_{lo}W^sT_{so}^{(\epsilon_k\epsilon_l)}\left(\frac{\eta}{\theta_4}\right)^2 \\
& -D_{ks}D_{ls}W^sT_{ss}^{(\epsilon_k\epsilon_l)}\left(\frac{\eta}{\theta_3}\right)^2 \\
& +2i(-1)^{m+k}D_{kk}D_{lk}T_{mk}^{(\epsilon_k\epsilon_l)}\frac{2\eta^3}{\theta_2\theta_3\theta_4}\}.
\end{aligned} \tag{4.2.3}$$

Then, the $|Q| = 1$ terms are

$$\begin{aligned}
\mathcal{A}_{(|Q|=1)} = & \frac{1}{8}\left\{-2N_o(m+\bar{m})T_{oo}(\xi_1\tau, \xi_2\tau)\left(\frac{k_1\eta}{\theta_1(\xi_1\tau|\tau)}\right)\left(\frac{k_2\eta}{\theta_1(\xi_2\tau|\tau)}\right)P^3\right. \\
& +2N_g(m-\bar{m})T_{og}(\xi_1\tau, \xi_2\tau)\left(\frac{k_1\eta}{\theta_1(\xi_1\tau|\tau)}\right)\left(\frac{2\eta}{\theta_2(\xi_2\tau|\tau)}\right)\left(\frac{2\eta}{\theta_2(0)}\right) \\
& +2N_f(m-\bar{m})T_{of}(\xi_1\tau, \xi_2\tau)\left(\frac{2\eta}{\theta_2(\xi_1\tau|\tau)}\right)\left(\frac{k_2\eta}{\theta_1(\xi_2\tau|\tau)}\right)\left(\frac{2\eta}{\theta_2(0)}\right) \\
& +2N_h(m+\bar{m})T_{oh}(\xi_1\tau, \xi_2\tau)\left(\frac{2\eta}{\theta_2(\xi_1\tau|\tau)}\right)\left(\frac{2\eta}{\theta_2(\xi_2\tau|\tau)}\right)P^3 \\
& -2i(m+\bar{m})D_{go}T_{go}^{(\epsilon_1)}(\xi_1\tau, \xi_2\tau)\left(\frac{k_1\eta}{\theta_1(\xi_1\tau|\tau)}\right)\left(\frac{\eta}{\theta_4(\xi_2\tau|\tau)}\right)\left(\frac{\eta}{\theta_4(0)}\right) \\
& -2i(m+\bar{m})D_{fo}T_{fo}^{(\epsilon_2)}(\xi_1\tau, \xi_2\tau)\left(\frac{\eta}{\theta_4(\xi_1\tau|\tau)}\right)\left(\frac{k_2\eta}{\theta_1(\xi_2\tau|\tau)}\right)\left(\frac{\eta}{\theta_4(0)}\right) \\
& +2(m+\bar{m})D_{ho}T_{ho}^{(\epsilon_3)}(\xi_1\tau, \xi_2\tau)\left(\frac{\eta}{\theta_4(\xi_1\tau|\tau)}\right)\left(\frac{\eta}{\theta_4(\xi_2\tau|\tau)}\right)P_3 \\
& -2(m-\bar{m})D_{gg}T_{gg}^{(\epsilon_1)}(\xi_1\tau, \xi_2\tau)\left(\frac{k_1\eta}{\theta_1(\xi_1\tau|\tau)}\right)\left(\frac{\eta}{\theta_3(\xi_2\tau|\tau)}\right)\left(\frac{\eta}{\theta_3(0)}\right) \\
& -2(m-\bar{m})D_{ff}T_{ff}^{(\epsilon_2)}(\xi_1\tau, \xi_2\tau)\left(\frac{\eta}{\theta_3(\xi_1\tau|\tau)}\right)\left(\frac{k_2\eta}{\theta_1(\xi_2\tau|\tau)}\right)\left(\frac{\eta}{\theta_3(0)}\right) \\
& -2(m+\bar{m})D_{hh}T_{hh}^{(\epsilon_3)}(\xi_1\tau, \xi_2\tau)\left(\frac{\eta}{\theta_3(\xi_1\tau|\tau)}\right)\left(\frac{\eta}{\theta_3(\xi_2\tau|\tau)}\right)P_3 \\
& +2(m-\bar{m})D_{fg}T_{fg}^{(\epsilon_2)}\frac{2\eta^3}{\theta_4(\xi_1\tau|\tau)\theta_2(\xi_2\tau|\tau)\theta_3(0)} \\
& -2(m-\bar{m})D_{hg}T_{hg}^{(\epsilon_3)}\frac{2\eta^3}{\theta_4(\xi_1\tau|\tau)\theta_3(\xi_2\tau|\tau)\theta_2(0)} \\
& +2(m-\bar{m})D_{gf}T_{gf}^{(\epsilon_1)}\frac{2\eta^3}{\theta_2(\xi_1\tau|\tau)\theta_4(\xi_2\tau|\tau)\theta_3(0)} \\
& +2(m-\bar{m})D_{hf}T_{hf}^{(\epsilon_3)}\frac{2\eta^3}{\theta_3(\xi_1\tau|\tau)\theta_4(\xi_2\tau|\tau)\theta_2(0)} \\
& +2i(m+\bar{m})D_{gh}T_{gh}^{(\epsilon_1)}\frac{2\eta^3}{\theta_2(\xi_1\tau|\tau)\theta_3(\xi_2\tau|\tau)\theta_4(0)} \\
& \left.-2i(m+\bar{m})D_{fh}T_{fh}^{(\epsilon_2)}\frac{2\eta^3}{\theta_3(\xi_1\tau|\tau)\theta_2(\xi_2\tau|\tau)\theta_4(0)}\right\}.
\end{aligned} \tag{4.2.4}$$

And finally, the $|Q| = 2$ terms are

$$\begin{aligned}
\mathcal{A}_{(|Q|=2)} &= \frac{1}{8} \left\{ - (m^2 + \bar{m}^2) T_{oo}(2\xi_1\tau, 2\xi_2\tau) \left(\frac{2k_1\eta}{\theta_1(2\xi_1\tau|\tau)} \right) \left(\frac{2k_2\eta}{\theta_1(2\xi_2\tau|\tau)} \right) P^3 \right. \\
&\quad + i(m^2 + \bar{m}^2) T_{og}(2\xi_1\tau, 2\xi_2\tau) \left(\frac{2k_1\eta}{\theta_1(2\xi_1\tau|\tau)} \right) \left(\frac{2\eta}{\theta_2(2\xi_2\tau|\tau)} \right) \left(\frac{2\eta}{\theta_2(0)} \right) \\
&\quad + i(m^2 + \bar{m}^2) T_{of}(2\xi_1\tau, 2\xi_2\tau) \left(\frac{2\eta}{\theta_2(2\xi_1\tau|\tau)} \right) \left(\frac{2k_2\eta}{\theta_1(2\xi_2\tau|\tau)} \right) \left(\frac{2\eta}{\theta_2(0)} \right) \\
&\quad \left. + (m^2 + \bar{m}^2) T_{oh}(2\xi_1\tau, 2\xi_2\tau) \left(\frac{2\eta}{\theta_2(2\xi_1\tau|\tau)} \right) \left(\frac{2\eta}{\theta_2(2\xi_2\tau|\tau)} \right) P^3 \right\}. \quad (4.2.5)
\end{aligned}$$

The amplitude stated above is contracted for the sake of brevity, the couplings to the different boundaries m and \bar{m} will of course effect the parameter ξ_j through a change of charge sign.

For comparison, this amplitude is the breaking of the $\mathbb{Z}_2 \times \mathbb{Z}_2$ direct channel annulus shown in equation (G.0.3).

With the direct channel amplitude fully specified, it is then a simple matter to perform an S transformation to obtain the transverse channel.

4.2.1 Tadpole Conditions

One finds that the untwisted sectors from the breaking's (4.2.3), (4.2.4) and (4.2.5) give rise to tadpoles that cancel consistently. These do present some subtleties that are similar in nature to those discussed in [25] for the simpler six dimensional model $T^4/\mathbb{Z}_2(H_1, H_2)$. However, these are made to reduce to consistent tadpole cancellation conditions with the constraints $m = \bar{m}$ and $H_1 = -H_2$ as was the case for the $T^4/\mathbb{Z}_2(H_1, H_2)$ model. It is noted that the choice for the fields that minimizes tachyonic excitations (which will be discussed thoroughly later) is $H_1 = -H_2$.

The twisted sector is more complicated. To illustrate this, I first consider the g -twisted sector. The R - R contributions from τ_{gh} and τ_{gf} reduce to their generic fixed point arrangements with an additional term which is proportional to α_1 .

In the case of τ_{gh} , with the deformations generated by (4.2.2), and the constraint $H_1 = -H_2$, one has the R - R contribution as

$$\begin{aligned}
\tilde{\mathcal{A}}_o^g &= \frac{2^{-5}}{8} \left\{ \left(\sqrt{v_1} [N_g + i(m - \bar{m}) + (m + \bar{m})\alpha_1] \right. \right. \\
&\quad \left. \left. - 4\sqrt{v_1} D_{gg} - 2\frac{1}{\sqrt{v_1}} D_{fg} + 2\frac{1}{\sqrt{v_1}} D_{hg} \right)^2 \right. \\
&\quad + 3 \left(\sqrt{v_1} [N_g + i(m - \bar{m}) + (m + \bar{m})\alpha_1] - 2\frac{1}{\sqrt{v_1}} D_{f:g} \right)^2 \\
&\quad + 3 \left(\sqrt{v_1} [N_g + i(m - \bar{m}) + (m + \bar{m})\alpha_1] + 2\frac{1}{\sqrt{v_1}} D_{h:g} \right)^2 \\
&\quad \left. + v_1 \left(N_g + i(m - \bar{m}) + (m + \bar{m})\alpha_1 \right)^2 \right\}. \quad (4.2.6)
\end{aligned}$$

This is just the fixed point structure of the generic $\mathbb{Z}_2 \times \mathbb{Z}_2$ for τ_{gh} after the substitution $N_g \rightarrow N_g + i(m - \bar{m}) + (m + \bar{m})\alpha_1$. So, after identification of conjugate multiplicities $(m - \bar{m}) = N_g = 0$, the expression (4.2.6) reduces to

$$2^{-5}(m + \bar{m})^2\alpha_1^2. \quad (4.2.7)$$

A similar case arises for the $NS - NS$ contributions, which after the identification $H_1 = -H_2$ and $m = \bar{m}$ has a residual term proportional to α_2^2 . In a reversed sense, those from the f -twisted sector are opposite, such that $R - R$ sector carries a residual contribution from α_2^2 , and the $NS - NS$ similarly has remaining term proportional to α_1^2 . For terms in the h -twisted sector, the resulting spectrum is inherently free of such residual terms, and so behaves as the tadpole term of the non-deformed case.

In the transverse channel, the constraint on the twisted sector is that it should cancel by itself. For the untwisted terms, the Klein bottle and Mobius contributions allow a constraint on the Chan-Paton factors other than zero. The Klein and the Mobius amplitude do not contain twisted terms with which to help cancellation of twisted terms in the annulus. In table G.1, such conditions are shown as $N_j = 0$ ($j \neq 0$).

In chapter 3 it was seen, in relation to the cancellation of the $D5$ tadpoles of the $\epsilon = +1$ cases, that the $NS-NS$ and $R-R$ sectors do not mutually cancel for models other than $(+, +, +)$. However, one could still obtain an spectrum that was anomaly free with respect to the cancellation of the $R-R$ charges of the $D5$'s and $O5$'s by ensuring that the $R-R$ conditions were satisfied. Non-zero $NS-NS$ tadpole terms have an interpretation as a correction to the vacuum energy through the low-energy effective action [25]. In the above case, the residual term is present for both the $R-R$ and $NS-NS$ sectors. Therefore, the model is not capable of cancelling the net $R-R$ charge.

Moreover, the form of the twisted tadpole terms are representative of the correct counting of the occupation of fixed points by the various brane types. Under magnetic deformation, equation (4.2.6) shows that the residual term is not consistent with this interpretation. The fixed point occupation counting for the magnetically charged branes are taken in to account by $i(m - \bar{m})$ and those of the uncharged ones by N_g . By arguments above, this will also be the case for the f -twisted sector.

These types of residual terms in the twisted sector are an artifact of the action on the world sheet bosonic and fermionic modes by the $\mathbb{Z}_2 \times \mathbb{Z}_2$ group generators. The six dimensional case considered [25] was an orbifold breaking of the form $T^4/\mathbb{Z}_2(H_1, H_2) \equiv (T^2(H_1) \times T^2(H_2))/\mathbb{Z}_2$. The action of the orbifold on the bosonic coordinates would then act in all internal directions, thereby allowing the same mode deformations, caused by the magnetic fields in both tori. In the case of the $\mathbb{Z}_2 \times \mathbb{Z}_2$, the set of generators are permutations of the operator $(+1, -1, -1)$ that act on $T_{45}^2 \times T_{67}^2 \times T_{89}^2$. Consequently, it is only possible to align the orbifold directions with those of the charged branes (in this model with $H_1, H_2 \neq 0$ and $H_3 = 0$) consistent with the $h = (-1, -1, +1)$ generator. This alignment effectively allows the h -twisted sector to be free of this complication.

Alternatively, for the choice of $\epsilon = +1$ (without discrete torsion) as discussed in [30] and section 3.3, the parent torus amplitude leaves such twisted terms absent in the resulting annulus amplitude. However, this removes the breaking terms that could otherwise define unitary representations for the $D9$ (that are not magnetically charged) and $D5$ branes. For the case ($\epsilon = +1$), one has either orthogonal or symplectic groups, and so the resulting models are less appealing phenomenologically, although the branes that carry magnetic charge are still unitary.

The method for keeping groups of unitary type while magnetizing two tori is discussed in chapter 5, this method was reported in [30].

4.2.2 Mass Shifting and Tachyonic Instabilities

In the presence of magnetized tori, tachyonic modes are present by virtue of the shift in mass that a magnetic deformation causes (4.1.13). This shifting occurs in the direct channel, since the deforming parameter ξ is now accompanied by the measure parameter τ as $\xi\tau$. These additional parts now provide a change in the mass squared as they can be written as powers of q .

I briefly review the respective contributions of the world sheet bosons and fermions to the mass shift (4.1.13). The world sheet fermion deformations are given by

$$\begin{aligned} O_2(m\xi_j\tau) &\sim_z \frac{1}{\eta}, \quad V_2(m\xi_j\tau) \sim_z \frac{q^{\frac{1}{2}}}{\eta}(q^{m\xi_j} + q^{-m\xi_j}) \\ C_2(m\xi_j\tau) &\sim_z \frac{q^{\frac{1}{8}}}{\eta}q^{-\frac{m\xi_j}{2}}, \quad S_2(m\xi_j\tau) \sim_z \frac{q^{\frac{1}{8}}}{\eta}q^{\frac{m\xi_j}{2}}. \end{aligned}$$

In the case of magnetically deformed world sheet bosonic modes, with and without an orbifold projection, the low lying modes are respectively

$$\begin{aligned} \frac{mk_j\eta}{\theta_1(m\xi_j\tau|\tau)} &\sim_z \frac{-mk_jq^{-\frac{1}{12}}}{\sin(m\pi\xi_j\tau)} = im|k_j|q^{-\frac{1}{12}} \sum_{n_j=0}^{\infty} q^{\frac{1}{2}|m\xi_j|(2n_j+1)}, \\ \frac{\eta}{\theta_2(m\xi_j\tau|\tau)} &\sim_z \frac{q^{-\frac{1}{12}}}{\cos(m\pi\xi_j\tau)} = q^{-\frac{1}{12}} \sum_{n_j=0}^{\infty} (-1)^{n_j} q^{\frac{1}{2}|m\xi_j|(2n_j+1)}. \end{aligned} \quad (4.2.8)$$

Where the index j labels the two directions of the j^{th} torus. The bosonic coordinates are not effected by the change in charge from say an m^2 to \bar{m}^2 coupling. For the deformation of the world sheet bosonic modes, the Landau number k_j is odd under $\xi_j \rightarrow -\xi_j$, as is the zero mode and thus the deformed lattice as a whole is even. This is reflected by the appearance of $|\xi_j|$ and $|k_j|$.

The dependence of k_j on the charge and field values can be seen by the Dirac quantization condition

$$k_j = 2\pi\alpha'qH_jv_j, \quad (4.2.9)$$

for the j^{th} torus.

Firstly, I discuss the instabilities that arise in the untwisted sector. In the case of the spacetime vector $V_2O_2O_2O_2$ and the scalar $O_2O_2O_2V_2$ the mass shift ΔM^2 is proportional to $2|H|$ for both \bar{m}^2 and m^2 couplings. The remaining untwisted scalars have internal vectors that lie in the tori with magnetic fields and so ΔM^2 has contributions from the magnetic moment terms. For $O_2V_2O_2O_2$ one finds that the shift in mass is $3|H|$ and $|H|$ for m^2 and \bar{m}^2 couplings respectively. In a reversed sense (because $H_1 = -H_2$) the relevant terms are $|H|$ and $3|H|$ for m^2 and \bar{m}^2 respectively for $O_2O_2V_2O_2$.

In the Ramond untwisted sector, for terms of the form S_2S_2 lying in the first two tori, the mass shift is $4|H|$ for m^2 couplings and zero for the \bar{m}^2 ones. Similarly, those of

Character	Diagram	Mass shift
τ_{gh}	$O_2O_2S_2S_2$	$\Delta M^2 \sim \pm(H_2 + H_3)$
	$S_2C_2O_2O_2$	$\Delta M^2 \sim \mp H_1$
τ_{gf}	$O_2O_2C_2C_2$	$\Delta M^2 \sim \pm(H_2 + H_3)$
	$C_2S_2O_2O_2$	$\Delta M^2 \sim \mp H_1$
τ_{hg}	$O_2C_2C_2O_2$	$\Delta M^2 \sim \pm(H_1 + H_2)$
	$C_2O_2O_2S_2$	$\Delta M^2 \sim \mp H_3$
τ_{hf}	$O_2S_2S_2O_2$	$\Delta M^2 \sim \pm(H_1 + H_2)$
	$S_2O_2O_2C_2$	$\Delta M^2 \sim \mp H_3$
τ_{fg}	$O_2C_2O_2C_2$	$\Delta M^2 \sim \pm(H_1 + H_3)$
	$C_2O_2S_2O_2$	$\Delta M^2 \sim \mp H_2$
τ_{fh}	$O_2S_2O_2S_2$	$\Delta M^2 \sim \pm(H_1 + H_3)$
	$S_2O_2C_2O_2$	$\Delta M^2 \sim \mp H_2$

Table 4.1: Twisted sector mass shifts for $\mathbb{Z}_2 \times \mathbb{Z}_2$ model

C_2C_2 have the same values for opposite couplings. The terms with C_2S_2 or S_2C_2 aligned with the first two tori don't have contributions from the magnetic moment couplings and so give ΔM^2 proportional to $2|H|$.

In conclusion, strings from the untwisted sector that arise from the couplings m^2 and \bar{m}^2 give either massless or massive states and so tachyonic excitations are absent. States from terms involving $\bar{m}m$ couplings remain massless since $q_L + q_R = 0$.

The terms that contribute massless modes in the $\mathbb{Z}_2 \times \mathbb{Z}_2$ twisted sector without magnetic fields are illustrated in table 4.1 (in the second column) alongside their mass shifts under magnetic deformation (the \pm refers to the net charge sign of the branes in the coupling, and is correlated for the two terms in a given character).

There are six distinct choices for the fields H_j that will minimize instabilities (for two magnetized tori)

$$\begin{aligned}
H_2 &= -H_3, H_1 = 0, H_3 > 0 \text{ or } H_3 < 0, \\
H_1 &= -H_2, H_3 = 0, H_2 > 0 \text{ or } H_2 < 0, \\
H_1 &= -H_3, H_2 = 0, H_1 > 0 \text{ or } H_1 < 0.
\end{aligned}$$

In the case at hand I consider only H_1 and H_2 to be nonzero. With this configuration, characters in the h -twisted sector are exactly massless. The characters of the remaining sectors contain tachyons. So again one sees that the h -sector is free of possible complications from the presence of magnetic fields.

It is clear that it is not possible to remove these instabilities by choice of fields due to the absence of Landau contributions and the sensitivity to charge sign from the magnetic moment parts.

4.3 Discussion

It has been shown in the previous section that the form of the $\mathbb{Z}_2 \times \mathbb{Z}_2$ ($\epsilon = -1$) with two background magnetic fields, gives low lying states in the transverse amplitude that

provide inconsistencies through residual terms proportional to the magnetic fields. In the conventional $\mathbb{Z}_2 \times \mathbb{Z}_2$ model (without magnetized $D9$'s), the tadpole conditions for the terms N_g , N_f and N_h must be (and are) identically zero.

There are no twisted sectors in the transverse Klein or Mobius with which to assist with cancellation of these terms. Therefore, the annulus amplitude defined with the presence of discrete torsion, cannot be magnetized to give a consistent spectrum. This is true for the case of choosing either one or two fields to be nonzero. What form these inconsistencies might have for the case of three internal fields is not clear, though it is expected that similar problems will arise.

In order to include magnetic backgrounds in models with transverse twisted sectors, one must have some control over what form these states have, as has been done in [30]. This will be discussed more concisely in chapter 5.

As an additional point, the aim of implementing background fields in this way was to obtain a solution of the form $U(8 - m)_9 \times U(m)_9 \times U(8)_5$. Here the original stack of $D9$'s could be broken to $U(6)_9 \times U(2)_9 \times U(8)_5$ using the solution of $m = 2$. In order to reduce the rank of all families of branes, one could then allow the existence of a background antisymmetric tensor [25], [27].

The B_{ab} field is introduced as a generalization of the momenta in the compact directions

$$p_{L,a} = m_a + \frac{1}{\alpha'}(g_{ab} - B_{ab})n^b,$$

$$p_{R,a} = m_a - \frac{1}{\alpha'}(g_{ab} + B_{ab})n^b,$$

for momenta and winding quantum numbers m_a and n^b . Retaining the symmetry of world sheet parity under Ω , the B_{ab} field takes on quantized values. The projector that is necessary in the trace of the partition function carries a normalization factor which is dependant on the rank of this field. This factor forces the tadpole conditions to be sensitive to the value of the rank r of the B_{ab} field. Thus the rank of the gauge group can be reduced accordingly.

The next step would be to allow the presence of discrete Wilson lines that would allow a reduction by half of the $D5$ stacks, thus obtaining a group of the form $U(3)_9 \times U(2)_5 \times U(1)_9$ (after using the antisymmetric field B_{ab} of appropriate rank).

The method for doing this kind of background setting is also reviewed in chapter 5, where I discuss work similar to the intended idea presented here that was implemented in [30].

Chapter 5

Conclusions

The three chapters that have been presented detail particular phenomenologically motivated aspects of the free fermionic heterotic and type I string limits.

The heterotic model described in the context of this work shows a construction based on the NAHE set $\{1, S, b_1, b_2, b_3\}$ and the additional vectors $\{\alpha, \beta, \gamma\}$. The particular choice of phase

$$C \begin{pmatrix} b_3 \\ \beta \end{pmatrix} = -1$$

is made. It was noted in contrast to model 3, which chooses this term as $+1$, that this causes an enhancement to the observable and hidden sector gauge groups. In particular, they are enhanced from $SU(3)$ to $SU(4)$.

The trace of the anomalous charge Q_A of this model is $\text{Tr}Q_A = -72$. It was shown that the spectrum does not contain Abelian VEVs that could cancel this contribution to allow D -flatness. The only VEVs that could be utilized to cancel the contribution of -72 arose from non-Abelian fields.

This is the first instance where the use of non-Abelian VEVs has been enforced in order for D -flatness, as opposed to other possible phenomenological reasons.

However, it was outlined that this particular model does not pertain to a realistic model. And so this study is discussed as an instance of an extended NAHE set based toy model which requires non-Abelian VEVs to satisfy the flat direction constraints. In examples such as that presented here, one can gain some intuition for phenomenology that arises from basis vectors that give rise to a large spectral content. While efforts have been made to quantify the effects that certain vectors and phases have on a models content, there is no general set of instructions to determine the precise phenomenology desired when attempting to design appropriate basis vectors and GSO phases. Therefore, this is yet another model which will help to highlight the relationship between the physics of models and their basis vectors/GSO phases. In particular, an enhancement to the observable and hidden sector gauge groups and more importantly, the need for non-Abelian VEVs to retain supersymmetry at the FI scale.

Models based on the NAHE set have provided a basis on which a great deal of study has been focused. The NAHE set contains the basis vectors $\{b_1, b_2, b_3\}$ which provide the $\mathbb{Z}_2 \times \mathbb{Z}_2$ structure of the one-loop partition function. The gauge group after this set is $SO(10) \times E_8 \times SO(6)^3$, which as stated before contains three $\mathbf{16}$'s of $SO(10)$, one from each of the vectors b_j .

Any study of string theory is motivated by the correspondence it has with the real world. Agreement with low energy physics, or the phenomenology of the standard model, is a basis on which to guide the efforts of research. The NAHE set has shown to be an underlying set with which to build and explore phenomenologically viable models within the heterotic limit.

In the type I limit, the models studied are freely acting shift \mathbb{Z}_2^s modulations of the \mathbb{Z}_2 and $\mathbb{Z}_2 \times \mathbb{Z}_2$ orbifolds. In contrast to the model that includes the $\mathbb{Z}_2 \times \mathbb{Z}_2$ orbifold geometry, the toy model is a pseudo $\mathbb{Z}_2 \times \mathbb{Z}_2$ geometry with only orbifold actions in the last two tori. This leads to a simplified spectrum with an absence of those terms corresponding to independent orbits (see appendix B), since the other $\mathbb{Z}_2 \times \mathbb{Z}_2$ generator acts only to shift the coordinates by $\frac{\pi R}{2}$.

The spectrum of the open sector admitted propagation of twisted sectors in the transverse channel. In turn, this allowed Chan-Paton factors to be interpreted as unitary terms. The gauge group therefore became unitary.

Adding in an additional orbifold generator to the trace of this model, and allowing the shift to act in all directions, one then has the next model based on the $\mathbb{Z}_2 \times \mathbb{Z}_2$ orbifold. This model proved to be more subtle both in its orientifold structure and its open descendants. To begin with, the torus partition function by itself defines an enhancement of the generic $\mathbb{Z}_2 \times \mathbb{Z}_2$ torus with additional $n + \frac{1}{2}$ massive states in the twisted sector. While the untwisted sector also has these types of states, it acquires a projection of the form $(1 + (-1)^{m_1+m_2+m_3})$. The low lying states in the torus shows that the number of fixed points, originally 16 for the generic $\mathbb{Z}_2 \times \mathbb{Z}_2$ model, are halved. Similar arguments are valid for the toy model.

In taking the orientifold projection of the torus amplitude, one finds a subtlety. Use of a generic orientifold gave rise to the counting of states in the Klein amplitude that give an inconsistent perfect square structure. The perfect square in the Klein amplitude represents the reflection coefficients of a closed string propagating between two O -plane's. The requirement that the coefficients of propagating closed string states between boundaries be perfect squares is condition that must be satisfied.

In this respect, a naive Ω projection gave rise to massive states of the form $W_{n+\frac{1}{2}}$ in the $O5_i-O5_j$ ($i \neq j$) couplings. As it would stand, this term maps under S to give rise to contributions that don't admit a perfect square structure. In this case, the eigenvalues of this coupling were forced to acquire different signs, so that the total was zero. As such, this term no longer appears in the counting and was then made so as to not interfere with the perfect squares.

A similar case was shown to arise in a T^4/\mathbb{Z}_2 model. However, this involved an eigenvalue reassignment (or sign redefinition of Ω) when using the unusual global form of Ω with the phase $(-1)^m$ as a model freedom. As such, a reassignment of eigenvalues was forced by taking a different choice of the parity operator. In the model discussed here, one begins with a conventional Ω which leads to the same reassignment for similar consistency conditions.

The additional modulation of a \mathbb{Z}_2 shift on the underlying $\mathbb{Z}_2 \times \mathbb{Z}_2$ spectrum allows this model to have orbits that are not related to the principle ones $\{(o, o), (o, g), (o, f), (o, h)\}$. As such there are two classes in a total of eight models that can be defined. The two classes are defined by the choices of $\epsilon = \epsilon_1\epsilon_2\epsilon_3 = \pm 1$ which is a sign freedom attached to the terms corresponding to the independent orbits. The spectral content is quite dif-

ferent between the two classes, while those models within each class differ with respect to the types of O -plane and D -brane present (which in turn effects a models supersymmetry). The only model that is fully supersymmetric is that defined by $\epsilon_j = +1$.

Models with $\epsilon = +1$ define the simplest of the two cases. It was shown in equation (3.3.2) that $\epsilon = +1$ choice does not admit the appropriate form of the twisted states so as to have twisted sectors in the transverse annulus. The open descendants are thus limited to untwisted states in the transverse channel.

The annulus amplitude of the $\mathbb{Z}_2 \times \mathbb{Z}_2$ ($\epsilon = +1$) models required a rescaling of the Chan-Paton charges, since there are no breaking terms present. The inclusion of the \mathbb{Z}_2 shift required an additional rescaling of the $D5$ charges, thus halving the corresponding group size. The gauge groups display different behavior in the case $(+, +, +)$ from the others in the same class. In this case the groups corresponding to all branes were unitary symplectic. In the cases that were permutations of $(+, -, -)$, one sees a change for the $D9$ -branes as orthogonal. The $D5$ -branes were orthogonal, whereas the $\bar{D}5$ -branes were unitary symplectic.

While the class of models belonging to $\epsilon = +1$ allow a rich spectrum with rank reduction of the $D5$ groups, the breaking terms that come from the twisted sectors in the transverse channel are absent. As such, unitary groups, and hence a more phenomenologically interesting spectrum (in the motivation to look at matter coupled to unitary groups) could not be obtained.

In the second class of models corresponding to $\epsilon = -1$, one has a vastly richer spectrum of states. In this case, it was seen that the torus admits the flow of twisted sectors in the transverse annulus. From this, one obtains breaking terms that allow the Chan-Paton charges as unitary for $D9$ and $D5$ couplings and symplectic for $\bar{D}5$ -branes.

However, the complexity of this amplitude causes a problem in the twisted sector of the direct channel $D5_i$ - $D5_j$ ($i \neq j$) couplings. In this case, the massless spectrum is entirely consistent with a gauge group of $U(8)_9 \times U(4)_{5_{\{1,2\}}}$ for the $D9$ and two $D5$'s and $USp(4)^4$ for the $\bar{D}5$ with the required halving of the Chan-Paton charges. The $n + \frac{1}{2}$ massive states for the $D5_i$ - $D5_j$ couplings does not give a proper particle interpretation. After taking into account all necessary factors, the coefficients of these terms are equal to $\frac{1}{2}$.

While a solution was not found that gives a proper particle interpretation at all lattice levels, it is regarded that such a solution should exist. The complexity of this model makes it very difficult to implement possible solutions. For example, one could not impose a rescaling of say the $D5$ branes alone, this would cause inconsistent particle counting in both the $D5$ - $D5$ and N - $D5$ sectors. The presence of the twisted terms in the transverse channel allows the Chan-Paton charges to be broken in such a way that the rescaling that was done for the $\epsilon = +1$ is taken into account by this breaking.

Various possibilities for the introduction of auxiliary Wilson lines were discussed. The term which causes the inconsistency will only admit a global phase for the particular lattice state that the $D5_i$ - $D5_j$ term has. Global in this context is simply meant that the phase must act outside the lattice state projector $(1 + (-1)_k^m)$, which would otherwise not be consistent with the corresponding torus amplitude states.

In trying to gain freedom in controlling phenomenologically interesting aspects of these models, such as gauge group rank and type, spectral content (such as matter families and supersymmetry) and the study of backgrounds has proved very forthcoming.

The work that has been presented in chapter 3 looks at the effect of discrete Wilson lines in the form of freely acting shifts. The aim was to obtain models that might be used in conjunction with other backgrounds, to yield a four dimensional gauge group of the form $SU(3) \times SU(2) \times U(1)$. However, the class of ϵ that is consistent with model building requirements only admits matter coupled to orthogonal or symplectic groups.

The motivation for using shifts in this manner was to set the foundation that would lead to a three generation model with a realistic gauge group. One could begin with the $\mathbb{Z}_2 \times \mathbb{Z}_2$ spectra for the case of $(+, +, -)$, which has a unitary configuration of $U(8) \times U(8)$ for the $D9$ and $D5$'s in the 1st and 2nd tori. The freely acting shift allows one to retain the full $\mathbb{Z}_2 \times \mathbb{Z}_2$ characters, with various changes in lattice contributions. This would then yield a low lying spectrum with gauge group $U(8) \times U(4)$. By use of an additional breaking mechanism (such as background magnetic fields), one could realize a group of the form $U(8-m) \times U(m) \times U(4)$. Switching on the background antisymmetric tensor, it would be possible to further control the rank of these groups to get close to or reproduce a standard model like structure. However, as has been shown, the $\epsilon = -1$ model cannot be straight forwardly magnetized.

The work done on freely acting shifts is an extension of the study discussed in [1]. Here, the shifts were used as integral parts of the $\mathbb{Z}_2 \times \mathbb{Z}_2$ generators as

$$\sigma_1(\delta_1, \delta_2, \delta_3) = \begin{pmatrix} \delta_1 & -\delta_2 & -1 \\ -1 & \delta_2 & -\delta_3 \\ -\delta_1 & -1 & \delta_3 \end{pmatrix}, \quad \sigma_2(\delta_1, \delta_2, \delta_3) = \begin{pmatrix} \delta_1 & -1 & -1 \\ -1 & \delta_2 & -\delta_3 \\ -\delta_1 & -\delta_2 & \delta_3 \end{pmatrix} \quad (5.0.1)$$

where δ is a shift operator. In all cases of these models, the terms corresponding to independent orbits are absent. As a consequence of defining shifts and orbifold operations as (5.0.1) the spectrum is projected by operators of the form $-\delta$. On the complex coordinates of the torus, this composite operation has the effect of providing shifted fixed points, as one can see from

$$z_i \sim -z_i + \frac{1}{2} \quad (5.0.2)$$

and so the fixed points coordinate set is $z_i^f = \{\frac{1}{4}, \frac{3}{4}\}$. One then sees in contrast to the freely acting case, that there are no fixed points at the origin. Those of the freely acting shift have the standard fixed points of $\{0, \frac{1}{2}\}$. In addition, of the cases arising from (5.0.1), most of the models are capable of providing matter coupled to unitary gauge groups.

The discussion on background magnetic deformations in chapter 4 looks at the effect of magnetizing the last two tori in the configuration $T_{45}^2 \times T_{67}^2 \times T_{89}^2$ of the $\epsilon = -1$ case of the $\mathbb{Z}_2 \times \mathbb{Z}_2$ open descendants.

Magnetic deformations are a very good way of breaking more precisely the gauge group rank of the $D9$ branes. The presence of such fields introduces additional massive states in the spectrum that correspond to lattices that depend on radii that are scaled according to $R_j \rightarrow R_j(1 + (2\pi\alpha'qH_j))^{\frac{1}{2}}$. Moreover, the Landau degeneracies that exist allow one some freedom (with the guidelines of spectral consistency, i.e. particle interpretation and symmetrization) to control certain matter contributions in the spectrum.

The magnetic deformation of the open descendants that correspond to $\epsilon_j = +1$ have been demonstrated in [30]. In this case, the group structure is a composite of unitary and orthogonal groups. The magnetic charges force the $D9$ stacks to split from the parent $D9$'s as $N \rightarrow N + m + \bar{m}$. As can be seen from this, the gauge groups corresponding to charged branes are unitary.

The deformations presented in this study show the effect on the low lying spectrum and structure of the annulus. The tadpoles in the untwisted sector present the usual subtleties where the reflection coefficients are no longer perfect squares. This is due to the structure of the transverse annulus (3.3.14) and that the boundary terms at either ends of the string are not invariant under the operation \mathcal{T} . However, after identification of the multiplicities $m = \bar{m}$, the invariance is restored and the tadpoles behave in manner similar to the $T^2(H) \times T^2(H)/\mathbb{Z}_2$ model (with the exception of two additional $D5$ sectors and the signs ϵ_j).

Therefore, the untwisted sector is well mannered with respect to cancellation of the tadpoles. The usual disagreement between the $NS-NS$ and $R-R$ sector appear where a negative sign is used for one of the ϵ_j factors.

The tadpoles of the twisted sector however present a deviation from the behavior of those of the untwisted ones. It was shown that after identification of conjugate multiplicities and $H_1 = -H_2$ (as demanded by the cancellation of the untwisted tadpoles), one is left with contributions depending on the magnetic fields.

These types of terms can be avoided in the $\mathbb{Z}_2 \times \mathbb{Z}_2$ formalism by the use of shifts integrated in the $\mathbb{Z}_2 \times \mathbb{Z}_2$ generators. Such work has been shown in [30] using projection operators of the form of equation (5.0.1), which was published independently of the finding in this work.

In particular, they consider a case with a winding shift acting in the second torus and a momentum shift acting in the third. The generic model defined by this arrangement defines a twisted sector which includes only a twist of the form $(+, -, -)$, which acts in the second and third torus. As such, they align two magnetic fields in the same directions as the twist and shift operators. This allows the model to be consistent in terms of symmetrization and free of problematic terms on the transverse channel.

The type I $\mathbb{Z}_2 \times \mathbb{Z}_2$ vacuum generically becomes unstable. Background magnetic fields introduce tachyonic modes in the direct channel. In the untwisted sector, the NS terms for two background fields can at least compensate for any possible instabilities (coming from the magnetic field/spin coupling) with contributions from the magnetically deformed bosons, as can be seen from equation (4.1.13). In the case of three fields, the magnetic/spin coupling terms are overwhelmed, and thus these contribute massive states.

The R untwisted terms are either at least stable (for two fields) or massive (for three fields) due to the presence of only spin- $\frac{1}{2}$ characters. The nature of the twisted characters of the $\mathbb{Z}_2 \times \mathbb{Z}_2$ inherently allows instabilities, which is demonstrated in table 4.1. At the time of writing there is yet no mechanism for allowing a stable type I $\mathbb{Z}_2 \times \mathbb{Z}_2$ vacuum. Such a mechanism would have to include a way of lifting the problematic sectors in mass.

While it is possible to discuss the stability in the case of three background fields, what conditions are forced upon such a configuration are not known. Indeed, what problems might occur (as did with the two field case) are not known. For the two field

case, the condition $H_1 = -H_2$ was a necessary requirement to achieve the untwisted tadpole conditions of the form (as well as partial stability in the twisted sector)

$$\begin{aligned}
N_o + m + \bar{m} &= 32 \\
D_{go} &= 32 \\
D_{fo} &= 32 \\
D_{ho} + \epsilon_3(m + \bar{m})k_1k_2 &= 32.
\end{aligned}
\tag{5.0.3}$$

Such constraints in the three field case are not known, although I would expect them to follow similar lines.

The study of three fields would be a necessary next step in understanding the $\mathbb{Z}_2 \times \mathbb{Z}_2$ with magnetic fields. Magnetizing all three tori would also mean that there is no directional preference given. In the one field case, all twisted sectors carry instabilities and the internal vectors of the untwisted sector also develop tachyon's.

The six dimensional case that involves background magnetization of T^4/\mathbb{Z}_2 that was studied in [25] is completely stable and is free of tachyonic instabilities and inconsistencies in all sectors.

In the interest of studying type I vacua with geometry of the type $\mathbb{Z}_2 \times \mathbb{Z}_2$, it is clear that the current approaches with magnetizing tori is incomplete if one is to assert stability in the vacuum. Continued research in the framework of this geometry with background magnetic fields would ideally seek to achieve the following points:

- Vacuum stability
- Standard model like components
- A way of “freezing” the additional moduli

The last point refers to factors one finds in the spectrum that are related to the Landau-level degeneracy, which manifest themselves as the numbers k_j , as can be seen in the amplitudes (4.2.4) and (4.2.5).

As motivated in the introduction, the study of different string limits related to the $\mathbb{Z}_2 \times \mathbb{Z}_2$ geometry is well founded. The heterotic limit in the free fermionic formalism based on the NAHE set (which contains the $\mathbb{Z}_2 \times \mathbb{Z}_2$ vectors b_1, b_2, b_3) harbors the $SO(10)$ group in the observable sector. Supplemented by additional vectors, this has been shown to give rise to models that reproduce the Minimal Supersymmetric Standard Model in the effective low energy theory.

A mechanism that would provide insight into vacuum selection and a framework with which to describe strings in a more dynamical sense are two very important questions that need to be answered. In addressing these points, it is prudent to continue the study of the different limits and their phenomenological aspects. This is the best guide for determining whether they apply to the real world. This also helps to highlight possible structures that promote new ideas for the resolution of aspects that are not yet fully understood. This is particularly relevant with respect to a mechanism of vacuum selection.

It may well be the case that the hidden vacuum selection mechanism will begin to show once a certain level of intuition is gained in how to interpret the relative limits. However, string phenomenology research has and should continue to provide important guidelines in how the theory of strings is interpreted and applied to the real world.

Appendix A

General Mobius Origin for the A_1 Shift

This is the Mobius origin with Chan-Paton charge parameterizations according to the class of models belonging to $\epsilon = \epsilon_1\epsilon_2\epsilon_3 = +1$. It is provided as a reference to show the explicitly lattice origin structure of the Mobius. And in particular, how the choice of different signs results in the change of group structure.

$$\begin{aligned}
\mathcal{M}_o = & -\frac{1}{4} \left\{ \left(n(1 - \epsilon_1 - \epsilon_2 - \epsilon_3) - d_{go}(1 - \epsilon_1 + \epsilon_2 + \epsilon_3) \right. \right. \\
& \left. \left. - d_{fo}(1 + \epsilon_1 - \epsilon_2 + \epsilon_3) - d_{ho}(1 + \epsilon_1 + \epsilon_2 - \epsilon_3) \right) \hat{\tau}_{oo}^{NS} \right. \\
& - \left(n(1 - \epsilon_1 - \epsilon_2 - \epsilon_3) - d_{go}\epsilon_1(1 - \epsilon_1 + \epsilon_2 + \epsilon_3) \right. \\
& \left. - d_{fo}\epsilon_2(1 + \epsilon_1 - \epsilon_2 + \epsilon_3) - d_{ho}\epsilon_3(1 + \epsilon_1 + \epsilon_2 - \epsilon_3) \right) \hat{\tau}_{oo}^R \\
& + \left(n(1 - \epsilon_1 + \epsilon_2 + \epsilon_3) - d_{go}(1 - \epsilon_1 - \epsilon_2 - \epsilon_3) \right. \\
& \left. - d_{fo}(-1 - \epsilon_1 - \epsilon_2 + \epsilon_3) - d_{ho}(-1 - \epsilon_1 + \epsilon_2 - \epsilon_3) \right) \hat{\tau}_{og}^{NS} \\
& - \left(n(1 - \epsilon_1 + \epsilon_2 + \epsilon_3) - d_{go}\epsilon_1(1 - \epsilon_1 - \epsilon_2 - \epsilon_3) \right. \\
& \left. - d_{fo}\epsilon_2(-1 - \epsilon_1 - \epsilon_2 + \epsilon_3) - d_{ho}\epsilon_3(-1 - \epsilon_1 + \epsilon_2 - \epsilon_3) \right) \hat{\tau}_{og}^R \\
& + \left(n(1 + \epsilon_1 - \epsilon_2 + \epsilon_3) - d_{go}(-1 - \epsilon_1 - \epsilon_2 + \epsilon_3) \right. \\
& \left. - d_{fo}(1 - \epsilon_1 - \epsilon_2 - \epsilon_3) - d_{ho}(-1 + \epsilon_1 - \epsilon_2 - \epsilon_3) \right) \hat{\tau}_{of}^{NS} \\
& - \left(n(1 + \epsilon_1 - \epsilon_2 + \epsilon_3) - d_{go}\epsilon_1(-1 - \epsilon_1 - \epsilon_2 + \epsilon_3) \right. \\
& \left. - d_{fo}\epsilon_2(1 - \epsilon_1 - \epsilon_2 - \epsilon_3) - d_{ho}\epsilon_3(-1 + \epsilon_1 - \epsilon_2 - \epsilon_3) \right) \hat{\tau}_{of}^R
\end{aligned}$$

$$\begin{aligned}
& + \left(n(1 + \epsilon_1 + \epsilon_2 - \epsilon_3) - d_{go}(-1 - \epsilon_1 + \epsilon_2 - \epsilon_3) \right. \\
& \left. - d_{fo}(-1 + \epsilon_1 - \epsilon_2 - \epsilon_3) - d_{ho}(1 - \epsilon_1 - \epsilon_2 - \epsilon_3) \right) \hat{\tau}_{oh}^{NS} \\
& - \left(n(1 + \epsilon_1 + \epsilon_2 - \epsilon_3) - d_{go}\epsilon_1(-1 - \epsilon_1 + \epsilon_2 - \epsilon_3) \right. \\
& \left. - d_{fo}\epsilon_2(-1 + \epsilon_1 - \epsilon_2 - \epsilon_3) - d_{ho}\epsilon_3(1 - \epsilon_1 - \epsilon_2 - \epsilon_3) \right) \hat{\tau}_{oh}^R \}. \quad (\text{A.0.1})
\end{aligned}$$

Appendix B

$\mathbb{Z}_2 \times \mathbb{Z}_2$ Boundary Operators

The $\mathbb{Z}_2 \times \mathbb{Z}_2$ generators including the identity lead to $16 = 4 \times 4$ distinct boundary conditions on the two dimensional sheet. These are portrayed in fig. B.1. The shaded blocks represent those which are not connected to the unshaded ones by the modular invariance group $SL(2, \mathbb{Z})/\mathbb{Z}_2$ which is generated by S and T transforms.

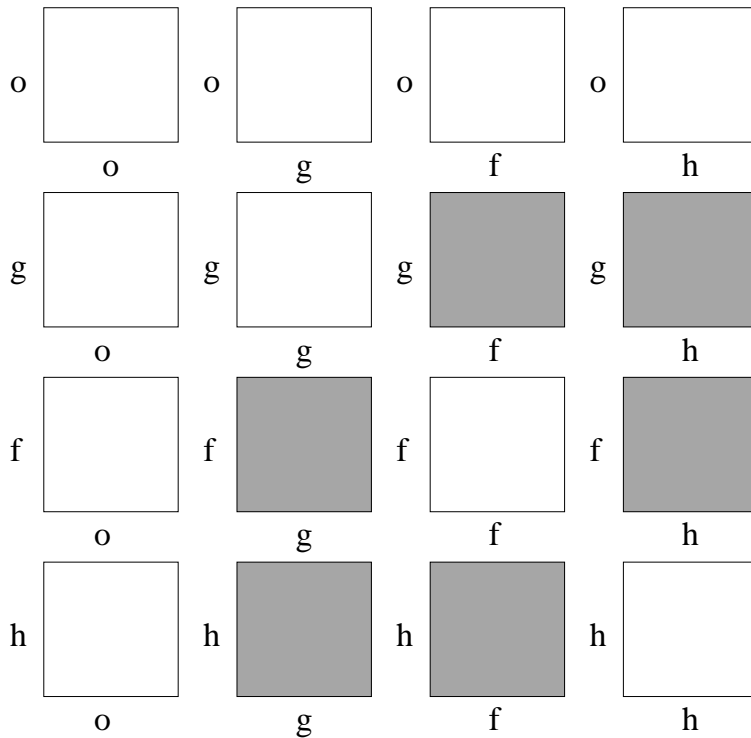


Figure B.1: Distinct boundary sets in the $\mathbb{Z}_2 \times \mathbb{Z}_2$

Appendix C

Tadpole Diagrams

In the transverse (or tube channel) the open strings attached to boundaries are interpreted in terms of closed strings propagating between them. In which case, the two types of boundaries (O -planes and branes) allow the topology of the tubes to be illustrated as in diagram C. At massless level, these are the tadpole diagrams for the Klein bottle (tube with crosscaps), the annulus (simple tube) and the Mobius strip (tube with one crosscap).

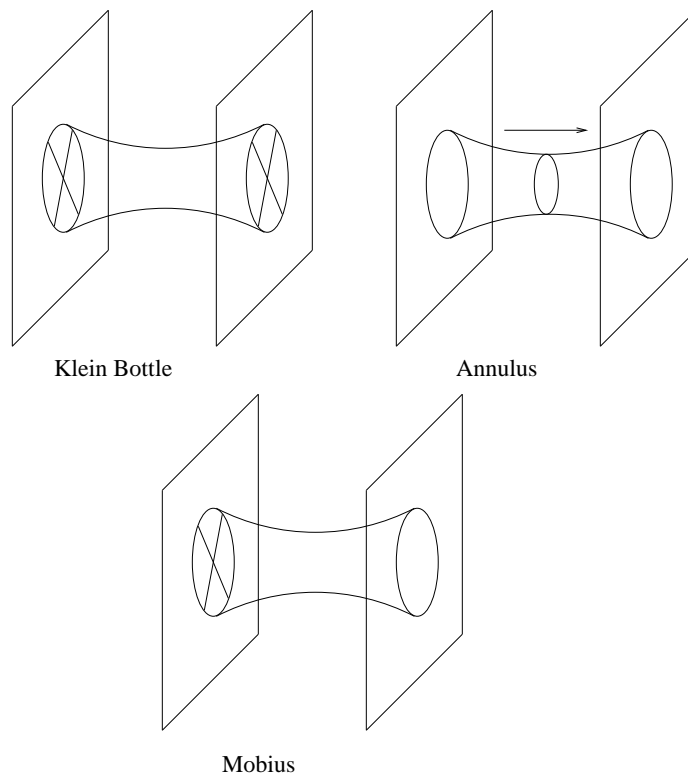


Figure C.1: Distinct boundary sets in the $\mathbb{Z}_2 \times \mathbb{Z}_2$

Appendix D

The Torus Amplitude from its Corresponding Action

Here, a simple case of the one-loop vacuum amplitude from the action of a simple scalar mode with mass M which exists in D dimensions [25] is shown. The action of this field is described by

$$S = \int d^D x \frac{1}{2} \left[\partial_\mu \phi \partial^\mu \phi - M^2 \phi^2 \right]. \quad (\text{D.0.1})$$

In the Euclidean basis, after integrating the fields over all paths, one has the vacuum energy Γ defined as

$$e^{-\Gamma} \sim \det^{-\frac{1}{2}}(-\Delta + M^2) \quad (\text{D.0.2})$$

and using the identity

$$\log(\det(Y)) = - \int_\Lambda^\infty \frac{dt}{t} \text{tr}(e^{-tY}) \quad (\text{D.0.3})$$

(Λ is an ultraviolet cutoff and t is the Schwinger parameter) Γ can be written as

$$\Gamma = -\frac{V}{2} \int_\Lambda^\infty \frac{dt}{t} e^{-tM^2} \int \frac{d^D p}{(2\pi)^D} e^{-tp^2}. \quad (\text{D.0.4})$$

Which leads to two results after performing the Gaussian integral over momentum, one for the scalar field and the second for a Dirac fermion for similar mass as

$$\Gamma = -\frac{V}{2(4\pi)^{\frac{D}{2}}} \int_\Lambda^\infty \frac{dt}{t^{\frac{D}{2}+1}} e^{-tM^2} \quad (\text{D.0.5})$$

and

$$\Gamma = \frac{2^{\frac{D}{2}} V}{2(4\pi)^{\frac{D}{2}}} \int_\Lambda^\infty \frac{dt}{t^{\frac{D}{2}+1}} e^{-tM^2}. \quad (\text{D.0.6})$$

respectively. So the total contribution can be defined in terms of a super trace which counts the signed multiplicities of the above which are extended to generic Bose or Fermi

fields, since their physics modes determine Γ . In addition, Γ is proportional to their number, and so

$$\Gamma_{\text{tot}} = -\frac{V}{2(4\pi)^{\frac{D}{2}}} \int_{\Lambda}^{\infty} \frac{dt}{t^{\frac{D}{2}+1}} \text{Str}(e^{-tM^2}). \quad (\text{D.0.7})$$

In moving now to describe the equivalent function in string theory, one uses the mass squared operator in the above expression. The mass levels of the modes are determined by

$$M^2 = \frac{2}{\alpha'}(L_o + \bar{L}_o), \quad (\text{D.0.8})$$

where L_o and \bar{L}_o are the left and right moving Hamiltonian's of a closed string, and are given by equation (3.1.17).

For the superstring, the critical dimension is $D = 10$. So, in conjunction with an insertion of a representation of the Dirac delta function which enforces the level matching condition $L_o = \bar{L}_o$ one has

$$\Gamma_{\text{tot}} = -\frac{V}{2(4\pi)^5} \int_{-\frac{1}{2}}^{\frac{1}{2}} ds \int_{\Lambda}^{\infty} \frac{dt}{t^6} \text{tr}(e^{-\frac{2}{\alpha'}(L_o + \bar{L}_o)t + 2\pi i(L_o - \bar{L}_o)s}). \quad (\text{D.0.9})$$

All calculations in the context of this paper are determined by the one loop amplitude, or torus. The Teichmüller τ_2 , is naturally identified with the complex Schwinger parameter. So, for the definition of the complex Schwinger parameter $\tau = \tau_1 + i\tau_2 = s + i\frac{t}{\alpha'\pi}$ with $q = e^{2\pi i\tau}$ and $\bar{q} = e^{-2\pi i\bar{\tau}}$, results in the torus amplitude

$$\mathcal{T} = \int_{\mathcal{F}} \frac{d^2\tau}{\tau_2^2} \frac{1}{\tau_2^4} \text{tr} q^{L_o} \bar{q}^{\bar{L}_o}. \quad (\text{D.0.10})$$

The fundamental region $\mathcal{F} = \{-\frac{1}{2} < \tau_1 \leq \frac{1}{2}, |\tau| \geq 1\}$ defines the region which covers the counting of distinct tori.

It is of some assistance to illustrate the role of the parameter τ_2 in its effect when S transforming amplitudes. The S transform of the Klein and annulus amplitudes will lead to factors that appear in the transverse channels.

Now, using the Gaussian integration of

$$\alpha'^{\frac{1}{2}} \int \exp(-\pi\alpha'\tau_2 p^2) = \frac{1}{\sqrt{\tau_2}} \quad (\text{D.0.11})$$

the measure that begins as

$$\int_{\mathcal{F}} \frac{d^2\tau}{\tau_2^2} \frac{1}{\tau_2^4} \quad (\text{D.0.12})$$

can thus be rewritten as (under compactification to $T^2 \times T^2 \times T^2$)

$$\int_{\mathcal{F}} \frac{d^2\tau}{\tau_2^2} \frac{1}{\tau_2} \sum_{\{m,n\}_i} q^{\frac{\alpha'}{4}p_{L,i}^2} \bar{q}^{\frac{\alpha'}{4}p_{R,i}^2}. \quad (\text{D.0.13})$$

Where $i = \{1, \dots, 6\}$ and the continuum of momentum states has been replaced by the discrete summation over momenta and winding states.

The Klein is based on the measure of the form $2i\tau_2$ in the direct channel, as can be seen by the Ω identification of the torus. The direct annulus has the measure $\frac{1}{2}i\tau_2$. As such, in S transforming to their respective transverse channels, one makes the substitutions of $2\tau_2 = \frac{1}{l}$ for the Klein and $\frac{\tau_2}{2} = \frac{1}{l}$ for the annulus. This allows the measure dependency of the Klein, annulus and Mobius amplitudes as il . The appropriate rescaling's show that the measure, as defined in equation (D.0.13), gives a factor of 2^2 for the transformation to the transverse Klein amplitude, and 2^{-2} for the annulus. The Poisson resummation formula of equation (3.1.46) then gives the additional factors of 2^3 and 2^{-3} for the Klein and annulus lattices.

Appendix E

Effect of Non-trivial Wilson Lines on Branes

This short discussion on the effect of a simple $U(1)$ gauge field on the branes connected by an open string follows that which was made in [31].

In the case of the 26 dimensional bosonic theory, one can have a simple and constant gauge field

$$A_{25}(x^D) = -\frac{\gamma}{2\pi R} = -i\frac{1}{\Lambda}\frac{\partial\Lambda}{\partial x^{25}}, \quad \Lambda(x^{25}) = \exp\left(-\frac{i\gamma x^{25}}{2\pi R}\right) \quad (\text{E.0.1})$$

with constant γ , and x^{25} is the coordinate for the compact space with topology S^1 . The measure of the gauge field around the compact transverse space picks up a phase according to

$$W_Q = \exp\left(iQ \oint A_{25} dx^{25}\right) = \exp(-iQ\gamma). \quad (\text{E.0.2})$$

The action of the bosonic open string which interacts with the gauge field is given by

$$\int d\tau \left(\frac{1}{2} \dot{X}^\mu \dot{X}_\mu - \frac{M^2}{2} - iQ_i A_\mu \dot{X}^\mu \Big|_{\sigma=0} - iQ_j A_\mu \dot{X}^\mu \Big|_{\sigma=\pi} \right) \quad (\text{E.0.3})$$

for Chan-Paton charges $|ij\rangle$. The gauge group in this case is $U(1)^n$ parameterized by $A_{25} = -\frac{1}{2\pi R} \text{diag}(\gamma_1, \dots, \gamma_n)$. The state $|ij\rangle$ is charged as Q_i under $U(1)_i$ and $U(1)_j$ and is neutral under the others. It can then be seen that the string mass is shift according to

$$M^2 = \frac{(Q_i\gamma_i + Q_j\gamma_j)}{(2\pi R)^2} + \dots \quad (\text{E.0.4})$$

By performing a T duality along the 25th coordinate, difference in string end points is described by

$$\Delta X'^{25} = X'^{25}(0) - X'^{25}(\pi) = (Q_i\gamma_i + Q_j\gamma_j)R' + \dots \quad (\text{E.0.5})$$

The distance between branes are therefore moved apart by $\Delta X'^{25}$. Correspondingly, the mass is altered.

Appendix F

Lattice Simplifications

I present here some simplifications of the lattice definition (3.2.2) which will be helpful in looking at the momentum towers that appear in all amplitudes.

A general lattice for the torus amplitude is defined as

$$\Lambda_{m+a,n+b} = \frac{q^{\frac{\alpha'}{4} \left(\frac{(m+a)}{R} + \frac{(n+b)R}{\alpha'} \right)^2} \bar{q}^{\frac{\alpha'}{4} \left(\frac{(m+a)}{R} - \frac{(n+b)R}{\alpha'} \right)^2}}{\eta(q)\eta(\bar{q})} \quad (\text{F.0.1})$$

for $q = \exp(2\pi i\tau)$ and $\tau = \tau_1 + i\tau_2$. This carries the quantum numbers $|m_i, n_i\rangle$ for a circle S_i^1 . The expanded form of this is

$$\Lambda_{m+a,n+b} = \frac{(-1)^{2\tau_1(m+a)(n+b)}}{|\eta(\tau)|^2} \exp \left[-\pi\tau_2\alpha' \left\{ \left(\frac{(m+a)}{R} \right)^2 + \left(\frac{(n+b)R}{\alpha'} \right)^2 \right\} \right] \quad (\text{F.0.2})$$

As such $\Lambda_{m+a,n+b}$ has the following expansions;

$$\Lambda_{m+a,0;0,0} = \frac{1}{|\eta(\tau)|^2} \exp \left[-\pi\tau_2\alpha' \left(\frac{(m+a)}{R} \right)^2 \right], \quad (\text{F.0.3})$$

$$\Lambda_{0,n+b;0,0} = \frac{1}{|\eta(\tau)|^2} \exp \left[-\pi\tau_2\alpha' \left(\frac{(n+b)R}{\alpha'} \right)^2 \right], \quad (\text{F.0.4})$$

$$\Lambda_{m+a,n+b;0,0} = \frac{1}{|\eta(\tau)|^2} \exp \left[-\pi\tau_2\alpha' \left(\left(\frac{(m+a)}{R} \right)^2 + \left(\frac{(n+b)R}{\alpha'} \right)^2 \right) \right]. \quad (\text{F.0.5})$$

Since the two directions of the torus are independent, one can decompose in the following manner

$$\Lambda_{m_1+a_1,n_1+b_1;m_2+a_2,n_2+b_2} = \Lambda_{m_1+a_1,n_1+b_1;0,0} \Lambda_{0,0;m_2+a_2,n_2+b_2} \quad (\text{F.0.6})$$

for all $\{m_i, n_i\} \in \mathbb{Z}$.

Appendix G

Amplitudes of the $\mathbb{Z}_2 \times \mathbb{Z}_2$ Partition Function

The sections of this work that deal with type I string mainly involve discussions of the phenomenology arising from models based on the $\mathbb{Z}_2 \times \mathbb{Z}_2$ model. As such, it is of some assistance to review the parent torus amplitude and the open descendants that follow in the cases of $\epsilon = \pm 1$. The following are simply a review of those defined and discussed in detail in [25].

The parent torus for this model is defined as

$$\begin{aligned} \mathcal{T} = & \frac{1}{4} \left\{ |T_{oo}|^2 \Lambda_1 \Lambda_2 \Lambda_3 + |T_{ok}|^2 \Lambda_k \left| \frac{2\eta}{\theta_2} \right|^4 + |T_{ko}|^2 \Lambda_k \left| \frac{2\eta}{\theta_4} \right|^4 + |T_{kk}|^2 \Lambda_k \left| \frac{2\eta}{\theta_3} \right|^4 \right. \\ & \left. + \epsilon (|T_{gh}|^2 + |T_{gf}|^2 + |T_{fg}|^2 + |T_{fh}|^2 + |T_{hg}|^2 + |T_{hf}|^2) \left| \frac{8\eta}{\theta_2 \theta_3 \theta_4} \right|^2 \right\}. \quad (\text{G.0.1}) \end{aligned}$$

The direct channel Klein follows as

$$\mathcal{K} = \frac{1}{8} \left\{ (P_1 P_2 P_3 + \frac{1}{2} P_k W_l W_s) T_{oo} + 2 \times 16 \epsilon_k (P_k + \epsilon W_k) T_{ko} \left(\frac{\eta}{\theta_4} \right)^2 \right\}, \quad (\text{G.0.2})$$

The direct channel open descendants take the forms

$$\begin{aligned} \mathcal{A}_{(-1)} = & \frac{1}{8} \left\{ \left(N_o^2 P_1 P_2 P_3 + \frac{D_{ko}^2}{2} P_k W_l W_s \right) T_{oo} \right. \\ & \left[(N_k^2 + D_{kk}^2) P_k + D_{lk}^2 W_k \right] T_{ok} \left(\frac{2\eta}{\theta_2} \right)^2 \\ & + 2 N_o D_{ko} P_k T_{ko}^{(\epsilon_k)} \left(\frac{\eta}{\theta_4} \right)^2 \\ & - 2 N_k D_{kk} P_k T_{kk}^{(\epsilon_k)} \left(\frac{\eta}{\theta_3} \right)^2 \\ & \left. + 2i (-1)^{k+l} N_l D_{kl} T_{kl}^{(\epsilon_k)} \frac{2\eta^3}{\theta_2 \theta_3 \theta_4} \right\} \end{aligned}$$

$$\begin{aligned}
& +D_{ko}D_{lo}W_mT_{mo}^{(\epsilon_k\epsilon_l)}\left(\frac{\eta}{\theta_4}\right)^2 \\
& -D_{km}D_{lm}W_mT_{mm}^{(\epsilon_k\epsilon_l)}\left(\frac{\eta}{\theta_3}\right)^2 \\
& +2i(-1)^{m+k}D_{kk}D_{lk}T_{mk}^{(\epsilon_k\epsilon_l)}\frac{2\eta^3}{\theta_2\theta_3\theta_4} \Big\} \tag{G.0.3}
\end{aligned}$$

for the $\epsilon = -1$ annulus, and

$$\begin{aligned}
\mathcal{A}_{(+1)} &= \frac{1}{2}\left\{\left(N^2P_1P_2P_3 + \frac{D_k^2}{2}P_kW_lW_s\right)T_{oo} \right. \\
& +2ND_kP_kT_{ko}^{(\epsilon_k)}\left(\frac{\eta}{\theta_4}\right)^2 \\
& \left. +D_kD_lW_mT_{mo}^{(\epsilon_k\epsilon_l)}\left(\frac{\eta}{\theta_4}\right)^2\right\} \tag{G.0.4}
\end{aligned}$$

for the $\epsilon = +1$ case.

The oriented amplitudes are

$$\begin{aligned}
\mathcal{M} &= -\frac{1}{8}\left\{\left(N_oP_1P_2P_3\hat{T}_{oo} + \frac{D_{ko}}{2}\epsilon_kP_kW_lW_s\hat{T}_{oo}^{(\epsilon_k)} \right. \right. \\
& -N_oP_k\epsilon_k\hat{T}_{ok}\left(\frac{2\hat{\eta}}{\hat{\theta}_2}\right)^2 \\
& \left. \left. -\left(D_{lo}\epsilon_kW_m\hat{T}_{om}^{(\epsilon_l)} + D_{ko}P_m\hat{T}_{ok}^{(\epsilon_k)}\right)\left(\frac{2\hat{\eta}}{\hat{\theta}_2}\right)^2\right\} \tag{G.0.5}
\end{aligned}$$

for the $\epsilon = -1$ model, and

$$\begin{aligned}
\mathcal{M} &= -\frac{1}{4}\left\{\left(NP_1P_2P_3\hat{T}_{oo} + \frac{D_k}{2}\epsilon_kP_kW_lW_s\hat{T}_{oo}^{(\epsilon_k)} \right. \right. \\
& -NP_k\epsilon_k\hat{T}_{ok}\left(\frac{2\hat{\eta}}{\hat{\theta}_2}\right)^2 \\
& \left. \left. -\left(D_l\epsilon_kW_m\hat{T}_{om}^{(\epsilon_l)} + D_kP_m\hat{T}_{ok}^{(\epsilon_k)}\right)\left(\frac{2\hat{\eta}}{\hat{\theta}_2}\right)^2\right\}. \tag{G.0.6}
\end{aligned}$$

The tadpole conditions are summarized in table G.1.

$\epsilon = -1$ Model		$\epsilon = +1$ Model
$N_o = 32,$	$N_g = N_f = N_h = 0$	$N = 16$
$D_{ko} = 32,$	$D_{kg} = D_{kf} = D_{kh} = 0$	$D_k = 16$

Table G.1: Tadpole conditions

This concludes all necessary detail for comparison to the $\mathbb{Z}_2 \times \mathbb{Z}_2$ models discussed in this study.

Appendix H

Singular Valued Decomposition

This an approach to finding a solution to the D -flat constraints that are imposed by equations (2.2.1) and (2.2.2). This method was first applied to the resolution of D -flat constraints by G. Cleaver.

The form of the these constraint equations becomes a set of linear equations of the form

$$\mathbf{D}\cdot\mathbf{x} = \mathbf{b}. \tag{H.0.1}$$

For an $M \times N$ matrix \mathbf{D} . A matrix element is written in terms of the charge $Q_j^{(i)}$ with $i = 1, \dots, A, \dots, N$ as $D_{ij} = Q_j^{(i)}$. The row $i = A$, corresponds to the constraint (2.2.1), and otherwise corresponds to (2.2.2). The j^{th} element of \mathbf{x} is the norm squared of the VEV for a field ϕ_j . The vector \mathbf{b} contains one non-zero entry for $i = A$, which has value $-\xi$, as appreciated by (2.2.1).

The singular value decomposition provides the matrix \mathbf{D} in the form

$$\mathbf{D}_{M \times N} = \mathbf{U}_{M \times N} \cdot \mathbf{W}_{N \times N}^{\text{diag}} \cdot \mathbf{V}_{N \times N}^{\text{T}} \tag{H.0.2}$$

for $M \geq N$. Here, \mathbf{U} is an $M \times N$ column orthogonal matrix, \mathbf{W} is an $N \times N$ diagonal matrix containing only semi-positive-definite elements and \mathbf{V}^{T} is the transpose of an $N \times N$ orthogonal matrix.

This decomposition is unique up to;

- forming linear combinations of any columns of \mathbf{U} and \mathbf{V} whose corresponding elements of \mathbf{W} are degenerate
- making the same permutation of the columns of \mathbf{U} , diagonal elements of \mathbf{W} and columns of \mathbf{V}

In this method, if $M < N$, then one appends an $(M - N) \times N$ zero matrix to \mathbf{D} so that $M \geq N$. When \mathbf{D} is singular, corresponding to the M constraints not all being linearly independent, there is a subspace of \mathbf{x} termed the *nullspace* that is mapped to $\mathbf{0}$ in \mathbf{b} space by \mathbf{D} . The subspace of \mathbf{b} that can be reached by the matrix \mathbf{D} is the range of \mathbf{D} , the dimension of which is $\text{rank}(\mathbf{D})$. With the dimension of the nullspace as $\text{nullity}(\mathbf{D})$, one has

$$\text{rank}(\mathbf{D}) + \text{nullity}(\mathbf{D}) = N \tag{H.0.3}$$

and $\text{rank}(\mathbf{D})$ is the number of independent constraint equations.

In the decomposition (H.0.2), the set of the l^{th} columns of \mathbf{U} corresponding to the l^{th} non-zero diagonal components of \mathbf{W} form an orthonormal set of basis vectors that span the range of \mathbf{D} . The columns of \mathbf{V} whose corresponding diagonal components of \mathbf{W} are zero form an orthonormal basis for the nullspace.

One begins with the full matrix $D_{ij} = Q_j^{(i)}$ for the i^{th} charges of the j^{th} field ϕ_j . Then one decomposes this to the form (H.0.2).

The matrix used in the calculation of the flat directions is \mathbf{D}' which is the original \mathbf{D} with the $i = A$ row removed. This enables one to extract a complete set of directions that are solutions of the form

$$\mathbf{D}' \cdot \mathbf{x}_p = \mathbf{0}. \tag{H.0.4}$$

This then gives a set of independent solutions \mathbf{x}_p (for p running over the number of zero components of \mathbf{W}) to (2.2.1). The next step, which helps to simplify the necessary analysis of the D -flat directions, involves rotating the bases \mathbf{x} so that these contain a set of common fields and at least one unique field. These rotated combinations can then be linearly combined to exact a solution of the constraint equation (2.2.2).

Left–Right Symmetric Model 1 Fields

F	SEC	$(C; L; R)$	Q_A	$Q_{1'}$	$Q_{2'}$	$Q_{3'}$	$Q_{4'}$	$Q_{5'}$	$Q_{7''}$	$Q_{8'}$	$SU(4)_{H_{1,2}}$
Q_{L_1}	$\mathbf{b}_1 \oplus$ $\mathbf{b}_1 + \zeta + 2\gamma$	$(4, 2, 1)$	-2	2	2	4	-2	-2	8	0	$(1, 1)$
Q_{R_1}		$(\bar{4}, 1, 2)$	-2	-2	-2	-4	-2	-2	-8	0	$(1, 1)$
L_{L_1}		$(1, 2, 1)$	-2	2	2	-20	-2	-2	0	0	$(1, 1)$
L_{R_1}		$(1, 1, 2)$	-2	-2	-2	20	-2	-2	0	0	$(1, 1)$
\mathcal{L}_{L_1}		$(1, 2, 1)$	2	2	2	4	2	2	-32	0	$(1, 1)$
\mathcal{L}_{R_1}		$(1, 1, 2)$	2	-2	-2	-4	2	2	32	0	$(1, 1)$
Q_{L_2}	$\mathbf{b}_2 \oplus$ $\mathbf{b}_2 + \zeta + 2\gamma$	$(4, 2, 1)$	-2	-2	2	4	2	-2	8	0	$(1, 1)$
Q_{R_2}		$(\bar{4}, 1, 2)$	-2	2	-2	-4	2	-2	-8	0	$(1, 1)$
L_{L_2}		$(1, 2, 1)$	-2	-2	2	-20	2	-2	0	0	$(1, 1)$
L_{R_2}		$(1, 1, 2)$	-2	2	-2	20	2	-2	0	0	$(1, 1)$
\mathcal{L}_{L_2}		$(1, 2, 1)$	2	-2	2	4	-2	2	-32	0	$(1, 1)$
\mathcal{L}_{R_2}		$(1, 1, 2)$	2	2	-2	-4	-2	2	32	0	$(1, 1)$
Q_{L_3}	$\mathbf{b}_3 \oplus$ $\mathbf{b}_3 + \zeta + 2\gamma$	$(4, 2, 1)$	-2	0	-4	4	0	4	8	0	$(1, 1)$
Q_{R_3}		$(\bar{4}, 1, 2)$	-2	0	4	-4	0	4	-8	0	$(1, 1)$
L_{L_3}		$(1, 2, 1)$	-2	0	-4	-20	0	4	0	0	$(1, 1)$
L_{R_3}		$(1, 1, 2)$	-2	0	4	20	0	4	0	0	$(1, 1)$
\mathcal{L}_{L_3}		$(1, 2, 1)$	2	0	-4	4	0	-4	-32	0	$(1, 1)$
\mathcal{L}_{R_3}		$(1, 1, 2)$	2	0	4	-4	0	-4	32	0	$(1, 1)$
Φ_1	Neveu- Schwarz	$(1, 1, 1)$	0	0	0	0	0	0	0	0	$(1, 1)$
Φ_2		$(1, 1, 1)$	0	0	0	0	0	0	0	0	$(1, 1)$
Φ_3		$(1, 1, 1)$	0	0	0	0	0	0	0	0	$(1, 1)$
Φ_{12}		$(1, 1, 1)$	0	-8	0	0	0	0	0	0	$(1, 1)$
$\bar{\Phi}_{12}$		$(1, 1, 1)$	0	8	0	0	0	0	0	0	$(1, 1)$
Φ_{23}		$(1, 1, 1)$	0	4	-12	0	0	0	0	0	$(1, 1)$
$\bar{\Phi}_{23}$		$(1, 1, 1)$	0	-4	12	0	0	0	0	0	$(1, 1)$
Φ_{31}		$(1, 1, 1)$	0	-4	-12	0	0	0	0	0	$(1, 1)$
$\bar{\Phi}_{31}$		$(1, 1, 1)$	0	4	12	0	0	0	0	0	$(1, 1)$
D_3	$\xi \equiv \mathbf{S} + \mathbf{b}_1 + \mathbf{b}_2 +$ $\alpha + \beta$ \oplus $\xi + \zeta$	$(4, 1, 1)$	0	0	4	8	0	0	-24	0	$(1, 1)$
\bar{D}_3		$(\bar{4}, 1, 1)$	0	0	-4	-8	0	0	24	0	$(1, 1)$
$\phi_{\alpha\beta}$		$(1, 1, 1)$	0	0	-12	0	0	0	0	0	$(1, 1)$
$\bar{\phi}_{\alpha\beta}$		$(1, 1, 1)$	0	0	12	0	0	0	0	0	$(1, 1)$
ϕ_1		$(1, 1, 1)$	0	4	0	0	0	0	0	0	$(1, 1)$
$\bar{\phi}_1$		$(1, 1, 1)$	0	-4	0	0	0	0	0	0	$(1, 1)$
ϕ_2		$(1, 1, 1)$	0	4	0	0	0	0	0	0	$(1, 1)$
$\bar{\phi}_2$		$(1, 1, 1)$	0	-4	0	0	0	0	0	0	$(1, 1)$
S_8		$(1, 1, 1)$	0	0	4	-16	0	0	-32	0	$(1, 1)$
\bar{S}_8		$(1, 1, 1)$	0	0	-4	16	0	0	32	0	$(1, 1)$

Table 1: *Model 1 fields.*

Left–Right Symmetric Model 1 Fields Continued

F	SEC	$(C; L; R)$	Q_A	$Q_{1'}$	$Q_{2'}$	$Q_{3'}$	$Q_{4'}$	$Q_{5'}$	$Q_{7''}$	$Q_{8'}$	$SU(4)_{H_{1,2}}$
D_1	$\xi \equiv \mathbf{S} + \mathbf{b}_2 + \mathbf{b}_3 +$ $\beta + \gamma$ \oplus $\xi + \zeta + 2\gamma$	$(4, 1, 1)$	0	2	2	4	0	0	8	-8	$(1, 1)$
\bar{D}_1		$(\bar{4}, 1, 1)$	0	-2	-2	-4	0	0	-8	8	$(1, 1)$
S_1		$(1, 1, 1)$	0	-2	6	-12	0	0	16	8	$(1, 1)$
\bar{S}_1		$(1, 1, 1)$	0	2	-6	12	0	0	-16	-8	$(1, 1)$
S_2		$(1, 1, 1)$	0	2	-6	-12	0	0	16	8	$(1, 1)$
\bar{S}_2		$(1, 1, 1)$	0	-2	6	12	0	0	-16	-8	$(1, 1)$
\mathcal{H}_1		$(1, 1, 1)$	0	2	2	-8	0	0	-16	0	$(1, 6)$
$\bar{\mathcal{H}}_1$		$(1, 1, 1)$	0	-2	-2	8	0	0	16	0	$(1, 6)$
D_2	$\xi \equiv \mathbf{S} + \mathbf{b}_1 + \mathbf{b}_3 +$ $\alpha + \gamma$ \oplus $\xi + \zeta + 2\gamma$	$(4, 1, 1)$	0	-2	2	4	0	0	8	-8	$(1, 1)$
\bar{D}_2		$(\bar{4}, 1, 1)$	0	2	-2	-4	0	0	-8	8	$(1, 1)$
S_3		$(1, 1, 1)$	0	2	6	-12	0	0	16	8	$(1, 1)$
\bar{S}_3		$(1, 1, 1)$	0	-2	-6	12	0	0	-16	-8	$(1, 1)$
S_4		$(1, 1, 1)$	0	-2	-6	-12	0	0	16	8	$(1, 1)$
\bar{S}_4		$(1, 1, 1)$	0	2	6	12	0	0	-16	-8	$(1, 1)$
\mathcal{H}_2		$(1, 1, 1)$	0	-2	2	-8	0	0	-16	0	$(1, 6)$
$\bar{\mathcal{H}}_2$		$(1, 1, 1)$	0	2	-2	8	0	0	16	0	$(1, 6)$
H_1	$\xi \equiv \mathbf{S} + \mathbf{b}_2 + \mathbf{b}_3 +$ $\alpha + 2\gamma$ \oplus $\xi + \zeta$	$(1, 1, 1)$	-4	-2	-2	2	2	2	-16	-4	$(1, 4)$
$\bar{H}_{1'}$		$(1, 1, 1)$	-4	2	2	-2	2	2	16	4	$(1, \bar{4})$
H_2		$(1, 1, 1)$	-4	-2	-2	2	2	2	-16	4	$(4, 1)$
$\bar{H}_{2'}$		$(1, 1, 1)$	-4	2	2	-2	2	2	16	-4	$(\bar{4}, 1)$
H_3	$\xi \equiv \mathbf{S} + \mathbf{b}_1 + \mathbf{b}_3 +$ $\alpha + 2\gamma$ \oplus $\xi + \zeta$	$(1, 1, 1)$	-4	2	-2	2	-2	2	-16	-4	$(1, 4)$
$\bar{H}_{3'}$		$(1, 1, 1)$	-4	-2	2	-2	-2	2	16	4	$(1, \bar{4})$
H_4		$(1, 1, 1)$	-4	2	-2	2	-2	2	-16	4	$(4, 1)$
$\bar{H}_{4'}$		$(1, 1, 1)$	-4	-2	2	-2	-2	2	16	-4	$(\bar{4}, 1)$
H_5	$\xi \equiv \mathbf{S} + \mathbf{b}_1 + \mathbf{b}_2 +$ $\alpha + 2\gamma$ \oplus $\xi + \zeta + 2\gamma$	$(1, 1, 1)$	-4	0	4	2	0	-4	-16	-4	$(1, 4)$
$\bar{H}_{5'}$		$(1, 1, 1)$	-4	0	-4	-2	0	-4	16	4	$(1, \bar{4})$
H_6		$(1, 1, 1)$	-4	0	4	2	0	-4	-16	4	$(4, 1)$
$\bar{H}_{6'}$		$(1, 1, 1)$	-4	0	-4	-2	0	-4	16	-4	$(\bar{4}, 1)$
S_5	$\mathbf{S} + \zeta + 2\gamma$	$(1, 1, 1)$	0	0	-8	-16	0	0	-32	0	$(1, 1)$
\bar{S}_5		$(1, 1, 1)$	0	0	8	16	0	0	32	0	$(1, 1)$
S_6		$(1, 1, 1)$	0	-4	4	-16	0	0	-32	0	$(1, 1)$
\bar{S}_6		$(1, 1, 1)$	0	4	-4	16	0	0	32	0	$(1, 1)$
S_7		$(1, 1, 1)$	0	4	4	-16	0	0	-32	0	$(1, 1)$
\bar{S}_7		$(1, 1, 1)$	0	-4	-4	16	0	0	32	0	$(1, 1)$

Table 1: *Model 1 fields continued.*

Basis	$Q^{(A)}$	S_5/S_5	D_3/D_3	D_2/D_2	$\mathcal{H}_2/\mathcal{H}_2$	$\mathcal{H}_1/\mathcal{H}_1$	$\bar{H}_{4'}$	$\bar{H}_{2'}$		
\mathbf{x}_1	12	0	-1	-1	-2	3	0	-2	2	\mathcal{L}_{R1}
\mathbf{x}_2	12	-1	3	-1	0	1	0	-2	2	\mathcal{L}_{L1}
\mathbf{x}_3	12	-1	3	-1	0	1	-2	0	2	\mathcal{L}_{L2}
\mathbf{x}_4	12	0	-1	-1	2	-1	-2	0	2	\mathcal{L}_{R2}
\mathbf{x}_7	24	-1	4	-4	-2	2	-4	-4	4	Q_{R3}
\mathbf{x}_5	24	-3	4	-4	2	6	-4	-4	4	Q_{L3}
\mathbf{x}_6	24	-1	8	-4	2	6	-4	-4	4	L_{R3}
\mathbf{x}_8	24	-3	0	-4	-2	2	-4	-4	4	L_{L3}
\mathbf{x}_9	-12	0	-1	1	0	-1	2	0	2	Q_{R2}
\mathbf{x}_{10}	-12	1	-3	1	-4	-1	2	0	2	L_{L2}
\mathbf{x}_{11}	-12	1	-1	1	-2	1	2	0	2	Q_{L2}
\mathbf{x}_{13}	-12	0	1	1	2	1	2	0	2	L_{R2}
\mathbf{x}_{12}	-12	0	1	1	2	1	0	2	2	L_{R1}
\mathbf{x}_{14}	-12	1	-3	1	0	-5	0	2	2	L_{L1}
\mathbf{x}_{15}	-12	0	-1	1	0	-1	0	2	2	Q_{R1}
\mathbf{x}_{16}	-12	1	-1	1	2	-3	0	2	2	Q_{L1}
\mathbf{x}_{17}	-24	1	-3	1	0	-1	2	2	2	$\bar{H}_{5'}$
\mathbf{x}_{18}	-24	1	-1	3	0	-3	2	2	2	H_5
\mathbf{x}_{19}	-24	-1	0	4	2	-2	4	4	4	\mathcal{L}_{L3}
\mathbf{x}_{20}	-24	5	-8	4	-2	-6	4	4	4	\mathcal{L}_{R3}
\mathbf{x}_{21}	-48	1	-6	6	2	-4	4	4	4	$\bar{H}_{6'}$
\mathbf{x}_{22}	-48	3	-2	2	-2	-4	4	4	4	H_6
\mathbf{x}_{40}	0	-3	4	0	-2	6	0	-4	4	H_1
\mathbf{x}_{37}	0	1	0	-4	-2	2	0	-4	4	$\bar{H}_{1'}$
\mathbf{x}_{41}	0	-3	4	0	6	-2	-4	0	4	H_3
\mathbf{x}_{29}	0	1	0	-4	-2	2	-4	0	4	$\bar{H}_{3'}$
\mathbf{x}_{34}	0	-1	2	-2	-2	4	0	-2	2	H_2
\mathbf{x}_{39}	0	-1	2	-2	2	0	-2	0	2	H_4
\mathbf{x}_{32}^v	0	0	0	0	-2	2	0	0	1	Φ_{12}
\mathbf{x}_{35}^v	0	-1	0	0	2	0	0	0	1	Φ_{23}
\mathbf{x}_{28}^v	0	-1	0	0	0	2	0	0	1	Φ_{31}
\mathbf{x}_{31}^v	0	-1	0	0	1	1	0	0	1	S_8
\mathbf{x}_{25}^v	0	0	0	0	-1	-1	0	0	1	$\phi_{\alpha\beta}$
\mathbf{x}_{33}^v	0	0	0	0	-1	1	0	0	1	$\phi_{1,2}$
\mathbf{x}_{30}^v	0	0	-1	-1	-1	1	0	0	1	S_4
\mathbf{x}_{27}^v	0	0	-1	-1	0	0	0	0	1	S_2
\mathbf{x}_{36}^v	0	1	-1	-1	-1	-1	0	0	1	S_3
\mathbf{x}_{24}^v	0	1	-1	-1	-2	0	0	0	1	S_1
\mathbf{x}_{23}^v	0	0	0	0	0	-2	0	0	1	S_7
\mathbf{x}_{38}^v	0	0	0	0	-2	0	0	0	1	S_6
\mathbf{x}_{26}^v	0	0	0	-1	-1	1	0	0	1	\bar{D}_1

Table 2: *D-Flat Direction Basis Set for Model 3.*

Bibliography

- [1] I. Antoniadis, G. D'Appollonio, E. Dudas and A. Sagnotti *Nucl. Phys.* **B565** (2000) 123-156.
- [2] M. Berkooz and R.G. Leigh, *Nucl. Phys.* **B483** (1997) 187.
- [3] J. Park, R. Rabadan and A.M. Uranga, *Nucl. Phys.* **B570** (2000) 38.
- [4] M. Bianchi, J.F. Morales and G. Pradisi, *Nucl. Phys.* **B573** (2000) 314.
- [5] I. Antoniadis, C. Bachas, and C. Kounnas, *Nucl. Phys.* **B289** (1987) 87.
- [6] H. Kawai, D.C. Lewellen, and S.H.H. Tye, *Nucl. Phys.* **B288** (1987) 1.
- [7] A.E. Faraggi and D.V. Nanopoulos, *Phys. Rev.* **D48** (1993) 3288.
- [8] A.E. Faraggi, *Int. J. Mod. Phys.* **A14** (1999) 1663.
- [9] C. Angelantonj, I. Antoniadis and K. Förger, *Nucl. Phys.* **B555** (1999) 116.
- [10] G.B. Cleaver, A. E. Faraggi, D. V. Nanopoulos, *Int. J. Mod. Phys.* **A16** (2001) 425.
- [11] G.B. Cleaver, A.E. Faraggi and C. Savage, *Phys. Rev.* **D63** (2001) 066001.
- [12] D.J. Gross, J.A. Harvey, J.A. Martinec and R. Rohm, *Phys. Rev. Lett.* **54** (1985) 502; *Nucl. Phys.* **B256** (1986) 253.
- [13] M. Dine, N. Seiberg and E. Witten, *Nucl. Phys.* **B289** (1987) 589.
- [14] J. Atick, L. Dixon and A. Sen, *Nucl. Phys.* **B292** (1987) 109.
- [15] D.J. Clements and A.E. Faraggi, *Phys. Rev.* **D65** (2002) 106003.
- [16] D.J. Clements and A.E. Faraggi, hep-th/0302006.
- [17] G. Cleaver, M. Cvetič, J. Espinosa, L. Everett and P. Langacker *Nucl. Phys.* **B545** (1999) 47.
- [18] A.E. Faraggi and E. Halyo, *Int. J. Mod. Phys.* **A11** (1996) 2357.
- [19] S. Kalara, J.L. Lopez and D.V. Nanopoulos, *Nucl. Phys.* **B353** (1990) 650.
- [20] A.E. Faraggi, *Nucl. Phys.* **B428** (1994) 111.

- [21] A.E. Faraggi and M. Masip, *Phys. Lett.* **B388** (1996) 524.
- [22] G.B. Cleaver and A.E. Faraggi, *Int. J. Mod. Phys.* **A14** (1999) 2335.
- [23] G.B. Cleaver, A.E. Faraggi, D.V. Nanopoulos, *Nucl. Phys.* **B620** (2002) 259-289.
- [24] A. Abouelsaood, C. G. Callan, C. R. Nappi and S. A. Yost, *Nucl. Phys.* **B280** (1987) 599.
- [25] C Angelantonj and A Sagnotti, *Phys. Rep.* **371** (2002) 1-150.
- [26] I Antoniadis, E Dudas and A Sagnotti, *Nucl. Phys.* **B544** (1999) 469-502.
- [27] C Angelantonj, *Nucl. Phys.* **B566** (2000) 126-150.
- [28] Mirjam Cvetič, Gary Shiu and Angel M. Uranga, *Nucl. Phys.* **B615** (2001) 3-32.
- [29] C. Angelantonj, I. Antoniadis, E. Dudas and A. Sagnotti, *Phys. Lett.* **B489** (2000) 223-232.
- [30] M. Larosa and G. Pradisi, *Nucl. Phys.* **B667** (2003) 261-309.
- [31] J. Polchinski, see *String Theory* Vol. 1, p263-268.
- [32] E. S. Franklin and A. A. Tseytlin *Phys. Lett.* **B163** (1985) 123.
- [33] C. Bachas, *Phys. Lett.* **B296** (1992) 77-84.
- [34] Kawai H, Lewellen D C and Tye S-H *Nucl. Phys.* **B288** (1987) 1.

Taking

$$S_I \sim (-g)^{\frac{1}{2}} \left[e^{-2\phi_I} (R + (d\phi)^2 + |\tilde{F}_3|^2) + e^{-\phi_I} |F_2|^2 \right] \quad (0.0.1)$$

Then

$$g_{\mu\nu} \rightarrow e^{-\phi_h} g_{\mu\nu}, \quad \phi_I = -\phi_h, \quad \tilde{F}_{I3} = \tilde{H}_{h3}, \quad A_{I1} = A_{hI} \quad (0.0.2)$$

I see that

$$\begin{aligned} (d\phi)^2 &= \partial_\mu \phi \partial_\nu \phi G^{\mu\nu} \\ R &= G^{\mu\nu} R_{\mu\nu} \end{aligned} \quad (0.0.3)$$

so that

$$(d\phi)^2, R \rightarrow e^{\phi_h} (d\phi)^2, e^{\phi_h} R \quad (0.0.4)$$

for the heterotic action of

$$\begin{aligned} S_{het} &\sim (-g)^{\frac{1}{2}} e^{-2\phi_h} (R + (d\phi)^2 + |\tilde{H}_3|^2 + |F_2|^2) \\ &\quad |\tilde{F}_3|^2 e^{\phi_h} |\tilde{F}_3|^2 |F_2|^2 \rightarrow e^{-3\phi_h} |F_2|^2 \end{aligned} \quad (0.0.5)$$